Hemodynamics and Heart Function

in the Venous Clipped

Chick Embryo

Hemodynamics and heart function in the venous clipped chick embryo

Sandra Stekelenburg-de Vos

Thesis Erasmus University Rotterdam – with ref. - with summary in Dutch

Hemodynamics and Heart Function in the Venous Clipped Chick Embryo

The influence of volume blood flow on cardiac development

Hemodynamiek en hartfunctie in het veneus geclipte kippenembryo

De invloed van bloed volume doorstroming op hartontwikkeling

Proefschrift

ter verkrijging van de graad van doctor aan de

Erasmus Universiteit Rotterdam

op gezag van de rector magnificus

Prof.dr. S.W.J. Lamberts

en volgens besluit van het College voor Promoties.

De openbare verdediging zal plaatsvinden op

woensdag 12 oktober 2005 om 13:45 uur

door

Sandra Stekelenburg-de Vos

geboren te Rotterdam

There must have been an angel by my side

Something heavenly led me to you

Look at the sky

It's the colour of love

'Kiss of life' by Sade, 1992

Aan mijn ouders

Voor Erik

Contents

Chapter 1

Introduction

1.1   Congenital heart disease

In the Netherlands each year 200.000 children are born according to figures from the Centraal Bureau voor de Statistiek. Approximately 2-3% of these children is affected with a congenital malformation, of which heart defects account for 20-25% [1]. This means that each year approximately 1400 children are born with a congenital cardiovascular malformation [1]. These malformations are the result of aberrant embryonic development of a normal structure, or failure of such a structure to progress beyond an early stage of embryonic or fetal development. The aetiology is still largely unclarified. Between 6-10% is attributed to genetic factors, 1% to toxic factors and 1% to intra-uterine infections [2]. In the majority of cases complex multifactorial genetic factors in combination with environmental influences are thought to be responsible [3].

Over the last decades therapeutic interventions have greatly improved and 85% of all children with congenital heart disease reach adulthood [4]. However, despite the advances in medical and surgical treatment, congenital heart disease still accounts for the largest component of infant mortality. Approximately 12% of all infants that die within the first year of life suffer from congenital heart disease [5]. After successful surgical repair many patients experience morbidity, sometimes accompanied by limited life expectancy [6]. Most frequent sequelae of congenital heart disease in adults are cardiac arrhythmias, valve insufficiency, pulmonary hypertension, endocarditis, and heart failure. These patients need life-long surveillance of their cardiac condition. In order to improve surgical outcome and the care for the (postoperative) adult patient we must increase our understanding of normal and abnormal cardiovascular developmental mechanisms.

1.2   The chick embryo model

In humans the heart is completely developed by the 10th week of pregnancy. This means that the embryonic heart has developed from a muscle wrapped tube into a septated four-chambered heart at the time most women undergo their first ultrasound scan. Moreover, the available ultrasound techniques do not allow a very detailed morphological examination of the heart until week 11 [7]. Thus to investigate cardiovascular development *in vivo* we need an animal model. We chose the chick embryo because it shares morphological characteristics of the human embryo during early cardiac development [8]. Furthermore, the chick embryo model is a relatively cheap model and due to its independency of the mother hen, it is also very accessible for manipulations.

The chick embryo has been used as a model to study hemodynamics and cardiovascular development for many decades. Chick embryonic development is completed in 21 days. Hamburger and Hamilton (HH) divided this period into 46 developmental stages based on morphological landmarks [9]. Using this classification system the developmental age of each embryo can be established accurately.

The heart is the first organ that forms and functions in the embryo. At HH10 (33-38hrs) the first heartbeat is detected and at HH12 (45-49hrs) blood flow is present. The heart is responsible for pumping blood to the embryo and the extra-embryonic circulation that provides the embryo with oxygen and nutrients and removes waste products. This means that its function is already crucial during the complicated process of cardiac development. Thus forces generated by cardiac contraction and relaxation, for instance blood pressure and blood flow, likely influence cardiovascular development [10].

The embryo grows rapidly. Embryonic weight increases 120-fold between HH12 and HH29 from 2.2 to 267.5mg and ventricular weight shows a 30-fold increase from 0.10 to 3.18mg [10]. Dorsal aortic blood flow increases parallel with embryonic growth [10], whereas the relative weight of the ventricle decreases [11]. This suggests that somehow cardiac output and metabolic demands are precisely coupled and that the cardiovascular system becomes increasingly effective.

Blood pressure waveforms are strikingly similar to those in mature circulations. The atrial pressure curve has a distinct A-wave. The ventricular pressure curve has a characteristic early diastolic passive rise and late diastolic active atrial accentuation [10]. Ventricular systole consists of an isovolumic contraction phase, ejection phase and isovolumic relaxation phase. The arterial pressure waveform shows distinct diastolic and systolic pressures, including a dicrotic notch [10].

Cardiac function in the embryo and adult animal is determined by preload, afterload, heart rate and myocardial contractility. Preload depends on the diastolic phase, in which the ventricle is filled with blood. Diastole can be partitioned into a passive filling component and an active filling component. During the passive phase blood flows from the atrium to the ventricle due to the pressure-gradient [12]. Hereafter, active filling is established by atrial contraction. During development the ratio of passive to active filling volume decreases because the active filling increases geometrically [13]. The atrioventricular flow pattern may influence ventricular chamber growth and thus may determine ventricular chamber volume [13]. Cardiac output depends on preload. In early stages of development the autonomic nervous system is not present yet [14,15] and cardiac output is controlled by the Frank-Starling

mechanism as in the human foetus [16]. Wagman *et al.* [17] demonstrated the presence of this mechanism in the chick embryo by volume injections that lead to increased dorsal aortic blood velocity and stroke volume.

Afterload, the force against which the ventricle contracts, decreases during development as the vascular bed grows rapidly [18]. Vascular resistance may be also controlled by receptor-mediated changes in vascular tone. Injections with ß-adrenergic agonists resulted in increased vascular resistance [19]. Atrial natriuretic peptide (ANP) causes vasodilatation and a decrease in passive filling resulting in decreased preload and cardiac output [20,21].

Heart rate increases from about 103 bpm at HH12 to more than 239 bpm at the time the embryo hatches [10,22]. Heart rate influences filling characteristics of the ventricle. Experimental pacing faster than intrinsic heart rate leads to a decrease in stroke volume, due to a reduction in passive filling [23], which can be reversed by volume loading during pacing [24]. This is again probably the result of the Frank-Starling principle. Environmental factors like temperature also influence cardiac function profoundly [25,26]. An increase in temperature results in an increase in heart rate, cardiac output and a decrease in vascular resistance, while a decrease in temperature results in opposite effects. Stroke volume seems not to be influenced, as it remains constant during temperature changes.

Myocardial contractility is the inherent capacity of the myocardium to contract independently of changes in preload or afterload. It is largely dependent on the amount of calcium reaching the myofilaments and the quantity and quality of myofilaments [27]. Pump performance increases with development, which is probably due to a better organization and more orderly arrangement of the myofibrils leading to increased myocardial contractility [28,29]. Also maturation in the calcium transport system could play a role [30].

As outlined earlier, cardiac function is already crucial during the complicated process of cardiac development. There seems to be an intricate relationship between form and function. Several studies have shown that alterations in hemodynamics can precede the onset of structural cardiac defects [31,37]. It is likely that blood pressure and blood flow are important determinants for development of the heart and vessels and that the final organization of the myocardium is in part determined by hemodynamic forces interacting with the developing ventricular walls [29]. Knowledge of developmental mechanisms is the key to understanding the link between aetiological factors and cardiac malformations [32].

1.3 The venous clip model

In 1997 Bianca Hogers and co-workers designed an intervention model for the chick embryo at the department of Anatomy and Embryology of the Leiden University Medical Center to obtain insight into the long-term hemodynamic effects of mechanical manipulation at the venous pole of the heart. She studied intracardiac blood flow patterns and their relation to the yolk sac circulation using India ink injections [33]. She described that blood derived from specific yolk sac regions follows specific developmental stage-dependent intracardiac routes. Permanent obstruction of the right lateral vitelline vein (venous clipping) with a microclip causes alterations in these intracardiac flow patterns [34]. Furthermore, after venous clipping the embryos displayed specific cardiovascular malformations consisting of a spectrum of outflow tract anomalies like ventricular septal defects, valve anomalies and pharyngeal arch artery malformations [34,35]. Next to the morphological malformations, Broekhuizen *et al.* also demonstrated long-term hemodynamic changes after venous clipping [36]. At HH34 (day 8 of incubation) heart rate was decreased, whereas peak systolic and mean systolic velocities, as well as peak and mean blood flow were increased after clipping [36]. However, at this point (HH34) cardiac malformations are already present, which makes it impossible to determine whether these hemodynamic changes are a direct effect of the clipping procedure or are caused by the cardiac malformations. The fact that intracardiac blood flow patterns change directly after clipping suggests that hemodynamics is influenced by this procedure and that hemodynamics plays a role in cardiac development [35]. Other studies have also shown that alterations in hemodynamics can precede the onset of structural defects [31,37]. Clipping causes a detour of venous inflow to the heart. After clipping, venous blood that is normally drained by the right lateral vitelline vein to the heart is redirected to the posterior vitelline vein via a small capillary vessel, which expands into a large anastomosis within a few hours. Hogers *et al.* [34] postulated that alterations in hemodynamic parameters could lead to changes in shear stress, which could alter the expression of shear stress responsive genes with downstream alterations in developmental processes resulting in cardiac malformations. Shear stress (τ) is the frictional force from blood flow on the endothelium, which can be calculated as follows: $\tau = 4\mu Q/\pi R^3$, in which μ is viscosity of blood, Q blood flow and R blood vessel radius. Endothelial cells sense changes in shear stress, which lead to changes in gene expression by activation of a shear stress responsive element in the promotor region of the gene [38]. The exact mechanism explaining how endothelial cells sense changes in shear stress is not clear yet. In a review by Resnick *et al.* [39] several endothelial proteins and structures termed shear stress sensors/receptors/transducers, localised to various compartments of the endothelial cell, are

described: cell-matrix and cell-cell junction molecules, membrane structures like ion channels and G-proteins, and the endothelial cytoskeleton [39]. After sensing a change in shear stress, second messenger cascades are activated leading to activation of shear stress responsive elements and activation or modulation of other transcription factors eventually affecting gene expression [40]. Endothelin-1 (ET-1), expressed by the endothelial cells, is a growth factor, which is shear stress responsive and part of the endothelin-1/endothelin-converting-enzym/endothelin-A receptor (ET-1/ECE-1/ETA) signalling cascade [38,41]. This cascade is important in cardiac development [42]. Cardiovascular malformations in the venous clip model are similar to malformations observed in knockout mice studies of the endothelin pathway [42-44]. This suggests that the endothelin pathway might be involved in the development of malformations induced by venous clipping.

In humans, complex multifactorial genetic factors in combination with environmental influences are held responsible for the development of cardiovascular malformations in the majority of cases [3]. These combinations lead to altered gene and protein expression, which in turn can lead to hampered blood flow patterns inside the embryonic heart. Both altered gene expression and hampered blood flow may result in cardiovascular malformations as described in the venous clip model. The venous clip model enables us to study the consequences of altered flow patterns on cardiovascular morphological and functional development.

Based on these prior studies regarding the development of cardiovascular malformations in the venous clip model we explored the following hypothesis in the present thesis. Venous clipping leads to instantaneous alterations in hemodynamic parameters, which cause changes in shear stress responsive gene expression, resulting in development of both long-term functional cardiac impairment and malformations. We also hypothesize that endothelin-1 is involved in the disturbed development in this model. The ultimate goal is to elucidate the relationship between cardiac morphogenesis and cardiac function.

1.4   Research objectives

We started this research project in order to learn more about cardiac function during embryonic development, and especially about the intricate relationship between cardiac morphogenesis and cardiac function. The venous clip model enabled us to study the influence of altered venous return patterns on hemodynamic parameters and cardiac morphogenesis. The objectives of this thesis were as follows:

1.   To study the instantaneous effects of clipping the right lateral vitelline vein on volume flow in the stage 17-chick embryo using dorsal aortic Doppler measurements. Data are presented in chapter 3.

2.   To determine the long-term consequences of the venous clip intervention for ventricular function as assessed by pressure-volume loop analysis one day (HH21) and two days (HH24) after the clip intervention. This is discussed in chapter 4.1 and 4.2 respectively.

3.   To assess the influence of the venous clip intervention on ventricular diastolic filling characteristics at stage 24 using simultaneous Doppler measurements over the dorsal aorta and atrioventricular canal. This is presented in chapter 5.1.

4.   To establish the influence of endothelin-1 or endothelin receptor antagonist infusion on ventricular diastolic filling characteristics at stage 24 using simultaneous Doppler measurements over the dorsal aorta and atrioventricular canal. Results are discussed in chapter 5.2.

1.5 References

1. Eurocat Website Database: www.eurocat.ulster.ac.uk, University of Ulster, 2003.

2. Buskens E, Grobbee DE, Frohn-Mulder IM, Wladimiroff JW, Hess J. Aspects of the aetiology of congenital heart disease. *Eur Heart J*. 1995;16:584-7.

3. Nora JJ. Causes of congenital heart diseases: old and new modes, mechanisms, and models. *Am Heart J*. 1993;125:1409-19.

4. Vriend JW, van der Velde ET, Mulder BJ. National registry and DNA-bank of patients with congenital heart disease: the CONCOR-project. *Ned Tijdschr Geneeskd*. 2004;148:1646-7.

5. Factsheet: cijfers en feiten aangeboren hartafwijkingen. The Netherlands Heart Foundation, 1998.

6. Mulder BJM. Inleiding. In: Mulder BJM, Pieper PG, Spitaels SEC, eds. *Aangeboren hartafwijkingen bij volwassenen*. Houten/Diegem: Bohn Stafleu Van Loghum; 1999.

7. Haak MC, Twisk JW, Van Vugt JM. How successful is fetal echocardiographic examination in the first trimester of pregnancy? *Ultrasound Obstet Gynecol*. 2002;20:9-13.

8. Sissman NJ. Developmental landmarks in cardiac morphogenesis: comparative chronology. *Am.J.Cardiol*. 1970;25:141-148.

9. Hamburger V, Hamilton HL. A series of normal stages in the development of the chick embryo. *J Morphol*. 1951;88:49-92.

10. Hu N, Clark EB. Hemodynamics of the stage 12 to stage 29 chick embryo. *Circ Res*. 1989;65:1665-1670.

11. Clark EB, Hu N. Hemodynamics of developing cardiovascular system. *Ann.N.Y.Acad.Sci.* 1990;588:41-47.

12. Clark EB. Hemodyanmic control of the embryonic circulation. In: Clark EB, Takao A, eds. *Developmental cardiology: Morphogenesis and function.* New York: Futura Publishing Co.; 1990:291-303.

13. Hu N, Connuck DM, Keller BB, Clark EB. Diastolic filling characteristics in the stage 12 to 27 chick embryo ventricle. *Pediatr Res*. 1991;29:334-337.

14. Pappano AJ. Ontogenetic development of autonomic neuroeffector transmission and transmitter reactivity in embryonic and fetal hearts. *Pharmacological Reviews*. 1977;29:3-33.

15. Higgins D, Pappano AJ. Developmental changes in the sensitivity of the chick embryo ventricle to beta-adrenergic agonist during adrenergic innervation. *Circ Res*. 1981;48:245-53.

16. Ursem NTC, Struijk PC, Hop WCJ, Clark EB, Keller BB, Wladimiroff JW. Heart rate and flow velocity variability as determined from umbilical Doppler velocimetry at 10-20 weeks of gestation. *Clin.Sci.* 1998;95:539-545.

17. Wagman AJ, Hu N, Clark EB. Effect of changes in circulating blood volume on cardiac output and arterial and ventricular blood pressure in the stage 18, 24 and 29 chick embryo. *Circ Res*. 1990;67:187-192.

18.	Clark EB, Hu N. Developmental hemodynamic changes in the chick embryo from stage 18 to 27. *Circ Res*. 1982;51:810-815.

19.	Clark EB, Hu N, Dooley JB. The effect of isoproterenol on cardiovascular function in the stage 24 chick embryo. *Teratology*. 1985;31:41-7.

20.	Nakazawa M, Kajio F, Ikeda K, Takao A. Effect of atrial natriuretic peptide on hemodynamics of the stage 21 chick embryo. *Pediatric Research*. 1990;27:557-560.

21.	Hu N, Hansen AL, Clark EB, Keller BB. Effect of atrial natriuretic peptide on diastolic filling in the stage 21 chick embryo. *Pediatr Res*. 1995;37:465-8.

22.	Broekhuizen MLA, Mast F, Struijk PC, Bie van der W, Mulder PGH, Gittenberger-De Groot AC, Wladimiroff JW. Hemodynamic parameters of stage 20 to stage 35 chick embryo. *Pediatr Res*. 1993;34:44-46.

23.	Dunnigan A, Hu N, Benson DW, Clark EB. Effect of heart rate increase on dorsal aortic flow in the stage 24 chick embryo. *Pediatr. Res*. 1987;22:442-444.

24.	Benson DW, Jr., Hughes SF, Hu N, Clark EB. Effect of heart rate increase on dorsal aortic flow before and after volume loading in the stage 24 chick embryo. *Pediatr Res*. 1989;26:438-41.

25.	Nakazawa M, Clark EB, Hu N, Wispé J. Effect of environmental hypothermia on vitelline artery blood pressure and vascular resistance in the stage 18, 21, and 24 chick embryo. *Pediatr Res*. 1985;19:651-4.

26.	Nakazawa M, Miyagawa S, Takao A, Clark EB, Hu N. Hemodynamic effects of environmental hyperthermia in stage 18, 21, and 24 chick embryos. *Pediatr Res*. 1986;20:1213-5.

27.	Nakanishi T, Seguchi M, Takao A. Development of the myocardial contractile system. *Experientia*. 1988;44:936-944.

28.	Manasek FJ. Histogenesis of the embryonic myocardium. *Am J Cardiol*. 1970;25:149-68.

29.	Clark EB, Hu N, Dummett JL, Vandekieft GK, Olson C, Tomanek R. Ventricular function and morphology in chick embryo from stages 18 to 29. *Am J Physiol*. 1986;250:H407-H413.

30.	Cheanvechai V, Hughes SF, Benson DW, Jr. Relationship between cardiac cycle length and ventricular relaxation rate in the chick embryo. *Pediatr Res*. 1992;31:480-2.

31.	Stewart DE, Kirby ML, Sulik KK. Hemodynamic changes in chick embryos precede heart defects after cardiac neural crest ablation. *Circ Res*. 1986;59:545-550.

32.	Clark EB. Cardiac embryology. Its relevance to congenital heart disease. *Am J Dis Child*. 1986;140:41-4.

33.	Hogers B, DeRuiter MC, Baasten AM, Gittenberger-de Groot AC, Poelmann RE. Intracardiac blood flow patterns related to the yolk sac circulation of the chick embryo. *Circ Res*. 1995;76:871-7.

34.   Hogers B, DeRuiter MC, Gittenberger-de Groot AC, Poelmann RE. Unilateral vitelline vein ligation alters intracardiac blood flow patterns and morphogenesis in the chick embryo. *Circ Res*. 1997;80:473-481.

35.   Hogers B, DeRuiter MC, Gittenberger-de Groot AC, Poelmann RE. Extraembryonic venous obstructions lead to cardiovascular malformations and can be embryolethal. *Cardiovasc Res*. 1999;41:87-99.

36.   Broekhuizen ML, Hogers B, DeRuiter MC, Poelmann RE, Gittenberger-de Groot AC, Wladimiroff JW. Altered hemodynamics in chick embryos after extraembryonic venous obstruction. *Ultrasound Obstet Gynecol*. 1999;13:437-45.

37.   Harh JY, Paul MH, Gallen WJ, Friedberg DZ, Kaplan S. Experimental production of hypoplastic left heart syndrome in the chick embryo. *Am J Cardiol*. 1973;31:51-6.

38.   Malek AM, Izumo S. Control of endothelial cell gene expression by flow. *J Biomech*. 1995;28:1515-28.

39.   Resnick N, Yahav H, Shay-Salit A, Shushy M, Schubert S, Zilberman LC, Wofovitz E. Fluid shear stress and the vascular endothelium: for better and for worse. *Prog Biophys Mol Biol*. 2003;81:177-99.

40.   Topper JN, Gimbrone MA. Blood flow and vascular gene expression: fluid shear stress as a modulator of endothelial phenotype. *Mol Med Today*. 1999;5:40-46.

41.   Nishida K, Harrison DG, Navas JP, Fisher AA, Dockery SP, Uematsu M, Nerem RM, Alexander RW, Murphy TJ. Molecular cloning and characterization of the constitutive bovine aortic endothelial cell nitric oxide synthase. *J Clin Invest*. 1992;90:2092-6.

42.   Kurihara Y, Kurihara H, Oda H, Maemura K, Nagai R, Ishikawa T, Yazaki Y. Aortic arch malformations and ventricular septal defect in mice deficient in endothelin-1. *J Clin Invest*. 1995;96:293-300.

43.   Yanagisawa H, Yanagisawa M, Kapur RP, Richardson JA, Williams SC, Clouthier DE, de Wit D, Emoto N, Hammer RE. Dual genetic pathways of endothelin-mediated intercellular signaling revealed by targeted disruption of endothelin converting enzyme-1 gene. *Development*. 1998;125:825-36.

44.   Clouthier DE, Hosoda K, Richardson JA, Williams SC, Yanagisawa H, Kuwaki T, Kumada M, Hammer RE, Yanagisawa M. Cranial and cardiac neural crest defects in endothelin-A receptor-deficient mice. *Development*. 1998;125:813-24.

Chapter 2

Methodology

This chapter describes the techniques and methods that were used to obtain different parameters of ventricular function in the chick embryo.

2.1 The venous clip procedure

At Hamburger and Hamilton stage 17 (2.5 days of incubation) the embryos were exposed by creating a window in the shell and removing the overlying membranes [1]. Then the vitelline membrane was removed adjacent to the right vitelline vein and a small incision in the yolk sac membrane was made. Subsequently, the right vitelline vein was obstructed with an aluminium microclip (Fig. 1). The microclips were made of a 0.2mm aluminium sheet. Cessation of blood flow proximal to the microclip was confirmed under microscopic surveillance. All experiments were performed *in ovo*. After this intervention hemodynamic measurements were made and/or the embryo was reincubated until a later developmental stage.
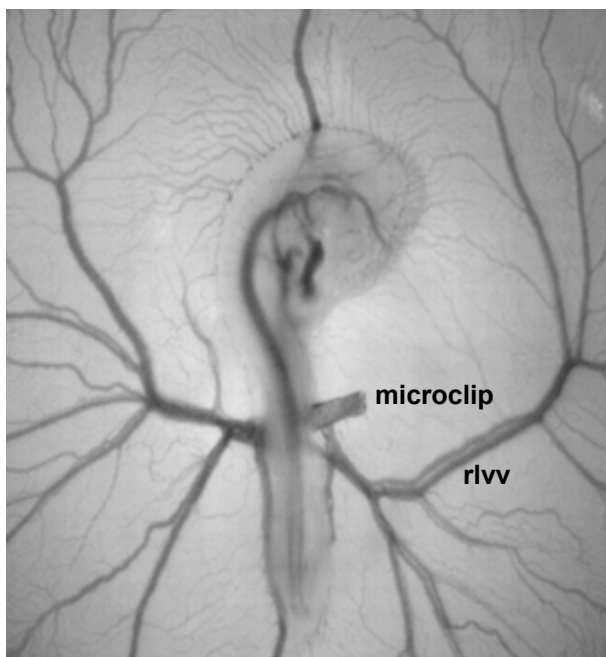

Figure 1.
Chick embryo at HH17.
The microclip obstructs the right lateral vitelline vein (rlvv) completely.

2.2   Doppler ultrasound

The principle of Doppler ultrasound lies in the Doppler effect. This natural phenomenon was first described by Christian Doppler, an Austrian physicist (1803-1853). When sound, emitted by an object, is received by a moving sound receiver then the frequency of the received sound is different from the original emitted signal. This is the Doppler shift. The change in frequency depends on the velocity of the moving receiver. We can use this relationship for determining blood flow velocities in chick embryos using a 20 MHz sound emitting pulsed Doppler probe. This Doppler probe serves as both emitter and receiver. The emitted signal is reflected by the red blood cells and its frequency is shifted by movements of the red blood cells. From the frequency shift the blood flow velocity is calculated using the following equation:

$V = (\Delta f \cdot c) / (2 \cdot f_0 \cdot \cos\alpha)$,

where V is velocity of the blood flow, Δf is the frequency shift, c is velocity of sound in tissue, f_0 is emitted frequency and α is the angle of insonation of the probe.

Dorsal aortic blood flow velocity measurements

In practice, dorsal aortic blood flow velocity measurements were carried out as follows: A 20-MHz pulsed Doppler meter (model 545C-4, Iowa Doppler Products, Iowa City, IA, USA) was used to measure the blood flow velocity. The Doppler audio signals were digitised at 12 kHz and stored on hard disk. Using complex fast Fourier transform analysis, the maximum velocity waveform was reconstructed. The Doppler probe consisting of a 750μm piezoelectric crystal was positioned at a 45º angle to the dorsal aorta at the level of the developing wing bud (Fig. 2). The sample volume was adjusted to cover the lumen of the dorsal aorta only, excluding other adjacent vessels. The internal aortic diameter was measured at the same level by video imaging with a stereo microscope (model SV 6, Carl Zeiss, Oberkochen, Germany) and a video camera (model SSC-M370CE, Sony Corporation, Tokyo, Japan). The video images were acquired with an image acquisition board (IMAQ PCI-1408, National Instruments, Austin, TX, USA) and subsequently analysed with a custom-built analysis program using IMAQ Vision software (National Instruments). Size calibration in the horizontal and vertical planes of the image was performed by videotaping a 10μm division scribed scale. For calculation of the aortic diameter, the magnification of the video image displaying the dorsal aorta was incorporated into the image analysis program.

Blood flow was calculated from the equation $Q = v\pi d^2/4$, where v is mean aortic blood flow velocity and d is the internal aortic diameter. Peak acceleration (dV/dt) was derived from the

dorsal aortic blood flow velocity by means of digital differentiation. Stroke volume was determined from the quotient of the dorsal aortic blood flow and the heart rate. Peak systolic velocity (PSV, mm/s), time-averaged velocity (TAV, mm/s), heart rate (bpm), peak blood flow (mm^3/s), mean blood flow (mm^3/s), peak acceleration (mm/s^2) and stroke volume (mm^3) were determined for each cardiac cycle. For each embryo a high quality waveform recording of 10 seconds was used for the analysis (fig.3). The 10-second recordings contained 20-27 heartbeats. For all hemodynamic parameters in each embryo, the average of all cardiac cycles was calculated.
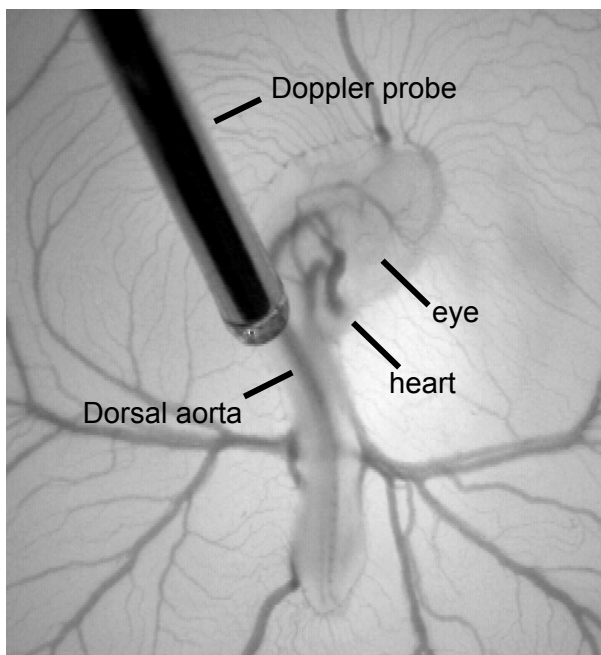
Figure 2. HH17 chick embryo.

This figure demonstrates the Doppler probe covering the dorsal aorta, positioned at the level of the developing wing bud of a normal stage 17-chick embryo.
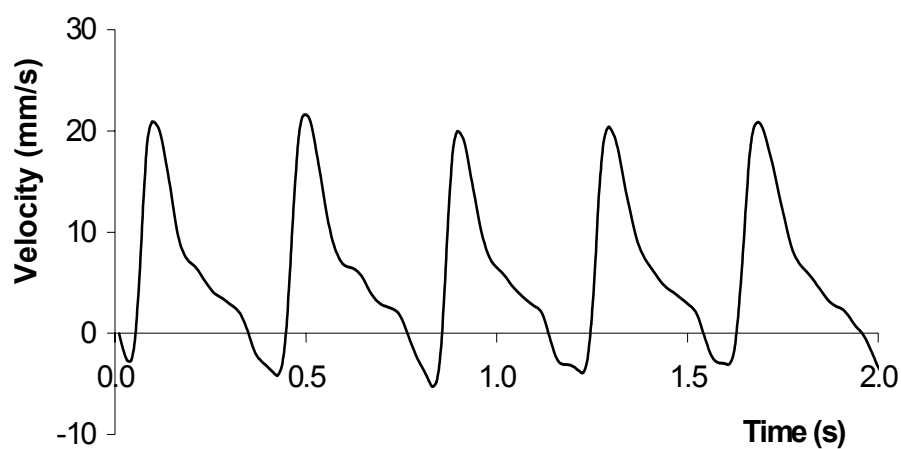
Figure 3.

Dorsal aortic blood flow velocity waveform of a stage 17 chick embryo.

Atrioventricular blood flow velocity measurements

To assess diastolic filling characteristics the atrioventricular (AV) blood flow velocity was measured with a second crystal positioned at the apex of the heart towards the AV orifice (Fig. 4). The Doppler audio signals from both the dorsal aorta and AV canal were digitized at 24 kHz and stored on hard disk. Passive filling (P) was defined in the AV flow velocity waveform from end-systole to the onset of the A-wave, and active filling (A) from the onset of the A-wave to the onset of systole (Fig. 5). Portions of passive and active filling overlapped each other at faster heart rates. The demarcation between the passive and active velocities was dependent on heart rate, but was most conspicuous at slower heart rate. Embryos were studied at similar heart rates to avoid the effect of heart rate on diastolic filling. Cycle length was defined as the time between consecutive beats obtained from the dorsal aortic velocity waveform. Dorsal aortic and both passive and active AV velocity profiles were integrated over time. Dorsal aortic blood flow was calculated as the product of the integrated velocity curve and the cross-sectional area of the dorsal aorta. Passive ventricular filling volume equaled dorsal aortic stroke volume multiplied by the fraction of passive filling area and active ventricular filling volume equaled dorsal aortic stroke volume multiplied by the fraction of the active filling area [2].

Figure 4.
HH24 chick embryo.
Simultaneous Doppler measurements of the dorsal aorta and the atrioventricular canal.
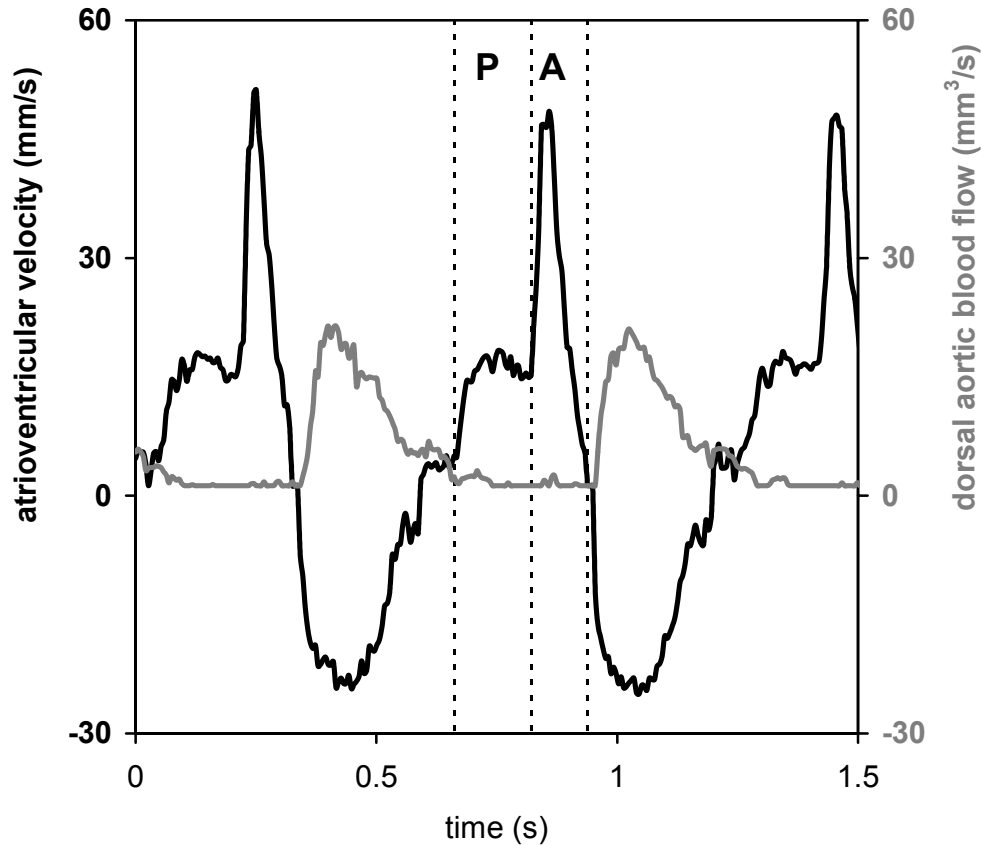
Figure 5.

Simultaneously acquired dorsal aortic blood flow (grey line) and atrioventricular blood flow velocity (black line). The diastolic phase consists of a passive (P) phase and an active (A) phase.

Reproducibility study of flow velocity waveforms in the chick embryo

To validate the method by which we obtained the velocity waveform recordings of the dorsal aorta in chick embryos using a 20-MHz pulsed Doppler meter, we conducted a study to assess the reproducibility. We measured 10 embryos of HH17 that showed no bleeding or deformities. All experiments were performed *in ovo*. In each of the 10 embryos, 3 independent measurements were made at 30-second time intervals. All the measurements were performed by one investigator in the same order; the egg was placed on the thermoelement under the dissecting microscope, the Doppler probe was positioned and the recording was made. In between the measurements the egg was removed from its position. The exact time interval between the measurements was documented. The mean coefficient of variation (C.V., %) for heart rate, peak systolic velocity and time-averaged velocity was calculated to determine the intraobserver reproducibility. In the calculations, the C.V. was adjusted for the trend due to cooling over the time points by performing an analysis of

variance. A common linear trend was assumed for each embryo in this analysis. The resulting S.D. of residuals was taken as the S.D. of measurement error. All calculations and statistical analyses were performed with SPSS 10.1 software (SPSS Inc, Chicago, IL, USA).

The mean coefficient of variation for heart rate (bpm), peak systolic velocity (PSV, mm/s) and time-averaged velocity (TAV, mm/s) was: 0.9% (range 0.8-1.0); 3.7% (range 2.8-4.9) and 4.6% (range 3.0-7.0), respectively. This indicates satisfactory intraobserver reproducibility for dorsal aortic waveform derived parameters.

2.3   Servo-null pressure system

Intraventricular pressure

Blood pressure was measured in the ventricle (Fig.6+7) using a servo-null system (model 900A, World Precision Instruments, Inc., Sarasota, Florida, USA) and a fluid filled (2M NaCl) 5-10μm glass micropipette attached to a microelectrode. Intraventricular pressure was calculated as the difference between the measured pressure and the pressure recorded when the tip of the pipette was placed in the extra-embryonic fluid adjacent to the ventricular puncture site

The working principle of the servo-null method is described in detail by Heineman & Grayson [3], and Chabert & Taber [4], and can be summarized as follows: A 1 mm glass capillary, with one end drawn to typically 6μm inner diameter, is placed in a small microelectrode. This microelectrode is mounted on a micromanipulator, which is used to insert the pipette tip into the embryonic heart. The microelectrode and capillary are fluid-filled with a highly conductive solution of 2M NaCl. The air on top of the fluid in the microelectrode is connected via a short flexible tube to the pressure pod, a small box near the microelectrode, in which the air pressure is measured continuously by a relatively fast responding pressure transducer. The pod pressure depends on the imbalance between air entering the pod from a pressure source through an electronically controlled valve, and air leaving the pod towards a vacuum sink.

Via an electrode connected to the embryo, the electric resistance between blood plasma and conducting solution in the pipette and microelectrode is monitored continuously. At a steady plasma pressure, a constant resistance is obtained, which is caused by the relatively low ion concentration of the blood plasma inside the narrow pipette tip. On a rising blood pressure, the ion concentration gradient is forced into the pipette, thereby increasing the electric resistance. The differential resistance is amplified by a factor *S*, 'sensitivity' and fed into the controlled valve of the pressure pod, thereby increasing the airflow into the pod. As a result,

the microelectrode pressure increases and forces the ion concentration gradient back to its equilibrium position. To avoid oscillation of this system at a resonance frequency, the feed back loop is stabilized by mixing the signal that reaches the valve with the measured pressure signal multiplied by a factor *D*, 'damping'. By this method, a stable system can be obtained, where the static pressure is measured accurately.
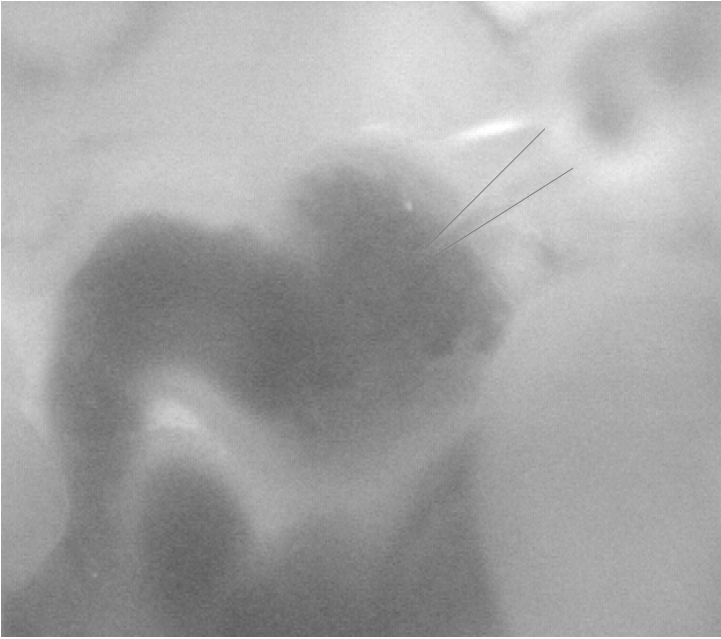
Figure 6.
Intraventricular pressure.
Ventricle and outflow tract of a stage 21 chick embryo. The pressure is measured inside the ventricular cavity using a glass micropipette.

Figure 7. Pressure signal.
The measured pressure signal is presented with the corresponding pictures of the ventricle
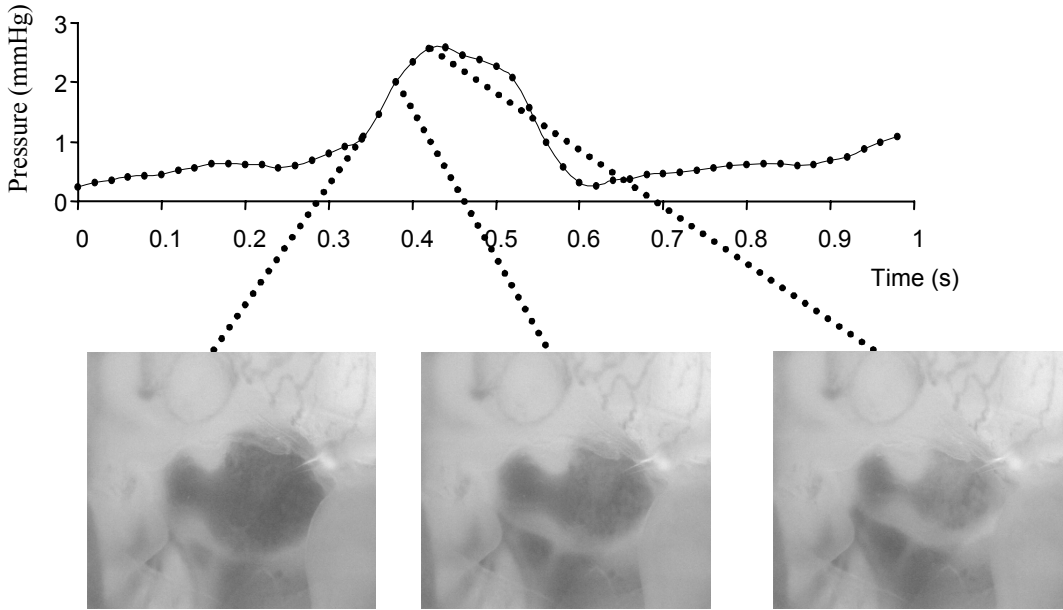
Frequency response of servo-null system

To establish the systems response to pressure oscillations in the blood, we tested the dynamic response of the system *in vitro* over the frequency range of 0.5-20Hz (as this frequency range is relevant to chick embryonic heart rate) by applying air pressure fluctuations on top of a liquid bath, in which the microelectrode with micropipette was inserted. The actual pressure was measured simultaneously, using a pressure transducer of known flat response up to 130Hz (Setra Systems, Inc., Boxborough, MA, USA). The servo-null system was adjusted to various settings with respect to 'sensitivity' and 'damping'.

The dynamic response of the servo-null system relative to the actual pressure is shown in figure 8. We conclude that at the HR frequency (2-3Hz) the signal amplitude is amplified (under damped) by about 1% only and the phase delay is about 5-6 degrees, or 7ms, or about ¼ of the frame time interval. For the 4th harmonic (10Hz)(at 4 times the HR frequency), where still 2-3% of the signal energy is present in the energy spectrum, the signal amplitude is amplified by about 20% and the phase delay is 25-30 degrees, or 8ms, or about ¼ of the frame time interval. We therefore conclude that the pressure is measured with sufficient accuracy.
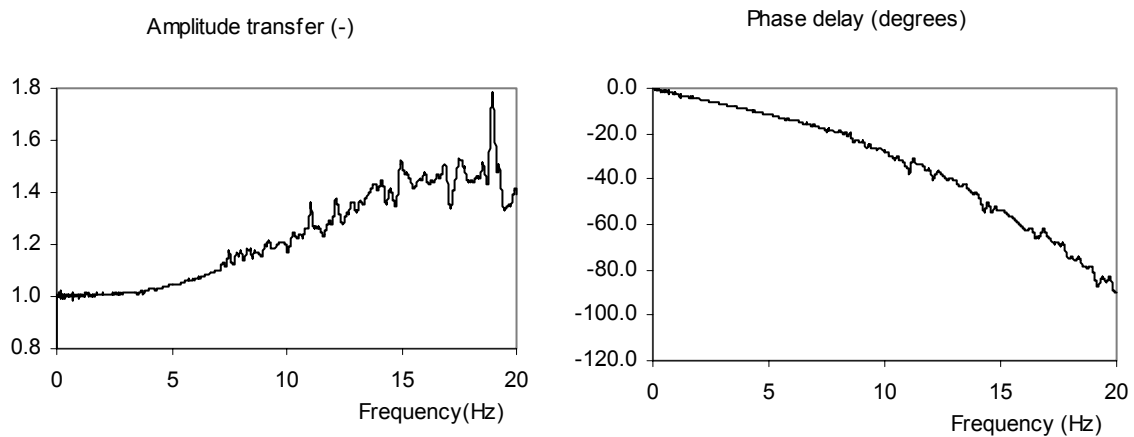
Figure 8. Dynamic frequency response curves of servo-null system.

The left panel demonstrates the amplitude transfer curve of the measured pressure signal over a frequency range of 0.5 to 20 Hz relative to the actual pressure. The right panel demonstrates the phase delay curve of the signal.

2.4 Intraventricular volume

During the pressure measurements the ventricle was visualised using video imaging with a stereo microscope (model SV 6, Carl Zeiss, Oberkochen, Germany) and a video camera (model SSC-M370CE, Sony Corporation, Tokyo, Japan). The video images were acquired simultaneously with the analog pressure signal at 50Hz and stored on a PC. Epicardial surface area was calculated from magnified video images displaying the ventricle using a custom-built analysis program (IMAQ Vision, National Instruments, Austin, TX, USA)(Fig.9). Ventricular volume (V) was derived from epicardial area (A) using a simplified ellipsoid geometric model: $V=0.65A^{3/2}$ as described by Keller et al [5].

For each embryo 2-4 consecutive (baseline) cardiac cycles were analyzed. Furthermore, to evaluate ventricular response to reduced venous return, a fourth order vitelline vein was incised to produce venous hemorrhage, which results in acute preload reduction. The cardiac cycles following hemorrhage were also recorded and subsequently analyzed to derive ventricular pressure-volume relations. By the latter procedure information can be obtained about ventricular contractility (through the end-systolic pressure volume relation) and diastolic stiffness (through the end-diastolic pressure volume relation).

Finally, maximum contraction of the heart with 2M NaCl was induced for determination of ventricular wall volume by video imaging (Fig.9). The solution (1-3µl) was applied directly on the ventricle. Cavity volume was calculated as total volume minus wall volume.
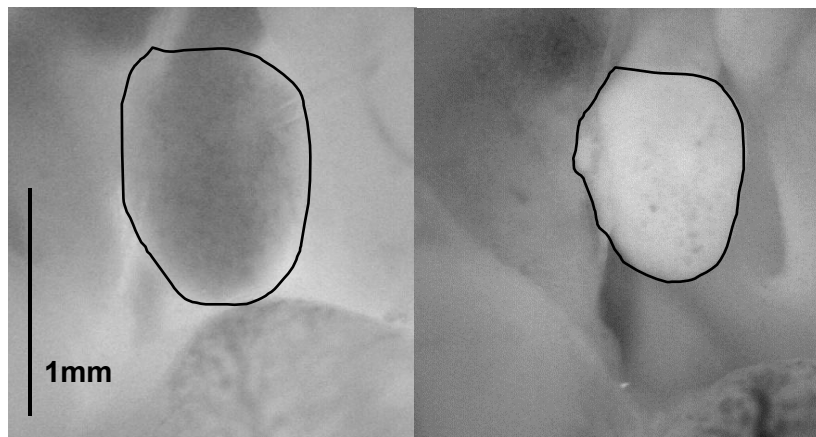
Figure 9.

The ventricle is traced to obtain the surface area, from which ventricular volume is calculated. At the end of the experiment 2 molar NaCl is applicated onto the ventricle to achieve maximum ventricular contraction, and ventricular wall volume is calculated. After subtraction of ventricular wall volume from all the obtained volumes during the cardiac cycle the ventricular blood volumes are obtained, which are used to create pressure-volume relations.

We validated this method in a set of four embryos at stage 21 in which wall volume obtained by video imaging was compared with wall volume obtained by the counting method of Cavalieri, detailed by Gundersen and Jensen [6]. The wall volume of the ventricles was determined by video imaging after 2M NaCl application, directly followed by fixation with 4% paraformaldehyde in 0.1M phosphate buffer. The hearts were embedded in paraffin, serially sectioned at 5-µm thickness, and stained with hematoxylin-eosin for stereologic examination. The number of points on a grid hitting 15 sections of the ventricle was counted. The first section was taken randomly and the other sections were taken systematically. From the counted numbers, the volumes could be calculated by Cavalieri's formula:

$V = \Sigma P \cdot M^{-2} \cdot a \cdot d$, where V is the volume in mm^3, ΣP is the total number of counted points on the 15 sections, M the magnification, a is the point area in mm^2, and d is the distance between the counted sections in mm.

The mean ventricular wall volume obtained by video imaging was $0.171 \pm 0.009\mu l$ and mean myocardial wall volume obtained by Cavalieri's method was $0.157 \pm 0.010\mu l$, which means that ventricular wall volume is overestimated by 8.9%. Therefore, we concluded that the video imaging procedure correlates well with stereologically obtained volumes and we chose not to correct for this overestimation in the calculations.

2.5 Assessment of ventricular function

By combining pressure and volume data, pressure-volume loops are obtained (Fig.10).
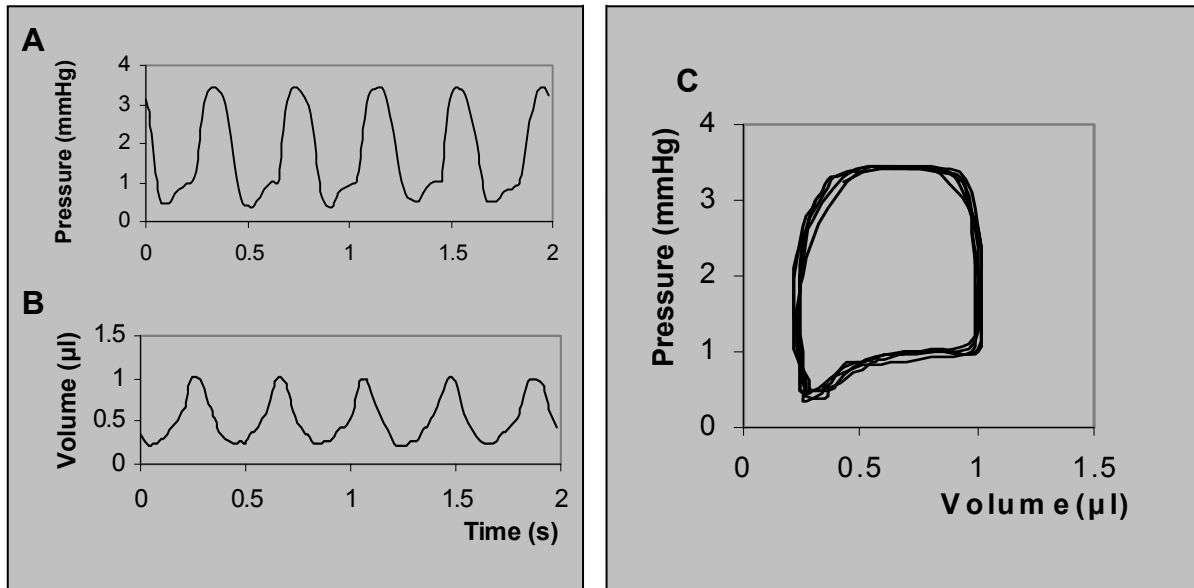
Figure 10.

Panels A and B show an intraventricular pressure signal with the corresponding volumes. In panel C these data are combined into pressure-volume loops.

Pressure-volume loops give information about ventricular function. A large number of parameters can be determined using pressure-volume loop analysis. Figure 11 demonstrates some basic principles of this analysis.
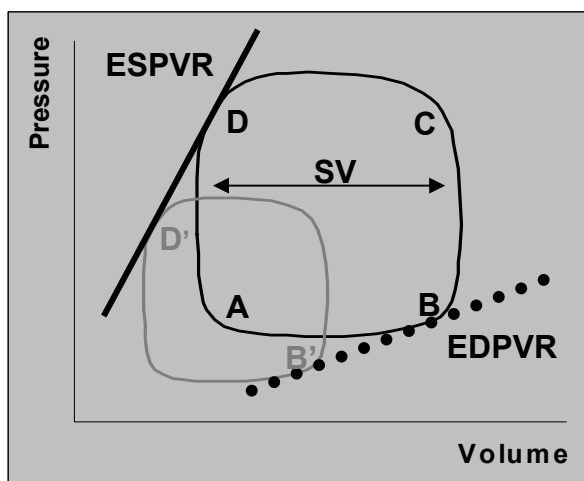
Figure 11. Pressure-volume loop analysis. At point A the atrioventricular cushions open and blood flows from the atrium into the ventricle during diastole. At point B the maximum volume is reached and the cushions close. Isovolumic contraction causes an increase in pressure up to point C, where the outflow tract cushions open and blood flows from the ventricle into the aorta during systole. At point D the outflow tract cushions close and isovolumic relaxation occurs back to point A. These steps are followed each cardiac cycle. The end-systolic pressure-volume relation (ESPVR) and the end-diastolic pressure-volume relation (EDPVR) are determined by the end-systolic points (D and D') and the end-diastolic points (B and B') of the baseline pressure-volume loop (black loop) and loop after preload reduction (grey loop). Stroke volume (SV) can also be obtained from the baseline loop.

From the baseline loops (black loop) the following parameters can be obtained: end-systolic and end-diastolic pressures and volumes (ESP, EDP, (mmHg); ESV, EDV, (µl)) and stroke volume (SV, µl) as the difference between EDV and ESV. Cardiac output (CO, µl/min) as HR multiplied by SV, ejection fraction (EF, %) as SV divided by EDV and stroke work (SW, (µl·mmHg) as the area of the pressure-volume loop. The latter three are ejection phase, afterload-dependent indices of systolic performance.

When preload is lowered the pressure-volume loops will shift downwards to the left (grey loop). This allows determination of the end-systolic and end-diastolic pressure-volume relationships as load-independent measures of systolic and diastolic ventricular function. The end-systolic pressure-volume relationship (ESPVR) is determined by the end-systolic points. The slope of this relation (E_{ES}, (mmHg/µl)) is a measure for ventricular contractility. The end-diastolic pressure-volume relationship (EDPVR) is determined by the end-diastolic points and reflects the passive properties of the ventricle. The slope of this relation (E_{ED} (mmHg/µl)) is a measure for diastolic ventricular stiffness.

Furthermore, from the pressure and volume data the following parameters can also be calculated: the maximum and minimum first derivatives of pressure (dP/dt_{MAX}, dP/dt_{MIN}, mmHg/s). dP/dt_{MAX} is an index of contractility from the isovolumic contraction phase that is afterload independent, however sensitive to change in preload. Peak filling rate (PFR, µl/s) represents the maximum first derivative of ventricular volume with respect to time (dV/dt), peak ejection rate (PER, µl/s) represents the minimum first derivative of ventricular volume with respect to time (dV/dt), and the relaxation time constant Tau (τ, ms) represents the time-constant of mono-exponential pressure decay during isovolumic relaxation (Fig.12). The isovolumic period is defined as the time-period between the moment of dP/dt_{MIN} and the time-point at which dP/dt reached 10% of dP/dt_{MIN} [7]. The relaxation time constant Tau (τ), an index of active (isovolumic) relaxation, can be calculated as the time-constant of mono-exponential pressure decay during isovolumic relaxation using P=A+B.exp(-t/tau), in which A and B are constants determined by the data [8]. In addition pressure-half-time (PHT, ms) can be determined as the time-interval between the moment of dP/dt_{MIN} and the moment that pressure has dropped to 50% of the instantaneous pressure at the moment of dP/dt_{MIN}.
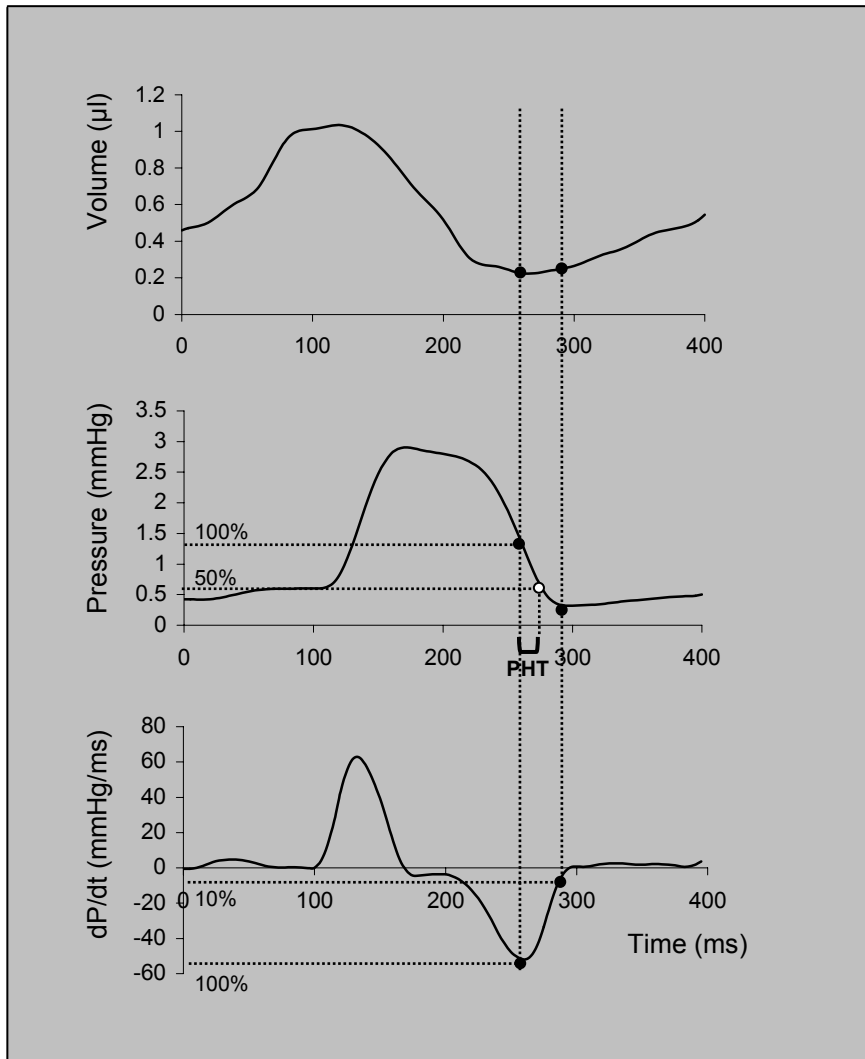
Figure 12.

This figure demonstrates how dP/dt_{MIN}, the relaxation time constant Tau and PHT are determined. The isovolumic period starts at the time-point of dP/dt_{MIN} and ends at the time-point at which dP/dt reaches 10% of dP/dt_{MIN}. PHT is calculated as the time-interval between the moment of dP/dt_{MIN} and the moment that pressure has dropped to 50% of the instantaneous pressure at the moment of dP/dt_{MIN}.

These parameters are a measure of different determinants of ventricular function. The use of this method during early embryonic development could improve our understanding of the intricate relationship between cardiac morphogenesis and cardiac function.

2.6 References

1. Hamburger V, Hamilton HL. A series of normal stages in the development of the chick embryo. *J Morphol*. 1951;88:49-92.

2. Hu N, Connuck DM, Keller BB, Clark EB. Diastolic filling characteristics in the stage 12 to 27 chick embryo ventricle. *Pediatr Res*. 1991;29:334-337.

3. Heineman FW, Grayson J. Transmural distribution of intramyocardial pressure measured by micropipette technique. *Am J Physiol*. 1985;249:H1216-1223.

4. Chabert S, Taber LA. Intramyocardial pressure measurements in the stage 18 embryonic chick heart. *Am J Physiol Heart Circ Physiol*. 2002;282:H1248-54.

5. Keller BB, Tinney JP, Hu N. Embryonic ventricular diastolic and systolic pressure-volume relations. *Cardiol Young*. 1994;4:19-27.

6. Gundersen HJ, Jensen EB. The efficiency of systematic sampling in stereology and its prediction. *J Microsc*. 1987;147 (Pt 3):229-63.

7. Leeuwenburgh BP, Steendijk P, Helbing WA, Baan J. Indexes of diastolic RV function: load dependence and changes after chronic RV pressure overload in lambs. *Am J Physiol Heart Circ Physiol*. 2002;282:H1350-H1358.

8. Yellin EL, Hori M, Yoran C, Sonnenblick EH, Gabbay S, Frater RW. Left ventricular relaxation in the filling and nonfilling intact canine heart. *Am J Physiol*. 1986;250:H620-629.

Chapter 3

Acute hemodynamic effects of venous clipping in the chick embryo

Introductory remarks

In the venous clip model cardiovascular malformations are induced by extra-embryonic venous obstruction. Previous studies using India ink injections clearly demonstrated that the venous clip procedure at HH17 leads to changes in blood flow patterns through the heart. These changes probably also affect hemodynamics. This chapter describes the direct influence of the venous clip procedure on hemodynamic parameters as assessed by Doppler blood flow velocimetry. Altered shear stress responsive gene expression could be the link between hemodynamic disturbances and the observed malformations.

3.1   Acutely altered hemodynamics following venous obstruction in the early chick embryo

Summary

In the venous clip model specific cardiac malformations are induced in the chick embryo by obstructing the right lateral vitelline vein with a microclip. Clipping alters venous return and intracardiac laminar blood flow patterns, with secondary effects on the mechanical load of the embryonic myocardium. We investigated the instantaneous effects of clipping the right lateral vitelline vein on hemodynamics in the stage-17 chick embryo. Thirty-two chick embryos HH 17 were subdivided into venous clipped (N=16) and matched control embryos (N=16). Dorsal aortic blood flow velocity was measured with a 20 MHz pulsed Doppler meter. A time series of eight successive measurements per embryo was made starting just before clipping and ending 5 h after clipping. Heart rate, peak systolic velocity, time-averaged velocity, peak blood flow, mean blood flow, peak acceleration and stroke volume were determined. All hemodynamic parameters decreased acutely after venous clipping and only three out of seven parameters (heart rate, time-averaged velocity and mean blood flow) showed a recovery to baseline values during the 5 h study period. We conclude that the experimental alteration of venous return has major acute effects on hemodynamics in the chick embryo. These effects may be responsible for the observed cardiac malformations after clipping.

Introduction

The earliest stage at which the beating embryonic human heart can be visualised is the sixth week of gestation, using ultrasonography. Detailed analysis of fetal cardiac and extracardiac flow velocity waveforms using combined high-resolution, 2-dimensional ultrasound and Doppler techniques is possible after 8 to 9 weeks onward [1]. The most essential events in human cardiovascular development, however, take place between 3-8 weeks of gestation, during which the embryonic heart develops from a muscle wrapped tube into the septated four-chambered heart, so animal models are required to study mechanisms of early cardiovascular development.

The chick embryo has been used as a model for many decades because in many aspects the embryonic chick heart resembles the developing human heart [2,3]. An intervention model for the chick embryo was designed to obtain insight into the long-term hemodynamic effects of altered venous return patterns on cardiac morphogenesis and malformations. Specific cardiac malformations were induced by permanently obstructing the right lateral vitelline vein with a microclip, (venous clip model [4]) thereby altering the intracardiac blood flow patterns. A spectrum of outflow tract anomalies can be induced by this intervention. Hogers *et al.* [4] postulated that alterations in hemodynamic parameters could lead to changes in shear stress, which could alter the expression of shear stress responsive genes with downstream alterations in developmental processes resulting in cardiac malformations. The observation of intracardiac blood flow pattern alterations during clipping, visualised by injected India ink, suggested that hemodynamics is influenced by clipping [5]. Other studies have also shown that alterations in hemodynamics can precede the onset of structural defects [6].

A previous study from our group has demonstrated that at stage 34 (day 8 of incubation) heart rate was decreased in embryos that had been clipped at stage 17 (stages according to Hamburger and Hamilton, 1951), whereas peak systolic and mean systolic velocities, as well as peak and mean blood flow were increased compared to normal embryos [7,8]. These results showed the presence of long term hemodynamic changes after clipping. However, at this point (stage 34) cardiac malformations are already present, so it is impossible to discriminate between the effects of cardiac malformations and any direct effects of clipping on hemodynamics.

By a modification of the method used for Doppler frequency detection it is now possible to obtain good quality waveforms directly after clipping at stage 17 [9]. This allows examination of the direct effects of clipping on hemodynamics, to improve our understanding of how cardiac anomalies may arise following venous obstruction. We hypothesise that cardiac

malformations induced by clipping are caused by instantaneous changes in blood flow through the heart resulting in altered activation of shear stress responsive genes. In the present work we show the instantaneous effects of clipping the right lateral vitelline vein on hemodynamics in the stage 17 (52-64 h of incubation) chick embryo.

Materials and Methods

Animals

Fertilized white Leghorn chick eggs *Gallus domesticus* L. were obtained from Charles River Laboratories (Extertal, Germany) and were incubated at 37-38°C, with the blunt end up and at a relative humidity of 70-80%. The embryos were exposed by creating a window in the shell and removing the overlying membranes. Only embryos that were at Hamburger and Hamilton stage 17 (HH17) [7] and that showed no bleeding or deformities were selected. A total of 32 embryos was included. The material was subdivided into venous clipped (n=16) embryos and control embryos (n=16). In the clipped group the vitelline membrane was removed adjacent to the right vitelline vein and a small incision in the yolk sac membrane was made. Subsequently, the right vitelline vein was obstructed with an aluminum microclip (Fig. 1). Cessation of blood flow proximal to the microclip was confirmed under microscopic surveillance. The microclips were made of a 0.2mm aluminum sheet. All experiments were performed *in ovo*. During the experiments the egg was placed on a thermoelement of 37°C. In between measurements the window in the shell was resealed with tape and the egg was reincubated.
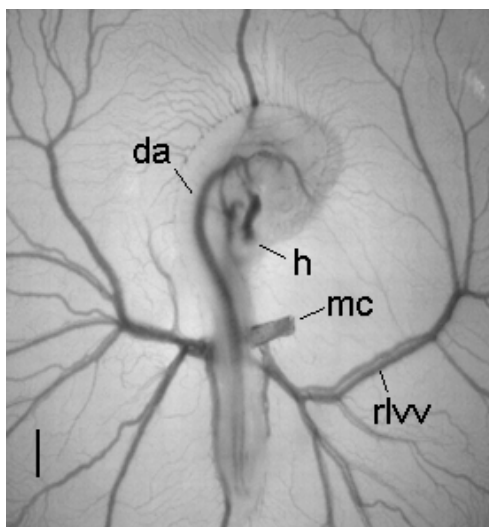
Figure 1. Stage 17 chick embryo with an aluminium microclip (mc) positioned at the right lateral vitelline vein (rlvv), causing cessation of blood flow proximal to the microclip. heart (h), dorsal aorta (da). Scale bar is 1 mm.

Hemodynamics in the chick embryo

The chick embryo has been used as a model to study hemodynamics and cardiovascular development for many decades. Chick embryonic development is completed in 21 days. Hamburger and Hamilton divided this period into 46 developmental stages based on morphological landmarks [7]. Using this classification system the developmental age of each embryo can be established accurately.

The heart is the first organ that forms and functions in the embryo. At HH10 (33-38hrs) the first heartbeat is detected and at HH12 (45-49hrs) blood flow is present. The heart is responsible for pumping blood to the embryo and the extra-embryonic circulation that provides the embryo with oxygen and nutrients and removes waste products. This means that its function is already crucial during the process in which the heart is transformed from a muscle wrapped tube into a 4-chambered septated heart. Thus forces generated by cardiac contraction and relaxation, for instance blood pressure and blood flow, likely influence cardiovascular development [10].

The embryo grows rapidly. Embryonic weight increases 100-fold between HH12 and HH29 from 2.22mg to 267.5mg and ventricular weight show a 30-fold increase from 0.1 to 3.18mg [10]. Dorsal aortic blood flow increases parallel with embryonic growth [10] and the relative weight of the ventricle decreases [11]. This suggests that somehow cardiac output and metabolic demands are coupled precisely and that the cardiovascular system is increasingly effective. Blood pressure waveforms are strikingly similar to those in mature circulations. The atrial pressure curve has a distinct A-wave. The ventricular pressure curve has a characteristic early diastolic passive rise and late diastolic active atrial accentuation [10]. Ventricular systole has an isovolumic contraction phase, ejection phase and isovolumic relaxation phase. The arterial pressure waveform shows distinct diastolic and systolic pressures, including a dicrotic notch [10].

Cardiac function in the embryo and adult animal is determined by preload, afterload, heart rate and myocardial contractility. Preload depends on the diastolic phase, in which the ventricle is filled with blood. Diastole can be partitioned into a passive filling component and an active filling component. During the passive phase blood flows from the atrium to the ventricle due to the pressure-gradient [12]. Hereafter, active filling is established by atrial contraction. During development the ratio of passive to active filling volume decreases because the active filling increases geometrically [13]. The atrioventricular flow pattern may be a mechanical-biologic link to ventricular chamber growth and a determination of ventricular chamber volume [13]. Cardiac output depends on preload. In early stages of development the

neurohumoral and autonomic nervous systems are not present yet and cardiac output is controlled by the Frank-Starling mechanism [14]. Wagman *et al.* demonstrated the presence of this mechanism in the chick embryo by volume injections that lead to increased dorsal aortic blood velocity and stroke volume.

Afterload, the force against which the ventricle contracts, decreases during development as the vascular bed grows rapidly [2]. Vascular resistance may be also controlled by receptor-mediated changes in vascular tone. Injections with ß-adrenergic agonists resulted in increased vascular resistance [15]. Atrial natriuretic peptide (ANP) causes vasodilatation and a decrease in passive filling resulting in decreased preload and cardiac output [16,17].

Heart rate increases from about 103 bpm at HH12 to more than 239 bpm at the time the embryo hatches [10,18]. Heart rate influences filling characteristics of the ventricle. Experimental pacing faster than intrinsic heart rate leads to a decrease in stroke volume, due to a reduction in passive filling [19], which can be reversed by volume loading during pacing [20]. This is again probably the result of the Frank-Starling principle. Environmental factors like temperature also influences cardiac function profoundly [21,22]. An increase in temperature results in an increase in heart rate, cardiac output and a decrease in vascular resistance, while a decrease in temperature results in opposite effects. Stroke volume seems not to be influenced, as it remains constant during temperature changes.

Pump performance increases with development, which is probably due to better organization and a more orderly arrangement of the myofibrils leading to increased myocardial contractility [23]. Also maturation in the calcium transport system [24] and

Functional changes in hemodynamics occur prior to any observable abnormal structural changes in heart or aortic arch arteries of embryos with cardiac neural crest ablations [6]. Embryos with neural crest ablations had significantly greater dorsal aortic blood flow velocity and lower systolic and diastolic blood pressures than controls. It is likely that blood pressure and blood flow are important determinants for development of the heart and vessels and that the final organization of the myocardium is in part determined by hemodynamic forces interacting with the developing ventricular walls [23]. Knowledge of developmental mechanisms is the key to understanding the link between etiologic factors and cardiac malformations [25].

Measurements

Eight dorsal aortic blood flow velocity measurements were made per embryo. The first velocity measurement (baseline) was done directly after exposure of the embryo. The second

measurement was performed directly after successful clipping of the right vitelline vein at approximately four min from the first measurement. For each clipped embryo a control embryo was measured, matched for the exact time interval between the first measurement before clipping and the second measurement directly after clipping. This was important since cooling of the embryo would take place despite the use of a thermoelement, and cooling of the embryo influences the outcome of the measurements [21,26]. The third measurement was performed 30 min after clipping, the fourth to eighth recordings occurred at 1, 2, 3, 4 and 5 h after clipping, respectively. The control embryos were subjected to the same measurement schedule as venous clipped embryos.

Materials

Dorsal aortic blood flow velocity was measured using a 20-MHz pulsed Doppler meter (model 545C-4, Iowa Doppler Products, Iowa City, IA, USA). The Doppler audio signals were digitized at 12 kHz and stored on hard disk. Using complex fast Fourier transform analysis, the maximum velocity waveform was reconstructed. A more detailed description of this method has been published previously [9]. The Doppler probe consisting of a 750μm piezoelectric crystal was positioned at a 45º angle to the dorsal aorta at the level of the developing wing bud. The sample volume was adjusted to cover the lumen of the dorsal aorta only, excluding other adjacent vessels. The internal aortic diameter was measured at the same level by video imaging using a stereo microscope (model SV 6, Carl Zeiss, Oberkochen, Germany) and a video camera (model SSC-M370CE, Sony Corporation, Tokyo, Japan). The video images were acquired with an image acquisition board (IMAQ PCI-1408, National Instruments, Austin, TX, USA) and subsequently analyzed using a custom-built analysis program using IMAQ Vision software (National Instruments). Size calibration in the horizontal and vertical planes of the image was performed by videotaping a scale divided into 10μm divisions. Aortic diameter was calculated by incorporating the magnified video image displaying the dorsal aorta into the image analysis program.

Blood flow Q was calculated from $Q=v\pi d^2/4$, where v is mean aortic blood flow velocity and d is the internal aortic diameter. Peak acceleration (dv/dt) was derived from the dorsal aortic blood flow velocity by means of digital differentiation. Stroke volume was determined from the quotient of the dorsal aortic blood flow and the heart rate. We determined peak systolic velocity (PSV, mm/s), time-averaged velocity (TAV, mm/s), heart rate (bpm), peak blood flow (mm^3/s), mean blood flow (mm^3/s), peak acceleration (mm/s^2) and stroke volume (mm^3) for each cardiac cycle. For each embryo a high quality waveform recording of 10 seconds was

used for the analysis. The 10-second recordings contain 20-27 heartbeats. For all hemodynamic parameters in each embryo, the average of all cardiac cycles was calculated.

Statistical analysis

Heart rate, PSV, TAV, peak blood flow, mean blood flow, peak acceleration and stroke volume data are presented as mean ± standard error of the mean (S.E.M.). Hemodynamic parameters were compared within and between groups. Paired t-tests were performed within each group to compare mean values at all time points with baseline values. Repeated measurements ANOVA, using SAS PROC MIXED, was performed on the net changes from baseline level to assess whether the profiles of the net changes paralleled each other. The values were standardized by taking the net changes from baseline level in order to adjust for biological variability. Net change profiles in a parallel position indicated a significant difference in the net changes throughout the 5-h study period between the clipped and control group. If the profiles differed significantly from parallelism, paired t-tests were performed at each time point to compare both groups. $P< 0.05$ was considered statistically significant. Statistical analyses were performed using SPSS 10.1 software and SAS 6.12 software (SAS Institute Inc, Cary, NC, USA).

Results

The means ± S.E.M. of all the measured parameters in the clipped embryos (n=16) and control embryos (n=16) at all time points are presented in table 1. The baseline values of all parameters did not significantly differ between both groups. The mean time required to place the microclip was 4 min (range 3.23-4.15), and the control group was matched for this 4 min period to differentiate between the influence of cooling of the embryo and clipping. All hemodynamic parameters decreased markedly during the venous clip procedure in the clipped group and the 4 min period in the control group.

The profiles of changes from baseline level of all the parameters did not significantly differ from parallelism ($P>0.05$), except for heart rate and peak acceleration ($P<0.05$).

Directly after clipping or the 4 min period (controls), heart rate decreased significantly in both groups (Fig. 2A). This decrease was not significantly different between the groups. However, at 30 min, 1 and 2 h the difference in heart rate between the clipped and control group was significant. In the clipped group it took 3 h for the heart rate to gradually return to baseline level, whereas the control group showed a recovery within 30 min.

The profile of the net changes in the PSV of the clipped group (Fig. 2B) was significantly below the profile of the control group ($P<0.001$). The clipped group demonstrated a 57%

decrease of PSV after clipping as compared with a 19% decrease in the control group. This decrease stabilized at 30 min after clipping at ± 22%. In the control group PSV was significantly elevated at all time points beyond 2 h compared to baseline level.

The profile of the net changes in TAV of the clipped group (Fig. 2C) was significantly lower than the profile of the control group ($P<0.001$). Following an initially significant decrease of 53% in the clipped group, TAV slowly stabilized at a level of 17% below baseline level. The control group recovered within 30 min and showed a significantly raised TAV at 4 and 5 h.

The profile of the net changes in peak blood flow of the clipped group (Fig. 2D) was significantly below the profile of the control group ($P<0.001$). Peak blood flow decreased by 58% directly after clipping as compared with 18% in the control group. This decrease in the clipped group stabilized significantly below the baseline level at 30 min after clipping. The control group displayed a significantly elevated peak blood flow after 3 h.

The profile of the net changes in mean blood flow of the clipped group (Fig. 2E) was significantly below the profile of the control group ($P<0.001$). In the clipped group mean blood flow was significantly lower directly after clipping, at 30 min and at 1 h after clipping as compared with baseline level. No significant differences existed at later time points. The control group only showed a significant decrease after the 4-min period and even demonstrated a significantly elevated level of mean blood flow at 4 and 5 h.

The profiles of net changes in peak acceleration (Fig. 2F) significantly ($P<0.05$) deviated from parallelism. The net changes in peak acceleration of the clipped group and the control group were significantly different at all time points. Within the clipped group peak acceleration was significantly decreased at all time points after clipping as compared with baseline level. The control group showed a significant decrease after the 4-min period only and a significant increase at all time points thereafter.

The profile of the net changes in stroke volume of the clipped group (Fig. 2G) was significantly lower than the profile of the control group ($P<0.001$). Stroke volume was significantly lower up to 1 h after clipping. At 4 and 5 h stroke volume was also significantly reduced. The control group demonstrated a significant decrease only immediately after the 4-min period.

Table 1. *Hemodynamic parameters of stage 17 clipped embryos and control embryos at all measurement points*

(N=16 for both groups) PSV, peak systolic velocity; TAV, time-averaged velocity.

		Baseline	4 min	30 min	1 h	2 h	3 h	4 h	5 h
Heart rate (bpm)	Clip	147±2	128±2	135±3	138±3	148±4	153±3	151±3	158±3
	Control	147±3	131±3	150±2	155±2	157±3	156±3	157±2	159±3
PSV (mm/s)	Clip	23.0±1.2	9.9±0.6	18.2±1.1	17.9±0.9	17.2±1.2	17.8±1.3	17.6±1.0	17.9±1.2
	Control	20.6±1.2	16.6±1.4	20.9±1.5	23.2±1.4	22.7±1.8	23.0±1.5	23.9±1.1	24.3±1.3
TAV (mm/s)	Clip	6.0±0.5	2.8±0.3	3.6±0.3	3.9±0.3	5.0±0.4	5.0±0.6	4.9±0.4	5.1±0.5
	Control	5.1±0.2	3.9±0.3	5.2±0.4	6.2±0.5	6.0±0.6	5.7±0.5	6.2±0.4	6.2±0.4
Peak blood flow (mm^3/s)	Clip	0.94±0.05	0.40±0.02	0.75±0.06	0.75±0.06	0.72±0.07	0.75±0.08	0.73±0.06	0.74±0.06
	Control	0.81±0.05	0.66±0.07	0.82±0.06	0.91±0.06	0.88±0.07	0.90±0.06	0.93±0.04	0.95±0.05
Mean blood flow (mm^3/s)	Clip	0.24±0.02	0.11±0.01	0.15±0.01	0.16±0.02	0.21±0.02	0.21±0.03	0.20±0.02	0.21±0.02
	Control	0.20±0.01	0.16±0.01	0.21±0.02	0.24±0.02	0.23±0.02	0.22±0.02	0.25±0.02	0.24±0.02
Peak acceleration (mm/s^2)	Clip	755±42	357±19	516±40	537±26	516±25	517±26	519±26	524±27
	Control	720±44	550±40	753±42	781±42	785±44	800±43	803±42	816±43
Stroke volume (mm^3)	Clip	0.099±0.007	0.053±0.004	0.064±0.005	0.071±0.007	0.085±0.008	0.084±0.013	0.081±0.007	0.079±0.008
	Control	0.082±0.005	0.071±0.006	0.082±0.006	0.094±0.007	0.090±0.010	0.087±0.008	0.094±0.007	0.091±0.006
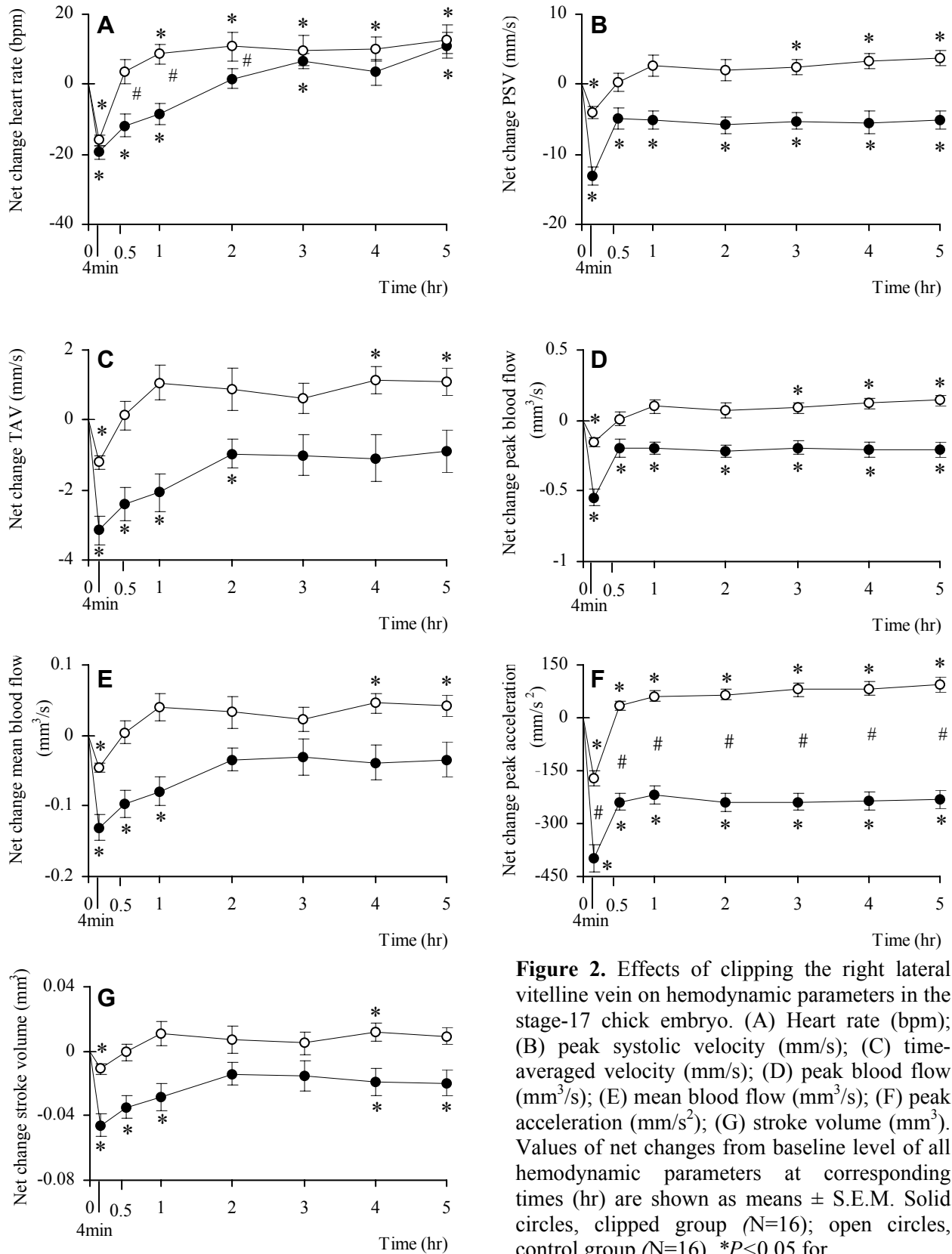
Figure 2. Effects of clipping the right lateral vitelline vein on hemodynamic parameters in the stage-17 chick embryo. (A) Heart rate (bpm); (B) peak systolic velocity (mm/s); (C) time-averaged velocity (mm/s); (D) peak blood flow (mm^3/s); (E) mean blood flow (mm^3/s); (F) peak acceleration (mm/s^2); (G) stroke volume (mm^3). Values of net changes from baseline level of all hemodynamic parameters at corresponding times (hr) are shown as means ± S.E.M. Solid circles, clipped group (N=16); open circles, control group (N=16). *$P<0.05$ for the comparison with baseline values within groups. The profiles in B–E and G are in a parallel position to each other, which indicates a significant difference in the net changes from baseline level throughout the 5 h study period. The profiles in A and F do not run parallel to each other, therefore paired t-tests were performed for these parameters to compare values between both groups at the different measurement points, # $P<0.05$.

45

Discussion

This study describes the instantaneous effects of clipping the right lateral vitelline vein on hemodynamics in the stage 17-chick embryo. The objective was to obtain insight into the direct effects of clipping on hemodynamics using Doppler ultrasonography. Because of the intricate relationship between hemodynamics and morphogenesis, this could improve our understanding as to how cardiac anomalies arise following venous obstruction. In the venous clip model, extraembryonic blood flow is manipulated without direct mechanical interference of the heart such as occurs by altering neural crest migration to the arterial pole of the heart [27] or of the cervical flexure [28]. Clipping causes a detour of venous inflow to the heart, which alters the intracardiac blood flow patterns, as has been visualised with India ink injections, and induces specific cardiac malformations [4]. After clipping, venous blood that is normally drained by the right lateral vitelline vein to the heart is redirected to the posterior vitelline vein via a small capillary vessel, which expands into a large anastomosis within a few hours. The alterations in intracardiac blood flow patterns observed immediately after clipping suggest that hemodynamics is influenced by clipping [5]. The present study demonstrates that there are major hemodynamic changes during the first 5 h after clipping and we hypothesise about the consequences of these hemodynamic changes in relation to cardiac development.

A significant reduction after clipping is demonstrated for all hemodynamic parameters with a recovery seen for only 3 out of 7 parameters (heart rate, time-averaged velocity and mean blood flow) during the 5-hour study period. In the control group all parameters recovered to baseline values and displayed an additional increase after 5 h, as could be expected in a normally developing embryo. It is likely that most if not all hemodynamic parameters in the clipped group will recover within the next stages of development, especially since Broekhuizen *et al.* [8] observed no significant differences in hemodynamic parameters at stage 24 between clipped and control embryos except for a lower peak acceleration.

In the clipped group it was evident that the magnitude of decrease of the hemodynamic parameters observed at the first measurement after clipping was mainly due to clipping, with additional effects due to cooling. In the control group the observed hemodynamic changes after the 4 min period were due to minor handling and due to cooling of the embryo. It is known that chick embryo hemodynamics is greatly influenced by temperature [21,22,26]. Prolonged incubation at low temperatures can even give rise to cardiac malformations [29]. De la Cruz *et al.* [29] observed cardiac malformations in 18.8% of the embryos that had survived during continuous incubation at 35.8ºC until hatching. In the clip study by Hogers *et al.* [4] the clipped embryos were only subjected to cooling for approximately 4 min as were our

embryos. In their study specific cardiac malformations were induced in 64% of the clipped embryos, which is much higher than the 18.8% cardiac malformations observed by de la Cruz *et al*. [29] during continuous incubation at a low temperature. This supports the conclusion of Hogers *et al*. [4] that the cardiac malformations observed by them are caused by obstruction of the right lateral vitelline vein.

When considering the first 30 min of the study period the clipped group was characterized by a significant drop in all hemodynamic parameters whereas in the control group there was a return to baseline level at 30 min. The clipped group also displayed a significantly larger decrease in each hemodynamic parameter as compared with the control group. The changes in the hemodynamic parameters during the first 30 min may be explained as follows. Blood, circulating in the segment of the yolk sac vascular bed that is normally drained by the right lateral vitelline vein, is blocked due to clipping and can therefore not return directly to the heart. Blood is captured in the vitelline vascular bed while the heart keeps on pumping blood into all segments of the vascular bed. Therefore, the actively circulating blood volume is decreased, which results in a drop in venous return or preload and subsequently cardiac stroke volume. The decrease in preload also results in a decrease in peak acceleration, reflecting cardiac contraction force.

During the remainder of the study period, observations in the clipped group showed a full recovery for time-averaged velocity and mean blood flow 5 h after clipping. All other parameters demonstrated a partial recovery that however, remained significantly below baseline level. From these observations it can be assumed that the embryo compensates to maintain a steady blood supply to all organs. With the development of the vitelline vascular bed, vascular resistance and impedance decreases [10,14,30]. Therefore, we postulate that when a part of the vitelline vascular bed is closed off from the rest of the vascular bed, the vascular resistance will rise. Even when the anastomosis is formed that permanently provides a detour of blood flow towards the heart, the venous vascular resistance will remain elevated because blood has to pass along a longer route to reach the heart. There is a new steady state in the hemodynamic situation that at least meets the demands of the embryo that are necessary to survive 5 h after clipping. When comparing the clipped and control group, all hemodynamic parameters of the latter are situated well above the baseline except for stroke volume. These findings probably reflect embryonic growth during the study period. As has been described by others, hemodynamic parameters increase with growth of the embryo [10,18].

The effects of venous clip on heart rate are more complex. There is an initial drop in heart rate in both the clipped and control group at 4 min, which however is not significantly different

between the groups. This suggests a cooling effect rather than a clipping effect. As outlined above, clipping causes an acute decrease in preload. It is known that heart rate does not respond to acute alterations in loading conditions [31]. However, at 30 min to 2 h after clipping heart rate remained significantly lower than in control embryos. This suggests a direct influence on the pacemaker function of the heart that prevents a quick and normal heart rate recovery. The cardiac autonomic nervous system is not functional until HH 41, which rules out any impact of this system on heart rate [32,33]. Nevertheless, there is evidence of the presence of ß-adrenergic receptors in the myocardium at day 2-2.5 of incubation and circulating neurohumoral agents [34]. The sudden and persistent decrease in preload following clipping may trigger a release of neurohumoral agents or a change in sensitivity for these agents resulting in a temporary decrease in heart rate.

The question arises as to how these hemodynamic changes relate to the development of cardiac malformations. During normal cardiac development, cardiac performance increases [2,23] and results in gradual changes in shear stress that either up- or downregulate the expression of shear stress responsive genes [35,36] . In vitro studies have demonstrated that endothelial cells are subjected to fluid shear stress as a result of blood flow and are aligned in the direction of the flow [36,37] and that especially changes in shear stress cause alterations in gene expression [38]. Shear stress depends directly on volume flow [39]. When major alterations occur in one of the hemodynamic parameters that directly influence the shear stress, it seems feasible that altered expression of shear stress responsive genes with secondary effects on cardiac development can be expected. Other studies have also shown that alterations in hemodynamics can precede the onset of structural defects [6]. The marked decrease in mean blood flow observed in this study may lead to an acute decrease in shear stress, which could be responsible for the induction of cardiac malformations by altering shear stress responsive gene expression.

In summary we conclude that obstruction of the right lateral vitelline vein results in major hemodynamic changes during the first 5 h after clipping. We suggest that these hemodynamic changes induce cardiovascular malformations by altering normal patterns of shear stress responsive gene expression.

3.2   References

1.   Splunder van IP, Stijnen T, Wladimiroff JW. Fetal atrioventricular flow-velocity waveforms and their relation to arterial and venous flow-velocity waveforms at 8 to 20 weeks of gestation. *Circulation*. 1996;94:1372-1378.

2.   Clark EB, Hu N. Developmental hemodynamic changes in the chick embryo from stage 18 to 27. *Circ Res*. 1982;51:810-815.

3.   Nakazawa M, Miyagawa S, Ohno T, Miura S, Takao A. Developmental hemodynamic changes in rat embryos at 11 to 15 days of gestation: normal data of blood pressure and the effect of caffeine compared to data from chick embryo. *Pediatr Res*. 1988;23:200-205.

4.   Hogers B, DeRuiter MC, Gittenberger-de Groot AC, Poelmann RE. Unilateral vitelline vein ligation alters intracardiac blood flow patterns and morphogenesis in the chick embryo. *Circ Res*. 1997;80:473-481.

5.   Hogers B, DeRuiter MC, Gittenberger-de Groot AC, Poelmann RE. Extraembryonic venous obstructions lead to cardiovascular malformations and can be embryolethal. *Cardiovasc Res*. 1999;41:87-99.

6.   Stewart DE, Kirby ML, Sulik KK. Hemodynamic changes in chick embryos precede heart defects after cardiac neural crest ablation. *Circ Res*. 1986;59:545-550.

7.   Hamburger V, Hamilton HL. A series of normal stages in the development of the chick embryo. *J Morphol*. 1951;88:49-92.

8.   Broekhuizen ML, Hogers B, DeRuiter MC, Poelmann RE, Gittenberger-de Groot AC, Wladimiroff JW. Altered hemodynamics in chick embryos after extraembryonic venous obstruction. *Ultrasound Obstet Gynecol*. 1999;13:437-45.

9.   Ursem NTC, Struijk PC, Poelmann RE, Gittenberger-de Groot AC, Wladimiroff JW. Dorsal aortic flow velocity in chick embryos of stage 16 to 28. *Ultrasound Med Biol*. 2001;27:919-24.

10.   Hu N, Clark EB. Hemodynamics of the stage 12 to stage 29 chick embryo. *Circ Res*. 1989;65:1665-1670.

11.   Clark EB, Hu N. Hemodynamics of developing cardiovascular system. *Ann.N.Y.Acad.Sci.* 1990;588:41-47.

12.   Clark EB. Hemodyanmic control of the embryonic circulation. In: Clark EB, Takao A, eds. *Developmental cardiology: Morphogenesis and function.* New York: Futura Publishing Co.; 1990:291-303.

13.   Hu N, Connuck DM, Keller BB, Clark EB. Diastolic filling characteristics in the stage 12 to 27 chick embryo ventricle. *Pediatr Res*. 1991;29:334-337.

14.   Wagman AJ, Hu N, Clark EB. Effect of changes in circulating blood volume on cardiac output and arterial and ventricular blood pressure in the stage 18, 24 and 29 chick embryo. *Circ Res*. 1990;67:187-192.

15. Clark EB, Hu N, Dooley JB. The effect of isoproterenol on cardiovascular function in the stage 24 chick embryo. *Teratology*. 1985;31:41-7.

16. Nakazawa M, Kajio F, Ikeda K, Takao A. Effect of atrial natriuretic peptide on hemodynamics of the stage 21 chick embryo. *Pediatric Research*. 1990;27:557-560.

17. Hu N, Hansen AL, Clark EB, Keller BB. Effect of atrial natriuretic peptide on diastolic filling in the stage 21 chick embryo. *Pediatr Res*. 1995;37:465-8.

18. Broekhuizen MLA, Mast F, Struijk PC, Bie van der W, Mulder PGH, Gittenberger-De Groot AC, Wladimiroff JW. Hemodynamic parameters of stage 20 to stage 35 chick embryo. *Pediatr Res*. 1993;34:44-46.

19. Dunnigan A, Hu N, Benson DW, Clark EB. Effect of heart rate increase on dorsal aortic flow in the stage 24 chick embryo. *Pediatr. Res.* 1987;22:442-444.

20. Benson DW, Jr., Hughes SF, Hu N, Clark EB. Effect of heart rate increase on dorsal aortic flow before and after volume loading in the stage 24 chick embryo. *Pediatr Res*. 1989;26:438-41.

21. Nakazawa M, Clark EB, Hu N, Wispé J. Effect of environmental hypothermia on vitelline artery blood pressure and vascular resistance in the stage 18, 21, and 24 chick embryo. *Pediatr Res*. 1985;19:651-4.

22. Nakazawa M, Miyagawa S, Takao A, Clark EB, Hu N. Hemodynamic effects of environmental hyperthermia in stage 18, 21, and 24 chick embryos. *Pediatr Res*. 1986;20:1213-5.

23. Clark EB, Hu N, Dummett JL, Vandekieft GK, Olson C, Tomanek R. Ventricular function and morphology in chick embryo from stages 18 to 29. *Am J Physiol*. 1986;250:H407-H413.

24. Cheanvechai V, Hughes SF, Benson DW, Jr. Relationship between cardiac cycle length and ventricular relaxation rate in the chick embryo. *Pediatr Res*. 1992;31:480-2.

25. Clark EB. Cardiac embryology. Its relevance to congenital heart disease. *Am J Dis Child*. 1986;140:41-4.

26. Wispé J, Hu N, Clark EB. Effect of environmental hypothermia on dorsal aortic blood flow in the chick embryo, stages 18 to 24. *Pediatr Res*. 1983;17:945-8.

27. Kirby ML, Gale TF, Stewart DE. Neural crest cells contribute to normal aorticopulmonary septation. *Science*. 1983;220:1059-61.

28. Manner J, Seidl W, Steding G. Correlation between the embryonic head flexures and cardiac development. An experimental study in chick embryos. *Anat Embryol (Berl)*. 1993;188:269-85.

29. de la Cruz MV, Campillo-Sainz C, Munoz-Armas S. Congenital heart defects in chick embryos subjected to temperature variations. *Circ Res*. 1966;18:257-62.

30. Yoshigi M, Ettel JM, Keller BB. Developmental changes in flow-wave propagation velocity in embryonic chick vascular system. *American Journal of Physiology*. 1997;273:H1523-9.

31. Keller BB, Tinney JP, Hu N. Embryonic ventricular diastolic and systolic pressure-volume relations. *Cardiol Young*. 1994;4:19-27.

32. Pappano AJ. Ontogenetic development of autonomic neuroeffector transmission and transmitter reactivity in embryonic and fetal hearts. *Pharmacological Reviews*. 1977;29:3-33.

33. Higgins D, Pappano AJ. Developmental changes in the sensitivity of the chick embryo ventricle to beta-adrenergic agonist during adrenergic innervation. *Circ Res*. 1981;48:245-53.

34. Lipshultz S, Shanfeld J, Chacko S. Emergence of beta-adrenergic sensitivity in the developing chicken heart. *Proc Natl Acad Sci U S A*. 1981;78:288-92.

35. Topper JN, Gimbrone MA. Blood flow and vascular gene expression: fluid shear stress as a modulator of endothelial phenotype. *Mol Med Today*. 1999;5:40-46.

36. Malek AM, Zhang J, Jiang J, Alper SL, Izumo S. Endothelin-1 gene suppression by shear stress: pharmacological evaluation of the role of tyrosine kinase, intracellular calcium, cytoskeleton, and mechanosensitive channels. *J Mol Cell Cardiol*. 1999;31:387-399.

37. Malek AM, Izumo S. Mechanism of endothelial cell shape change and cytoskeletal remodeling in response to fluid shear stress. *J. Cell. Sci.* 1996;109:713-726.

38. Fisher AB, Chien S, Barakat AI, Nerem RM. Endothelial cellular response to altered shear stress. *Am J Physiol Lung Cell Mol Physiol*. 2001;281:L529-533.

39. Goldsmith HL, Turitto VT. Rheological aspects of thrombosis and haemostasis: basic principles and applications. ICTH-Report--Subcommittee on Rheology of the International Committee on Thrombosis and Haemostasis. *Thromb Haemost*. 1986;55:415-435.

Chapter 4

Pressure-Volume loop analysis after venous clipping

Introductory remarks

Cardiac pressure-volume loop analysis enables determination of end-systolic elastance and end-diastolic stiffness of the developing ventricle. These parameters represent intrinsic myocardial properties and are relatively independent of loading conditions. We tested the hypothesis that venous clipping could lead to long-term changes in ventricular function. We performed pressure-volume loop analysis of the embryonic chick heart at stage 21 and stage 24, respectively one day and two days after the venous clip procedure. The use of this method in early stages of development could contribute to a better understanding of the relationship between cardiac function and morphogenesis during normal and abnormal cardiac development. In this chapter the impact of early venous obstruction on embryonic cardiovascular function in later development is presented.

4.1 Systolic and diastolic ventricular function assessed by pressure-volume loops in the stage 21 venous clipped chick embryo

Summary

Cardiac pressure-volume relations enable quantification of intrinsic ventricular diastolic and systolic properties independent of loading conditions. The use of pressure-volume loop analysis in early stages of development could contribute to a better understanding of the relationship between hemodynamics and cardiac morphogenesis. The venous clip model is an intervention model for the chick embryo, in which permanent obstruction of the right lateral vitelline vein temporarily reduces the mechanical load on the embryonic myocardium and induces a spectrum of outflow tract anomalies.

We used pressure-volume loop analysis of the embryonic chick heart at stage 21 (3.5 days of incubation) in order to investigate whether the development of ventricular function is affected by venous clipping at stage 17, as compared to normal control embryos.

Steady state hemodynamic parameters demonstrated no significant differences between the venous clipped and control embryos. However analysis of pressure-volume relations showed a significantly lower end-systolic elastance in the clipped embryos (E_{ES}, slope of the end-systolic pressure-volume relation: 5.68 ± 0.85 *vs*. 11.76 ± 2.70mmHg/μl, p<0.05) indicating reduced contractility. Diastolic stiffness tended to be increased in the clipped embryos (E_{ED},

slope of end-diastolic pressure-volume relation: 2.74±0.56 vs. 1.67±0.21, p=0.103) but the difference did not reach statistical significance.

The results of the pressure-volume loop analysis show that one day after venous obstruction, development of ventricular function is affected, with reduced contractility. Pressure-volume analysis may be applied in the chick embryo and is a sensitive technique to detect subtle alterations in ventricular function.

Introduction

Animal models are required to study mechanisms of early cardiovascular development. The chick embryo has been used as a model for many decades because the embryonic chick heart resembles the developing human heart in many aspects [1,2]. Especially the intricate relationship between hemodynamics and cardiac morphogenesis has been a major study topic in this model.

The venous clip model is an intervention model for the chick embryo, in which permanent obstruction of the right lateral vitelline vein temporarily reduces the mechanical load on the embryonic myocardium and induces a spectrum of outflow tract anomalies [3]. This model was designed to obtain insight into the effects of altered venous return patterns on cardiac morphogenesis and malformations [4].

In the chick embryo, information on cardiac function can be assessed through blood flow velocities and pressure waveform recordings [1,5-7]. In a previous study using a 20MHz Doppler velocity meter, we have demonstrated that the experimental alteration of venous return caused by venous clipping has major acute effects on hemodynamics in the HH (Hamburger and Hamilton) stage 17 chick embryo [3,8]. Peak systolic velocity, peak blood flow, and stroke volume are all significantly decreased for up to 5 hours after clipping. However, dorsal aortic Doppler measurements give indirect information on cardiac function. Direct information can be assessed using cardiac pressure-volume loop analysis [9]. This method enables assessment of ventricular diastolic and systolic properties independent of loading conditions. Pressure-volume analysis has been widely used in both human and animal studies [10-12]. Only a few studies have been done during embryonic or fetal development; in (near term) fetal lambs and chick embryos [9,13-15].

The use of pressure-volume loop analysis in early stages of development could contribute to a better understanding of cardiovascular developmental processes and especially the relationship between cardiac function and cardiac morphogenesis as cardiac morphogenesis depends on the interaction between genetics and epigenetic influences like fluid mechanical forces [16].

Since mechanical load influences cardiac development and clipping the right lateral vitelline vein alters mechanical load we tested the hypothesis that clipping could lead to long-term changes in ventricular function. For this purpose a custom-made workstation was used to simultaneously measure intraventricular pressure and capture video images of the beating ventricle. We performed pressure-volume loop analysis of the embryonic chick heart at stage

21 in order to investigate whether the development of ventricular function is affected by venous clipping at stage 17 as compared to normal control embryos.

Materials and Methods

Animals

Fertilized white Leghorn chick eggs (*Gallus gallus* (L.)) were obtained from Charles River Laboratories (Extertal, Germany) and were incubated at 37-38°C, with the blunt end up and at a relative humidity of 70-80%. The embryos were exposed by creating a window in the shell and removing the overlying membranes. Twenty-one embryos that were at HH stage 17 and that showed no bleeding or deformities were selected [8]. The material was subdivided into venous clipped embryos (n=11), in which the right vitelline vein was obstructed with an aluminum microclip, and control embryos (n=10). A more detailed description of the clipping procedure has been published previously [3]. During the experiments the egg was placed on a thermoelement of 37°C. Experiments were approved by the Animal Experimentation Review Board of the Erasmus MC and were performed in accordance with Dutch Law for animal experimentation

Intraventricular pressure

Blood pressure was measured in the ventricle at HH stage 21 (Fig.1) using a servo-null system (model 900A, World Precision Instruments, Inc., Sarasota, Florida, USA) and a fluid filled (2M NaCl) 5-10µm glass micropipette attached to a microelectrode.

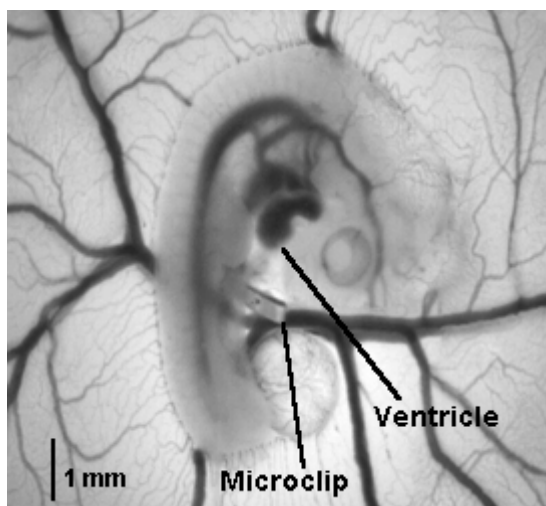

Figure 1. Stage 21-chick embryo (3.5 days of incubation).

Intraventricular pressure was calculated as the difference between the measured pressure and the pressure recorded when the tip of the pipette was placed in the extra-embryonic fluid

adjacent to the ventricular puncture site. Pressure data were sampled at 50Hz and stored on a PC. The working principle of this pressure transducer is described in detail by Heineman [17]. The dynamic response of the system was tested over the frequency range of 0.5-20Hz (as this frequency range is relevant to chicken embryonic heart rate) by applying air pressure fluctuations on top of a liquid bath in which the probe with micropipette was inserted. The actual pressure was measured simultaneously, using a pressure transducer of known flat response up to 130Hz (Setra Systems, Inc., Boxborough, MA, USA). The dynamic response of the servo-null system relative to the actual pressure is shown in figure 2
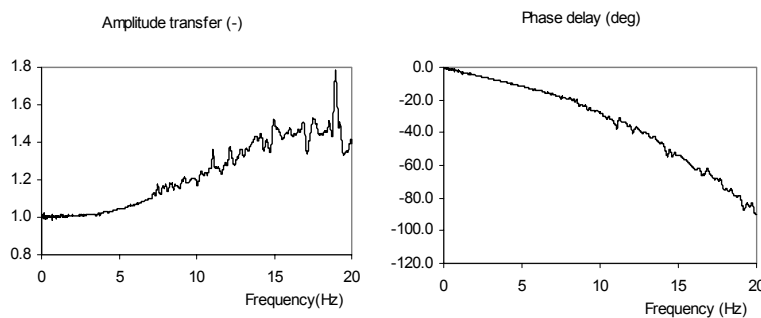
Figure 2. Dynamic frequency response of the servo-null system. Panel A demonstrates the amplitude transfer curve of the measured pressure signal over a frequency range of 0.5 to 20Hz relative to the actual pressure. Panel B demonstrates the phase delay curve of the signal.

We conclude that at the HR frequency (2-3Hz) the signal amplitude is amplified (under damped) by about 1% only and the phase delay is about 5-6 degrees, or 7ms, or about ¼ of the frame time interval. For the 4th harmonic (10Hz)(at 4 times the HR frequency), where still 2-3% of the signal energy is present in the energy spectrum, the signal amplitude is amplified by about 20% and the phase delay is 25-30 degrees, or 8ms, or about ¼ of the frame time interval. We therefore conclude that the pressure is measured with sufficient accuracy.

Furthermore, to avoid aliasing of higher frequencies into the low frequency domain, pressure data were filtered with a 2nd order low-pass Butterworth filter (Krohn-Hite Corporation, Brockton, MA, USA) set at the sampling frequency.

Intraventricular volume

During the pressure measurements the ventricle was visualised using video imaging with a stereo microscope (model SV 6, Carl Zeiss, Oberkochen, Germany) and a video camera (model SSC-M370CE, Sony Corporation, Tokyo, Japan). The video images were acquired simultaneously with the analog pressure signal at 50Hz and stored on a PC. Epicardial surface area was calculated from magnified video images displaying the ventricle using a custom-built analysis program (IMAQ Vision, National Instruments, Austin, TX, USA). Ventricular

volume (V) was derived from epicardial area (A) using a simplified ellipsoid geometric model: $V=0.65A^{3/2}$ as described by Keller *et al* [9].

For each clipped and control embryo 2-4 consecutive (baseline) cardiac cycles were analyzed. Furthermore, to evaluate ventricular response to reduced venous return, a fourth order vitelline vein was incised to produce venous hemorrhage, which results in acute preload reduction. The cardiac cycles following hemorrhage were also recorded and subsequently analyzed to derive ventricular pressure-volume relations. By the latter procedure information can be obtained about ventricular contractility (through the end-systolic pressure volume relation) and diastolic stiffness (through the end-diastolic pressure volume relation).

Finally, maximum contraction of the heart with 2M NaCl was induced for determination of ventricular wall volume by video imaging. The solution (1-3μl) was applied directly on the ventricle. Cavity volume was calculated as total volume minus wall volume. We validated this method by a separate study in a set of four embryos at stage 21 in which wall volume obtained by video imaging was compared with wall volume obtained by the counting method of Cavalieri, detailed by Gundersen and Jensen [18]. The wall volume of the ventricles was determined after 2M NaCl application by video imaging, directly followed by fixation with 4% paraformaldehyde in 0.1M phosphate buffer. The hearts were embedded in paraffin, serially sectioned at 5-μm thickness, and stained with hematoxylin-eosin for stereologic examination. The number of points on a grid hitting 15 sections of the ventricle was counted. The first section was taken randomly and the other sections were taken systematically. From the counted numbers, the volumes could be calculated by Cavalieri's formula:

$V = \Sigma P . M^{-2} . a . d$, where V is the volume in mm^3 , ΣP is the total number of counted points on the 15 sections, M the magnification, a is the point area in mm^2 , and d is the distance between the counted sections in mm.

The mean ventricular wall volume obtained by video imaging was 0.171 ± 0.009μl and mean myocardial wall volume obtained by Cavalieri's method was 0.157 ± 0.010μl, which means that ventricular wall volume is overestimated by 8.9%. Therefore, we conclude that the video imaging procedure correlates well with stereologically obtained volumes and we chose not to correct for this overestimation in the calculations.

Calculations

All data were interpolated using a natural spline function (LabVIEW 6.0, National Instruments, Austin, TX, USA). Data analysis and calculations were performed using custom-made software (Circlab, Leiden University Medical Center, Leiden, the Netherlands). For

each variable the mean value of 2-4 consecutive cardiac cycles was calculated. Pressure and volume data were plotted as pressure-volume loops (Fig. 3). End-systole is represented by the upper-left corner of the pressure-volume loops and was defined as the moment in the cardiac cycle with the maximum instantaneous pressure to volume ratio or time-varying elastance $E(t)$ = $P(t)/[V(t)-Vd]$ [19]. Vd represent volume at zero pressure and was determined using an iterative approach as described by Kono *et al* [20].

The lower-right corner of the pressure-volume loop represents end-diastole as the onset of ventricular contraction and was defined as the point at which the first derivative of the pressure waveform rose sharply from baseline. End-systolic and end-diastolic ventricular pressures and volumes (ESP, EDP, mmHg; ESV, EDV, µl) were determined as the instantaneous values $P(t)$ and, respectively, $V(t)$ at these time-points. Heart rate (HR, bpm) was calculated from the beat-to-beat cycle length. Stroke volume (SV, µl) was calculated as the difference between EDV and ESV. Cardiac output (CO, µl/min) was calculated as HR multiplied by SV. Ejection fraction (EF, %) was determined by SV divided by EDV. Stroke work (SW, µl·mmHg) was calculated as the area of the pressure-volume loop. The maximum and minimum first derivatives of pressure were determined (dP/dt_{MAX}, dP/dt_{MIN}, mmHg/s). Peak filling rate (PFR, µl/s) and peak ejection rate (PER, µl/s) were identified as the maximum and minimum first derivatives of ventricular volume with respect to time ($dV(t)/dt$). The relaxation time constant Tau (τ, ms) was calculated as the time-constant of mono-exponential pressure decay during isovolumic relaxation. The isovolumic period was defined as the time-period between the moment of dP/dt_{MIN} and the time-point at which $dP(t)/dt$ reached 10% of dP/dt_{MIN} [21]. In addition we calculated pressure-half-time (PHT, ms) as the time-interval between the moment of dP/dt_{MIN} and the moment that pressure has dropped to 50% of the instantaneous pressure at the moment of dP/dt_{MIN}.

In addition to these steady state indices we employed the baseline pressure-volume loops combined with loops obtained after venous hemorrhage to determine systolic and diastolic pressure-volume relationships as load-independent measures of systolic and diastolic ventricular function. Systolic function was characterized by end-systolic elastance (E_{ES}, mmHg/µl), which is the linear slope of the end-systolic pressure-volume relation (ESPVR) (Fig. 4). Also the position of the ESPVR defined as the volume-intercept at 2mmHg (ESV_2, µl) was determined in order to quantify the volume-intercept at a physiological pressure, rather than at pressure equals zero [22].

Diastolic ventricular function was determined by calculating diastolic stiffness (E_{ED} mmHg/μl) as the slope of the end-diastolic pressure-volume relation (EDPVR): $EDP = a + E_{ED} \cdot EDV$ [23].

Statistical analysis

Data are presented as mean ± SEM. For comparison of the clipped embryos with control embryos unpaired *t* tests were performed using SPSS 10.1 software (SPSS Inc, Chicago, IL, USA). When Levene's test showed inhomogeneity of variance or when the data were not normally distributed according to the Shapiro-Wilk test, a log (ln) transformation was performed before testing group differences [24]. Values *p*<0.05 were considered statistically significant.

Results

Steady state hemodynamic parameters were determined from baseline pressure and volume signals and corresponding pressure-volume loops as depicted in Figure 3. Results are summarized in Table 1. and do not reveal any significant difference between clipped and control embryos.

Figure 4. shows representative pressure-volume loops from a clipped and a control embryo. The grey lines represent loops at baseline, whereas the black lines are loops obtained after hemorrhage induced by incision of a fourth order vitelline vein. End-systolic and end-diastolic pressure-volume points are marked and the resulting pressure-volume relations are indicated. Note that, compared to the control embryo, in the clipped embryo the ESPVR was less steep indicating reduced contractility, whereas the EDPVR was steeper indicating increased diastolic stiffness (reduced compliance). The summarized results are shown in Table 2. and show a significantly reduced contractility ($p=0.037$) in the clipped embryos indicated by a 52% reduction in E_{ES}. Diastolic stiffness tended to be increased in the clipped embryos as indicated by the 64% increase in E_{ED}, however the difference did not reach statistical significance ($p=0.103$). Ventricular wall volume was obtained after application of 2M NaCl and was not significantly different between the clipped and control embryos ($0.195\pm0.013\mu l$ vs. $0.181\pm0.017\mu l$, NS).
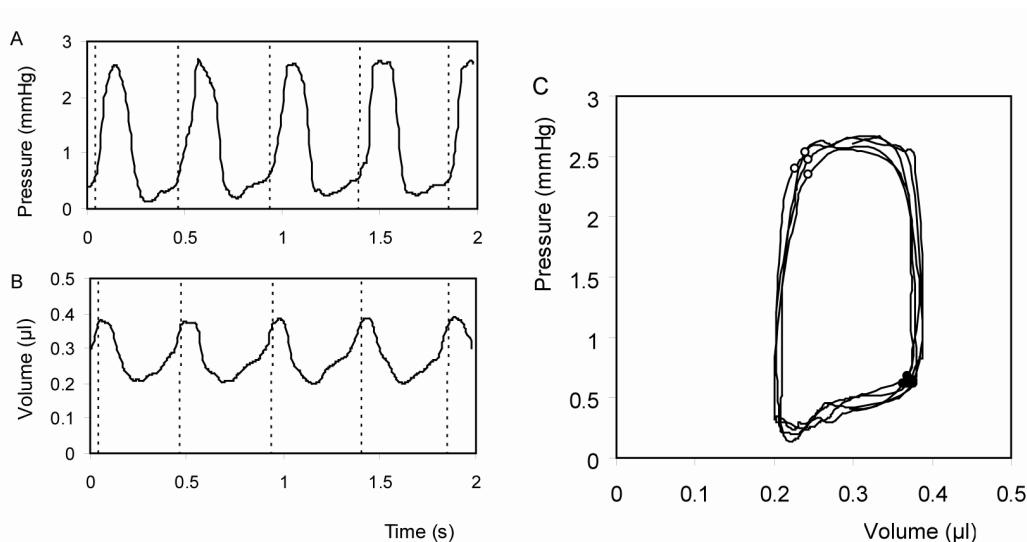
Figure 3. Representative stage 21 baseline pressure-volume loops (C) built up from simultaneously acquired pressure (A) and volume data (B). Solid circles depict end-diastolic points, and open circles depict end-systolic points (C). Also end-diastolic points are represented by dotted lines in panels A and B.

Table 1. Hemodynamic parameters derived from baseline pressure-volume loops at stage 21.

	Clip (n=11)	Control (n=10)
HR (bpm)	131±2	140±5
ESP (mmHg)	2.20±0.07	2.14±0.13
EDP (mmHg)	0.84±0.05	0.71±0.06
dP/dt_{MAX} (mmHg/s)	41.3±1.8	37.8±2.6
dP/dt_{MIN} (mmHg/s)	-43.2±2.7	-40.0±3.3
ESV (µl)	0.20±0.02	0.20±0.02
EDV (µl)	0.41±0.02	0.41±0.02
SV (µl)	0.25±0.02	0.24±0.01
CO (µl/min)	32.2±2.3	32.6±1.3
EF (%)	59.3±3.0	57.7±2.5
SW (µl•mmHg)	0.44±0.03	0.42±0.03
PFR (µl/s)	3.17±0.36	3.55±0.40
PER (µl/s)	-4.33±0.39	-4.11±0.42
Tau (ms)	31.41±3.16	39.02±6.20
PHT (ms)	22.67±1.66	25.43±4.54

Values are means ± SEM. None of the parameters were significantly different between clipped and control embryos. dP/dt_{MIN}, PER, Tau and PHT were not normally distributed. Consequently t-tests were performed after log transformation (using absolute values for dP/dt_{MIN} and PER) as described in the methods section.

Table 2. End-systolic ventricular elastance (E_{ES}), end-diastolic ventricular stiffness (E_{ED}) and ESV at P=2mmHg obtained from pressure-volume relations.

	Clip (n=11)	Control (n=10)
E_{ES} (mmHg/µl)	5.68±0.85*	11.76±2.70
E_{ED} (mmHg/µl)	2.74±0.56	1.67±0.21
ESV_2 (µl)	0.16±0.02	0.18±0.01

Values are means ± SEM. * $p < 0.05$. E_{ES}, E_{ED} and ESV_2 demonstrated inhomogeneity of variances. Therefore, a log (ln) transformation was performed prior to performing t-tests.

Figure 4. Representative pressure-volume loops of a clipped and a control embryo at stage 21. Both baseline-loops (grey lines) and loops after venous hemorrhage (black lines) are depicted of a clipped (A) and control embryo (B). The end-systolic points (open circles) and end-diastolic p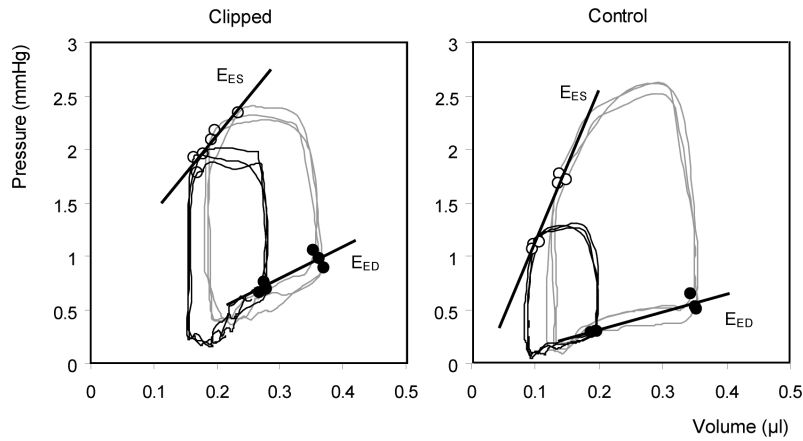oints (solid circles) were determined and were used to assess the end-systolic pressure-volume relation (ESPVR) and end-diastolic pressure-volume relation (EDPVR). From these relations the end-systolic elastance (E_{ES}) and the end-diastolic stiffness (E_{ED}) were obtained, which are defined by the slopes of both relations, respectively

Discussion

The venous clip model is an intervention model for the chick embryo, in which permanent obstruction of the right lateral vitelline vein temporarily reduces the mechanical load on the embryonic myocardium and induces a spectrum of outflow tract anomalies, e.g. double outlet right ventricle, dextroposition of the aorta, and ventricular septal defects. The same types of anomalies can be present in humans. There is an intricate relationship between hemodynamics and cardiac morphogenesis. Pressure-volume loop analysis enables determination of end-systolic elastance and end-diastolic stiffness of the developing ventricle. These parameters represent intrinsic myocardial properties and are relatively independent of loading conditions. The use of pressure-volume loop analysis in early stages of development could contribute to a better understanding of the relationship between cardiac function and morphogenesis during normal and abnormal cardiac development.

The cardiac cycle consists of four distinct phases: the isovolumic contraction phase, the ejection phase, the isovolumic relaxation phase and diastolic filling phase. Parameters that reflect the first two phases are dP/dt_{MAX} (isovolumic contraction phase), and cardiac output, ejection fraction, stroke work, and end-systolic elastance (ejection phase). From these parameters only the end-systolic elastance was significantly changed in the clipped embryos. This may reflect the high sensitivity of this load-independent parameter of contractility compared to the other parameters that are also changed by alterations in pre- and afterload.

The reduced end-systolic elastance indicating reduced contractile state can be explained by observations of Hogers *et al* [25]. They observed less developed ventricles after venous clipping and a delay in cardiac looping. They did not observe normal embryos between stage 19 and 23 after clipping. All embryos displayed cardiovascular malformations. They found that stages 22-24 are critical for survival. A mortality rate between 10 and 22% is described. At later stages of development approximately 64% of the embryos displayed cardiac malformations [4]. Normally, myocardial contraction force increases with development [5,26-29]. After clipping ventricular contractility development may lag behind as a consequence of impaired cardiac development. Mechanical load regulates ventricular growth [30,31]. Venous obstruction temporarily reduces mechanical load on the myocardium and thus probably slows down the ventricular growth and differentiation process [3]. During normal development the ventricular wall volume will increase in size. Since a delay in ventricular development was observed by Hogers *et al.* [25], we would have expected wall volume to be smaller in the clipped embryos. However, after applying 2M NaCl to achieve maximum ventricular contraction, ventricular wall volume was similar between the groups. Potentially the reduced contractility in the clipped embryos limits their maximal contracture leading to an overestimation in wall volume.

The third phase of the cardiac cycle, the active phase of relaxation represented by Tau, reflects the energy consuming process of relaxation. In the mature heart ventricular relaxation rate is an important determinant of the early diastolic pressure-volume relation [32]. There were no significant differences in the active phase of relaxation between the two groups.

The end-diastolic pressure-volume relationship reflects passive relaxation properties of the ventricle, which contribute to the passive relaxation phase during diastolic filling. The relation was quantified by its slope, the end-diastolic stiffness, which was 64% higher in the clipped group. Although this was not a significant difference, this finding suggests reduced compliance after clipping. Myocardial compliance increases with development [9,28,33]. A higher end-diastolic stiffness after venous obstruction may result from impaired cardiac development after clipping. Changes in structure of the ventricular wall may affect the stiffness of the ventricle, especially the addition and organisation of myofibrils may limit cell distensibility [34]. Normally, myofibrils become more organised with development, and assume a more orderly arrangement, presumably parallel to stress lines [5]. After venous obstruction this could be impaired. Next to the organisation of myofibrils, titin is also important for passive stiffness [35]. Titin contains passive spring-like properties that help restore stretched muscle to its resting length [36]. Diastolic pressure results from the tension that develops when

passive myocardium is stretched beyond its slack length. In dogs with tachycardia-induced dilated cardiomyopathy it has been demonstrated that titin isoform ratio changes cause an increase in myocardial stiffness [37]. We speculate that titin isoform expression ratios may have been changed by clipping, causing increased passive stiffness.

Changes in diastolic function may be a critical regulatory pathway during cardiac morphogenesis [34]. Recently Schroder *et al*. found an increase in microtubule density and β-tubulin protein after reduced mechanical load in the stage 27 embryonic heart after left atrial ligation at stage 21 [31]. They observed increased myocardial stiffness in response to reduced mechanical load. They hypothesized that because microtubules mediate the transport of materials necessary for the production of new cellular structures, they may also play a role in mediating the adaptive response of the developing myocardium to altered mechanical load. Since in the venous clip model mechanical load is reduced it could be possible, that changes in microtubule density and organisation caused the tendency of increased diastolic stiffness in the clipped embryos. A decrease in workload may affect the number of contractile units or their function within the myocyte. Recently we observed a reduction in the diastolic passive-filling component of ventricular filling in favor of the active component in clipped embryos at stage 24 [38]. We speculate that a stiffer ventricular wall causes this decrease in passive filling, which is compensated by the active contraction of the atrium. It seems that at stage 21 the ventricle is just starting to become stiffer.

Study limitations:

There are several limitations to the present study. Like Tobita and Keller [29,39] we assumed that the embryonic ventricle is a thick-walled ellipsoidal shell with a fixed ratio of semiminor and semimajor axis diameter during systole. This could lead to error in the calculation of ventricular wall volume and cavity volume.

As demonstrated by our study in which the calculation of ventricular wall volume and assessing cavity volume was compared to volumes obtained by Cavalieri 's method, there is a overestimation of ventricular wall volume by 8.9%. In theory this means that cavity volumes are underestimated by about 0.016-0.017μL. Since this represents, even for the smallest volumes (mean end-systolic volume was 0.20μL), only about 8.7% of cavity volume we chose not to correct for this factor. Furthermore since this would cause a rightward shift of the entire pressure-volume loops, it has no consequences for the slopes of the pressure-volume relations.

We considered trabecular spaces to be part of the wall. These spaces do not close completely after application of 2M NaCl, but for the calculation of ventricular volume this is not very important. These spaces are present during both diastole and systole. This results in a slight overestimation of total volumes throughout the cardiac cycle. Therefore, when wall volume is subtracted from the total volumes this overestimation is cancelled out. Any remaining trabecular space volume can be considered dead volume, as this blood does not contribute to cardiac output.

Because we only obtained pressure and volume data before and after hemorrhage and not during this preload reduction we chose linear relationships to describe the ESPVR and EDPVR. This may have influenced our results, but since the pressure-volume relations were based on only two conditions (rather than on data acquired continuously during preload reduction) there was no justification for applying a non-linear fit. Possible non-linearities might have been detected when the ESPVR had been determined over a wider pressure range. However, systolic pressure was similar in both groups, thus comparison of E_{ES} between groups is unlikely to be importantly affected by a pressure-dependent non-linearity.

There were distinct differences in variances of the E_{ES} and E_{ED} between the clipped and control embryos before log (ln) transformation. Several factors may be involved. The chick embryos are not genetically identical, this could cause biological variability. Also the clipping experiment could have been partially successful, which could affect the outcome. There could have been some influence of the extent of hemorrhage. In theory, loading conditions do not influence the end-systolic pressure-volume relation or the end-diastolic pressure-volume relation. However, in the small chick embryo this might be different. Also the position of the embryo and/or micropipette could have been changed during the incision of a fourth order vitelline vein. This could have caused some variation as well. Furthermore, temperature differences could have influenced the measurements as time to insert the micropipette into the ventricle varied between experiments. However, whereas these effects may increase within-group variability, they would not be expected to systematically affect the differences between the groups.

Because of the necessity to end the experiments with the use of 2M NaCl it was impossible to obtain good histological examinations of the measured embryonic hearts. Therefore, we compared our results with scanning electron microscope and histological findings of Hogers *et al.*, who developed the venous clip model. Any existing discrepancies in morphological findings between our data and those of Hogers *et al.* could therefore not be detected.

In summary, development of ventricular function in the embryonic heart is affected by mechanical load. Pressure-volume loop analysis shows that one day after venous obstruction the clipped embryo has a reduced contractility compared to stage-matched control embryos. The morphological correlates of these findings require further study. Pressure-volume analysis may be applied in the chick embryo and is a sensitive technique to detect subtle alterations in ventricular function.

4.2 Impaired systolic and diastolic ventricular function after permanent extra-embryonic venous obstruction, a pressure-volume loop assessment in the stage 24-chick embryo

In preparation

Summary

Fluid mechanical forces affect cardiac development. In the chick embryo, permanent obstruction of the right lateral vitelline vein reduces the mechanical load on the embryonic myocardium, which has been shown to induce a spectrum of outflow tract anomalies. Insight into the effects of this intervention on the mechanical function of the developing myocardium could contribute to a better understanding of the relationship between hemodynamics and cardiac morphogenesis.

Cardiac pressure-volume relations enable a load-independent quantification of intrinsic ventricular systolic and diastolic properties. We determined ventricular function by pressure-volume loop analysis of *in-ovo* chick embryos (n=15) at stage 24 (4.5 days of incubation) after venous obstruction at stage 17. Control embryos (n=15) were used for comparison.

End-systolic volume was significantly higher in clipped embryos ($0.36 \pm 0.02 \mu l$ vs. $0.29 \pm 0.02 \mu l$, *p*=0.002). End-systolic pressure and end-diastolic pressure were also increased as compared to control animals (2.93 ± 0.07mmHg vs. 2.70 ± 0.08mmHg, p=0.036 and 1.15 ± 0.06mmHg vs. 0.82 ± 0.05mmHg, p<0.001). No significant differences were demonstrated for other baseline hemodynamic parameters.

Analysis of pressure-volume relations showed a significantly lower end-systolic elastance in the clipped embryos (E_{ES}, slope of end-systolic pressure-volume relation: 2.91 ± 0.24 vs. 7.53 ± 0.66mmHg/μl, p<0.005) indicating reduced contractility. Diastolic stiffness was significantly increased in the clipped embryos (E_{ED}, slope of end-diastolic pressure-volume relation: 1.54 ± 0.21vs 0.60 ± 0.08, p<0.005), indicating reduced compliance.

We conclude that venous obstruction interferes with normal myocardial development resulting in impaired intrinsic systolic and diastolic ventricular function. These changes in ventricular function may precede morphological derangements in later developmental stages.

Introduction

Human cardiac development takes place within the first 10 weeks of pregnancy. Despite technological advancements in ultrasonography we are still unable to adequately visualize the embryonic heart this early in gestation. Therefore, animal models are required to study *in-vivo* embryonic cardiovascular development. The chick embryo is an attractive model because it enables direct visualization of the heart and its cardiac development is comparable to that of mammalian embryos [40].

Recent studies indicate that cardiac morphogenesis depends on the interaction between genetics and epigenetic influences like fluid mechanical forces [16]. We previously developed an intervention model for the chick embryo (the venous clip model) in which intracardiac blood flow patterns and mechanical load on the embryonic myocardium are altered, leading to a spectrum of outflow tract anomalies [3,4] As blood flow is acutely decreased for up to 5 hrs after clipping at stage 17 [3,8], this model supports the hypothesis that alterations in shear stress play an important role in the development of cardiac anomalies presumably through shear stress responsive gene expression.

Insight into the effects of this intervention on the mechanical function of the developing myocardium could contribute to a better understanding of the relationship between hemodynamics and cardiac morphogenesis. Previous studies described that venous clipping can influence systolic and diastolic ventricular function. Using pressure-volume loop analysis we demonstrated the presence of a less contractile ventricle one day after clipping (HH21)[41]. Furthermore, 2 days after clipping (HH24), we showed that diastolic ventricular filling is disturbed using simultaneous Doppler measurements of the dorsal aorta and atrioventricular canal [38].

In the present study we explored the effects of clipping on intrinsic systolic and diastolic ventricular function at stage 24, 2 days after venous obstruction. Pressure-volume loop analysis of the embryonic chick heart was performed using a custom-made workstation to simultaneously measure intraventricular pressure and capture video images of the beating ventricle for ventricular volume assessment.

Materials and Methods

Animals and venous clip procedure

Fertilized white Leghorn chick eggs (*Gallus gallus* (L.)) were obtained from Charles River Laboratories (Extertal, Germany) and were incubated at 37-38°C, with the blunt end up and at a relative humidity of 70-80%. The embryos were exposed by creating a window in the shell and removing the overlying membranes. Thirty embryos of stage 17 that showed no bleeding or deformities were selected. The material was subdivided into venous clipped embryos (n=15), in which the right vitelline vein was obstructed with an aluminum microclip, and control embryos (n=15). A more detailed description of this procedure has been published previously [3]. During the experiments the egg was placed on a thermo element of 37°C. After the intervention the window in the shell was resealed with tape. Experiments were approved by the Animal Experimentation Review Board of the Erasmus MC and were performed in accordance with Dutch Law for animal experimentation.
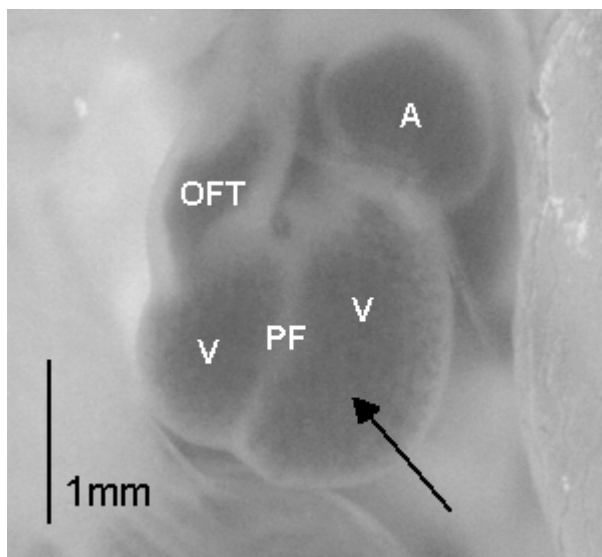
Figure 1. Frontal view of embryonic chick heart at stage 24 (4.5 days of incubation).
A, atrium; V, ventricle; PF, primary fold; OFT, outflow tract. The future right and left ventricle are functioning as one ventricle at this developmental stage. Therefore, we used the entire ventricular area to determine volume. The ventricle was punctured with the glass micropipette in the area indicated by the arrow.

Intraventricular pressure

Embryos were reincubated until stage 24 (4.5 days of incubation). After removing the tape, the embryo was gently turned towards the left side to obtain a clear frontal view of the ventricle (Fig.1). The thoracic wall was opened using a pair of fine forceps. Blood pressure was measured in the ventricle using a servo-null system (model 900A, World Precision Instruments, Inc., Sarasota, Florida, USA) and a fluid filled (2mol/l NaCl) 5-10μm glass micropipette attached to a microelectrode. Intraventricular pressure was calculated as the difference between the measured pressure and the pressure recorded when the tip of the

pipette was placed in the extra-embryonic fluid adjacent to the ventricular puncture site. Pressure data were sampled at 50Hz and stored on a PC. The working principle of this pressure transducer is described in detail by Heineman [17]. The dynamic response of the system was tested over the frequency range of 0.5-20Hz (as this frequency range is relevant to chicken embryonic heart rate) as published previously and was found to be of sufficient accuracy [41]. Furthermore, to avoid aliasing of higher frequencies into the low frequency domain, pressure data were filtered with a 2nd order low-pass Butterworth filter (Krohn-Hite Corporation, Brockton, MA, USA) set at the sampling frequency.

Ventricular cavity volume

During the pressure measurements the ventricle was visualised using video imaging with a stereo microscope (model SV 6, Carl Zeiss, Oberkochen, Germany) and a video camera (model SSC-M370CE, Sony Corporation, Tokyo, Japan). The video images were captured simultaneously with the analog pressure signal at 50Hz and stored on a PC. Epicardial surface area was calculated from magnified video images displaying the ventricle using a custom-built analysis program (IMAQ Vision, National Instruments, Austin, TX, USA). Total volume (V) was derived from epicardial area (A) using a simplified ellipsoid geometric model: $V=0.65A^{3/2}$ as described by Keller *et al* [9]. Ventricular wall volume was determined using the same approach at the end of each study after induction of maximum ventricular contraction with application of (1-3μl) 2mol/l NaCl directly on the ventricle. Ventricular cavity volume was calculated as total volume minus wall volume.

Experimental protocol

For each embryo 4-5 consecutive baseline cardiac cycles were recorded. Subsequently, a fourth order vitelline vein was incised to produce venous hemorrhage, which results in acute preload reduction. The cardiac cycles following hemorrhage were also recorded and subsequently analyzed to derive systolic and diastolic ventricular pressure-volume relations.

Calculations

Time-dependent pressure and volume signals were interpolated using a natural spline function (LabVIEW 6.0, National Instruments, Austin, TX, USA) and subsequently analyzed using custom-made software (Circlab, Leiden University Medical Center, Leiden, the Netherlands). Pressure and volume data were plotted as pressure-volume loops. End-systole is represented by the upper-left corner of the pressure-volume loops and was defined as the moment in the

cardiac cycle with the maximum instantaneous pressure to volume ratio or time-varying elastance $E(t) = P(t)/[V(t)-Vd]$ [19]. Vd represents volume at zero pressure and was determined using an iterative approach as described by Kono *et al* [20]. The lower-right corner of the pressure-volume loop represents end-diastole as the onset of ventricular contraction and was defined as the point at which the first derivative of the pressure waveform rose sharply from baseline. End-systolic and end-diastolic ventricular pressures and volumes (ESP, EDP; ESV, EDV) were determined as the instantaneous values $P(t)$ and, respectively, $V(t)$ at these time-points. Heart rate (HR) was calculated from the beat-to-beat cycle length. Stroke volume (SV) was calculated as the difference between EDV and ESV. Cardiac output (CO) was calculated as HR multiplied by SV. Ejection fraction (EF) was determined by SV divided by EDV. Stroke work (SW) was calculated as the area of the pressure-volume loop. From the volume signal peak filling rate (PFR) and peak ejection rate (PER) were identified as the maximum and minimum first derivatives of ventricular volume with respect to time (dV/dt). From the pressure signal the maximum and minimum first derivatives of pressure were determined (dP/dt$_{MAX}$, dP/dt$_{MIN}$). The isovolumic relaxation period was defined as the time-period between the moment of dP/dt$_{MIN}$ and the time-point at which dP/dt reached 10% of dP/dt$_{MIN}$ [21]. The relaxation time constant Tau (τ) was calculated as the time-constant of mono-exponential pressure decay during isovolumic relaxation using $P=A+B.exp(-t/tau)$, in which A and B are constants determined by the data [42]. Pressure-half-time (PHT) was calculated as the time-interval between the moment of dP/dt$_{MIN}$ and the moment that pressure has dropped to 50% of the instantaneous pressure at the moment of dP/dt$_{MIN}$. For each parameter the mean value of 4-5 consecutive cardiac cycles was calculated.

In addition to these steady state indices we employed the baseline pressure-volume loops combined with loops obtained after venous hemorrhage to determine systolic and diastolic pressure-volume relationships as load-independent measures of systolic and diastolic ventricular function. Systolic function was characterized by end-systolic elastance (E$_{ES}$), which is the linear slope of the end-systolic pressure-volume relation (ESPVR) (Fig. 2). The position of the ESPVR was defined as the volume-intercept at 2.8mmHg (ESV$_{2.8}$). Diastolic ventricular function was determined by calculating diastolic stiffness (E$_{ED}$) as the slope of the end-diastolic pressure-volume relation (EDPVR): $EDP=c+E_{ED}\cdot EDV$, in which c is a constant [23].

Statistical analysis

Data are presented as mean ± SEM. For comparison of the clipped embryos with control embryos unpaired *t* tests were performed using SPSS 10.1 software (SPSS Inc, Chicago, IL, USA). When data were not normally distributed according to the Shapiro-Wilk test, a log (ln) transformation was performed before testing group differences [24]. Values *p*<0.05 were considered statistically significant.

Results

Steady state hemodynamic parameters were determined from baseline pressure and volume signals and corresponding pressure-volume loops. Results are summarized in Table 1. All parameters were normally distributed except Tau and PHT. These parameters were transformed prior to statistical testing. ESV was significantly higher in clipped embryos ($0.36\pm0.02\mu l$ vs. $0.29\pm0.02\mu l$, $p=0.002$). Also ESP and EDP were increased as compared to control animals (2.93 ± 0.07mmHg vs. 2.70 ± 0.08mmHg, p=0.036 and 1.15 ± 0.06mmHg vs. 0.82 ± 0.05mmHg, p<0.001). All other baseline parameters demonstrated no significant differences.

Figure 2. shows representative pressure-volume loops from a clipped and a control embryo. The black loops represent baseline, whereas the grey loops were obtained after hemorrhage induced by incision of a fourth order vitelline vein. End-systolic and end-diastolic pressure-volume points are marked and the resulting end-systolic and end-diastolic pressure-volume relations are indicated. Note that, compared to the control embryo, in the clipped embryo the ESPVR was less steep indicating reduced contractility, whereas the EDPVR was steeper indicating increased diastolic stiffness (reduced compliance).
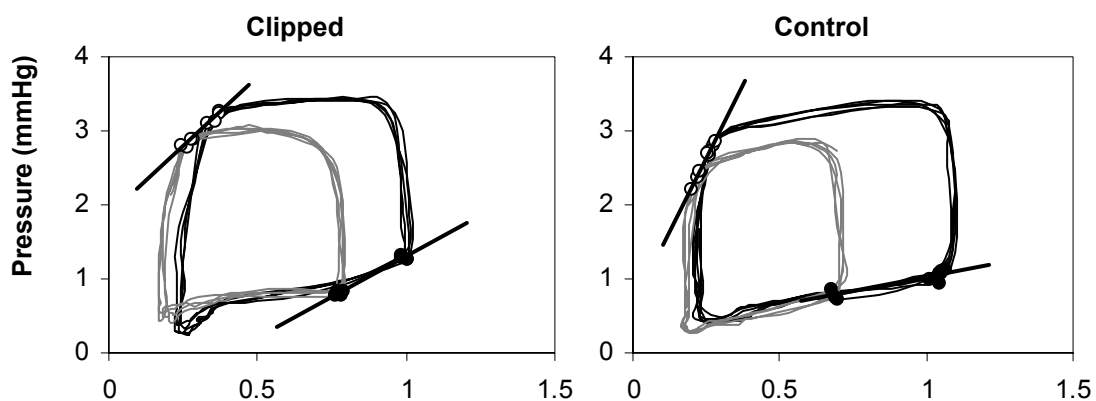
Figure 2. Representative pressure-volume loops of a clipped and a control embryo at stage 24. Both baseline-loops (black) and loops after venous hemorrhage (grey) are depicted of a clipped (A) and control embryo (B). The end-systolic points (open circles) and end-diastolic points (solid circles) were determined and were used to assess the end-systolic pressure-volume relation (ESPVR) and end-diastolic pressure-volume relation (EDPVR). From these relations the end-systolic elastance (E_{ES}) and the end-diastolic stiffness (E_{ED}) were obtained, which are defined by the slopes of both relations, respectively.

The summarized results are presented in Table 2. and show a significantly reduced contractility ($p<0.001$) in the clipped embryos indicated by a 61% reduction in E_{ES}. Diastolic stiffness was increased in the clipped embryos as indicated by 157% increase in E_{ED}, ($p<0.001$).

Ventricular wall volume was obtained after application of 2mol/l NaCl and was not significantly different between the clipped and control embryos (0.809±0.037µl vs. 0.783±0.046µl, NS).

Table 1. Hemodynamic parameters derived from baseline pressure-volume loops at stage 24.

	Clip (n=15)	Control (n=15)
HR (bpm)	160±4	164±3
ESP (mmHg)	2.93±0.07*	2.70±0.08
EDP (mmHg)	1.15±0.06*	0.82±0.05
dP/dt_{MAX} (mmHg/s)	64.8±3.1	69.3±3.5
dP/dt_{MIN} (mmHg/s)	-52.0±2.7	-52.9±2.1
ESV (µl)	0.36±0.02*	0.29±0.02
EDV (µl)	0.97±0.03	0.91±0.04
SV (µl)	0.72±0.03	0.69±0.04
CO (µl/min)	115±4	112±7
EF (%)	74.3±1.8	74.7±1.6
SW (µl•mmHg)	1.66±0.07	1.62±0.11
PFR (µl/s)	14.9±0.8	13.6±0.9
PER (µl/s)	-12.0±0.5	-11.4±0.8
Tau (ms)	27.4±1.9	27.4±1.8
PHT (ms)	18.2±1.0	17.8±0.8

Values are means ± SEM.* p<0.05. Tau and PHT were not normally distributed. Consequently t-tests were performed after a log (ln) transformation as described in the methods section.

Table 2. End-systolic ventricular elastance (E_{ES}), end-diastolic ventricular stiffness (E_{ED}) and ESV at P=2.8mmHg obtained from pressure-volume relations.

	Clip (n=15)	Control (n=15)
E_{ES} (mmHg/µl)	2.91±0.24*	7.53±0.66
E_{ED} (mmHg/µl)	1.54±0.21*	0.60±0.08
$ESV_{2.8}$ (µl)	0.31±0.02	0.30±0.01

Values are means ± SEM. * $p < 0.005$. E_{ED} was not normally distributed. Therefore, a log (ln) transformation was performed prior to performing t-tests.

Discussion

Pressure-volume analysis has been widely used in both human and animal studies [10-12]. Only a few studies have been conducted during embryonic or fetal development; in (near term) fetal lambs and chick embryos [9,13-15]. We used this method to study the impact of early venous obstruction (HH17) on embryonic cardiovascular function in later development. The venous clip model is an intervention model for the chick embryo, in which permanent obstruction of the right lateral vitelline vein temporarily reduces the mechanical load on the embryonic myocardium and induces a spectrum of outflow tract anomalies, e.g. double outlet right ventricle, dextroposition of the aorta, and ventricular septal defects [4]. The same types of anomalies can be found in humans.

The findings of the present study extend the results that we obtained in a younger developmental stage, at HH21 [41]. The end-systolic elastance was already significantly lower (52% reduction) at stage 21 and this is even more pronounced at stage 24 (61% reduction). This indicates that the disturbed ventricular function is not repaired, but there seems to be an ongoing process that results in a less contractile ventricle. At stage 21 the diastolic stiffness tended to be higher, however this was not significant. At stage 24, we demonstrated aggravation of the process causing a stiffer ventricular wall, as well as a significantly increased diastolic stiffness, leading to a less compliant ventricle. As the embryonic ventricle is relatively non-compliant and compliance increases during development [9,28,33], our data suggest that this process lags behind after venous clipping.

Both the decreased end-systolic elastance and the increased end-diastolic stiffness are in line with observations made by Hogers *et al* [25]. They observed less developed ventricles after venous clipping and a delay in cardiac looping. Between stage 19 and 23 all embryos displayed cardiovascular malformations. Furthermore, they found that stages 22-24 are critical for survival, with a mortality rate up to 22%. Mechanical load regulates ventricular growth [30,31]. Venous obstruction temporarily reduces mechanical load on the myocardium and thus probably slows down the ventricular growth and differentiation process, leading to decreased end-systolic elastance and increased end-diastolic stiffness. Recently, we also observed changes in ventricular diastolic filling in stage 24 using simultaneous Doppler measurements of the dorsal aorta and atrioventricular canal. We found a reduced diastolic passive-filling component of ventricular filling, which was compensated by an increased active-filling component in clipped embryos at stage 24 [38]. The findings of the current study support our hypothesis that a stiffer ventricular wall causes this decrease in passive filling, which is compensated by increased atrial contraction.

The changes in intrinsic characteristics of the ventricle also caused elevation of the ESV, ESP, and EDP. Probably these elevations result from adaptation of the embryonic ventricle in order to maintain cardiac output at an adequate level to assure steady blood supply to all organs. To meet the demands of the growing embryo cardiac output increases during normal development [6,7]. The increase in dorsal aortic blood flow parallels embryonic growth, and this suggests that cardiac output and metabolic demands are coupled through feedback mechanisms [6].

Alterations in hemodynamics can precede the onset of structural defects [43]. The venous clip procedure causes changes in intracardiac blood flow patterns and decreased dorsal aortic blood volume flow, eventually leading to a spectrum of outflow tract anomalies [4]. Alterations in blood volume flow influence the shear stress on the vessel wall [44]. During normal cardiac development, cardiac performance increases [1,5] and results in gradually increasing shear stress that either induces or represses the expression of shear stress responsive genes in the endothelium and/or endocardium [45,46]. In vitro studies have demonstrated that especially changes in shear stress cause alterations in gene expression [47]. After venous obstruction blood volume flow is acutely decreased [3]. Therefore, it is possible that alterations in shear stress are involved in the development of cardiac anomalies after venous clipping. Recently our group demonstrated developmental stage-related cardiovascular expression of the transcription factor KLF-2 (Krüppel-like factor-2), ET-1 (endothelin-1) and NOS-3 (nitric oxide synthase-3), which are shear stress responsive genes [48]. Especially the ET-1 pathway seems to be important in cardiovascular development. ET-1 knockout mice demonstrate a spectrum of cardiovascular malformations, which strongly resemble those seen in our venous clip model [49]. This finding suggests that the endothelin cascade is important in heart development and might be involved in the development of the malformations induced by venous clipping.

The question as to how the ET-1 pathway could be responsible for the impaired ventricular function at stage 21 and 24 remains to be answered. Our group is currently working on ET-1 expression patterns in the embryonic heart after venous obstruction. ET-1 expression seems to be decreased in certain areas of the heart after venous clipping (unpublished data). We assume that the changes in intra-cardiac blood flow patterns leading to shear stress changes as described by Hogers *et al*. are responsible for this observation [4]. We speculate that this impairment of the ET-1 pathway causes the functional changes, observed in this study.

There are several limitations to the present study. Like Tobita and Keller [29,39] we assumed that the embryonic ventricle is a thick-walled ellipsoidal shell with a fixed ratio of semi minor and

semi major axis diameter during systole. This could lead to error in the calculation of ventricular wall volume and cavity volume.

We considered trabecular spaces to be part of the wall. These spaces do not close completely after application of 2mol/l NaCl, but for the calculation of ventricular volume this is not very important. These spaces are present during both diastole and systole. This results in a slight overestimation of total volumes throughout the cardiac cycle. Therefore, when wall volume is subtracted from the total volumes this overestimation is cancelled out. Any remaining trabecular space volume can be considered dead volume, as this blood does not contribute to cardiac output.

Because we only obtained pressure and volume data before and after hemorrhage and not during this preload reduction we chose linear relationships to describe the ESPVR and EDPVR. This may have influenced our results, but since the pressure-volume relations were based on only two conditions (rather than on data acquired continuously during preload reduction) there was no justification for applying a non-linear fit. Possible non-linearities might have been detected when both relations would have been determined over a wider pressure range.

Because of the necessity to end the experiments with the use of 2mol/l NaCl it was impossible to obtain good histological examinations of the measured embryonic hearts. Therefore, we compared our results with scanning electron microscope and histological findings of Hogers *et al*., who developed the venous clip model. Although not expected, possible discrepancies in morphological findings between our data and those of Hogers *et al*. could therefore not be detected.

Considering these limitations, however we have no reason to assume that potential errors are different for the control and experimental groups.

In summary, development of ventricular function in the embryonic heart is affected by mechanical load. Pressure-volume loop analysis shows that two days after venous obstruction clipped embryos have reduced contractility and increased diastolic stiffness compared to stage-matched control embryos. Therefore, we conclude that venous obstruction interferes with normal myocardial development resulting in adverse effects on intrinsic systolic and diastolic ventricular function. These changes in ventricular function may precede morphological derangements in later developmental stages.

Acknowledgements

4.3 References

1. Clark EB, Hu N. Developmental hemodynamic changes in the chick embryo from stage 18 to 27. *Circ Res*. 1982;51:810-815.

2. Nakazawa M, Miyagawa S, Ohno T, Miura S, Takao A. Developmental hemodynamic changes in rat embryos at 11 to 15 days of gestation: normal data of blood pressure and the effect of caffeine compared to data from chick embryo. *Pediatr Res*. 1988;23:200-205.

3. Stekelenburg-De Vos S, Ursem NT, Hop WC, Wladimiroff JW, Gittenberger-De Groot AC, Poelmann RE. Acutely altered hemodynamics following venous obstruction in the early chick embryo. *J Exp Biol*. 2003;206:1051-1057.

4. Hogers B, DeRuiter MC, Gittenberger-de Groot AC, Poelmann RE. Unilateral vitelline vein ligation alters intracardiac blood flow patterns and morphogenesis in the chick embryo. *Circ Res*. 1997;80:473-481.

5. Clark EB, Hu N, Dummett JL, Vandekieft GK, Olson C, Tomanek R. Ventricular function and morphology in chick embryo from stages 18 to 29. *Am J Physiol*. 1986;250:H407-H413.

6. Hu N, Clark EB. Hemodynamics of the stage 12 to stage 29 chick embryo. *Circ Res*. 1989;65:1665-1670.

7. Broekhuizen MLA, Mast F, Struijk PC, Bie van der W, Mulder PGH, Gittenberger-De Groot AC, Wladimiroff JW. Hemodynamic parameters of stage 20 to stage 35 chick embryo. *Pediatr Res*. 1993;34:44-46.

8. Hamburger V, Hamilton HL. A series of normal stages in the development of the chick embryo. *J Morphol*. 1951;88:49-92.

9. Keller BB, Tinney JP, Hu N. Embryonic ventricular diastolic and systolic pressure-volume relations. *Cardiol Young*. 1994;4:19-27.

10. Kass DA, Yamazaki T, Burkhoff D, Maughan WL, Sagawa K. Determination of left ventricular end-systolic pressure-volume relationships by the conductance (volume) catheter technique. *Circulation*. 1986;73:586-595.

11. Teitel DF, Klautz R, Steendijk P, van der Velde ET, van Bel F, Baan J. The end-systolic pressure-volume relationship in the newborn lamb: effects of loading and inotropic interventions. *Pediatr Res*. 1991;29:473-482.

12. Georgakopoulos D, Mitzner WA, Chen CH, Byrne BJ, Millar HD, Hare JM, Kass DA. In vivo murine left ventricular pressure-volume relations by miniaturized conductance micromanometry. *Am J Physiol*. 1998;274:H1416-H1422.

13. Lewinsky RM, Szwarc RS, Benson LN, Ritchie JW. The effects of hypoxic acidemia on left ventricular end-systolic elastance in fetal sheep. *Pediatr Res*. 1993;34:38-43.

14. Weil SR, Russo PA, Hechman JL, Balsara RK, Pasiecki V, Dunn JM. Pressure-volume relationschip of the fetal lamb heart. *Ann Thorac Surg*. 1993;55:470-475.

15. Keller BB, Yoshigi M, Tinney JP. Ventricular-vascular uncoupling by acute conotruncal occlusion in the stage 21 chick embryo. *Am J Physiol*. 1997;273:H2861-H2866.

16. Hove JR, Koster RW, Forouhar AS, Acevedo-Bolton G, Fraser SE, Gharib M. Intracardiac fluid forces are an essential epigenetic factor for embryonic cardiogenesis. *Nature*. 2003;421:172-177.

17. Heineman FW, Grayson J. Transmural distribution of intramyocardial pressure measured by micropipette technique. *Am J Physiol*. 1985;249:H1216-1223.

18. Gundersen HJ, Jensen EB. The efficiency of systematic sampling in stereology and its prediction. *J Microsc*. 1987;147 (Pt 3):229-63.

19. Sagawa K, Maughan L, Suga H, Sunagawa K. *Cardiac contraction and the pressure-volume relationship*. New York: Oxford University Press; 1988:36-39.

20. Kono A, Maughan WL, Sunagawa K, Hamilton K, Sagawa K, Weisfeldt ML. The use of left ventricular end-ejection pressure and peak pressure in the estimation of the end-systolic pressure-volume relationship. *Circulation*. 1984;70:1057-1065.

21. Leeuwenburgh BP, Steendijk P, Helbing WA, Baan J. Indexes of diastolic RV function: load dependence and changes after chronic RV pressure overload in lambs. *Am J Physiol Heart Circ Physiol*. 2002;282:H1350-H1358.

22. Steendijk P, Baan J, Jr., Van der Velde ET, Baan J. Effects of critical coronary stenosis on global systolic left ventricular function quantified by pressure-volume relations during dobutamine stress in the canine heart. *J Am Coll Cardiol*. 1998;32:816-26.

23. Pak PH, Maughan L, Baughman KL, Kass DA. Marked discordance between dynamic and passive diastolic pressure- volume relations in idiopathic hypertrophic cardiomyopathy. *Circulation*. 1996;94:52-60.

24. Bland JM, Altman DG. Transforming data. *BMJ*. 1996;312:770.

25. Hogers B, Gittenberger-de Groot AC, DeRuiter MC, Mentink MMT, Poelmann RE. Cardiac inflow malformations are more lethal and precede cardiac outflow malformations. Chick embryonic venous clip model. In: Hogers B, ed. *The role of blood flow in normal and abnormal heart development*. Wageningen: Ponsen & Looijen BV; 1998:79-100.

26. Nakanishi T, Seguchi M, Takao A. Development of the myocardial contractile system. *Experientia*. 1988;44:936-944.

27. Godt RE, Fogaca RT, Nosek TM. Changes in force and calcium sensitivity in the developing avian heart. *Can J Physiol Pharmacol*. 1991;69:1692-1697.

28. Anderson PA. The heart and development. *Semin Perinatol*. 1996;20:482-509.

29. Tobita K, Keller BB. Maturation of end-systolic stress-strain relations in chick embryonic myocardium. *Am J Physiol Heart Circ Physiol*. 2000;279:H216-H224.

30. Clark EB, Hu N, Frommelt P, Vandekieft GK, Dummett JL, Tomanek RJ. Effect of increased pressure on ventricular growth in stage 21 chick embryos. *Am J Physiol*. 1989;257:H55-H61.

31.   Schroder EA, Tobita K, Tinney JP, Foldes JK, Keller BB. Microtubule involvement in the adaptation to altered mechanical load in developing chick myocardium. *Circ Res*. 2002;91:353-359.

32.   Gilbert JC, Glantz SA. Determinants of left ventricular filling and of the diastolic pressure-volume relation. *Circ Res*. 1989;64:827-852.

33.   Friedman WF. The intrinsic physiologic properties of the developing heart. *Prog Cardiovasc Dis*. 1972;15:87-111.

34.   Hu N, Connuck DM, Keller BB, Clark EB. Diastolic filling characteristics in the stage 12 to 27 chick embryo ventricle. *Pediatr Res*. 1991;29:334-337.

35.   Granzier H, Labeit S. Cardiac titin: an adjustable multi-functional spring. *J Physiol*. 2002;541:335-42.

36.   Epstein ND, Davis JS. Sensing stretch is fundamental. *Cell*. 2003;112:147-150.

37.   Wu Y, Bell SP, Trombitas K, Witt CC, Labeit S, LeWinter MM, Granzier H. Changes in titin isoform expression in pacing-induced cardiac failure give rise to increased passive muscle stiffness. *Circulation*. 2002;106:1384-1389.

38.   Ursem NTC, Stekelenburg-de Vos S, Wladimiroff JW, Poelmann RE, Gittenberger-de Groot AC, Hu N, Clark EB. Ventricular diastolic characteristics in stage-24 chick embryos after extra-embryonic venous obstruction. *J Exp Biol*. 2004;207:1487-1490.

39.   Tobita K, Keller BB. End-systolic myocardial stiffness is a load-independent index of contractility in stage 24 chick embryonic heart. *Am J Physiol*. 1999;276:H2102-2108.

40.   Sissman NJ. Developmental landmarks in cardiac morphogenesis: comparative chronology. *Am.J.Cardiol*. 1970;25:141-148.

41.   Stekelenburg-de Vos S, Ursem NT, Wladimiroff JW, Delfos R, Poelmann RE. Systolic and Diastolic Ventricular Function Assessed by Pressure-Volume Loops in the Stage 21 Venous Clipped Chick Embryo. *Pediatr Res*. In press.

42.   Yellin EL, Hori M, Yoran C, Sonnenblick EH, Gabbay S, Frater RW. Left ventricular relaxation in the filling and nonfilling intact canine heart. *Am J Physiol*. 1986;250:H620-629.

43.   Stewart DE, Kirby ML, Sulik KK. Hemodynamic changes in chick embryos precede heart defects after cardiac neural crest ablation. *Circ Res*. 1986;59:545-550.

44.   Goldsmith HL, Turitto VT. Rheological aspects of thrombosis and haemostasis: basic principles and applications. ICTH-Report--Subcommittee on Rheology of the International Committee on Thrombosis and Haemostasis. *Thromb Haemost*. 1986;55:415-435.

45.   Topper JN, Gimbrone MA. Blood flow and vascular gene expression: fluid shear stress as a modulator of endothelial phenotype. *Mol Med Today*. 1999;5:40-46.

46.   Malek AM, Zhang J, Jiang J, Alper SL, Izumo S. Endothelin-1 gene suppression by shear stress: pharmacological evaluation of the role of tyrosine kinase, intracellular calcium, cytoskeleton, and mechanosensitive channels. *J Mol Cell Cardiol*. 1999;31:387-399.

47. Fisher AB, Chien S, Barakat AI, Nerem RM. Endothelial cellular response to altered shear stress. *Am J Physiol Lung Cell Mol Physiol*. 2001;281:L529-533.

48. Groenendijk BC, Hierck BP, Gittenberger-De Groot AC, Poelmann RE. Development-related changes in the expression of shear stress responsive genes KLF-2, ET-1, and NOS-3 in the developing cardiovascular system of chicken embryos. *Dev Dyn*. 2004;230:57-68.

49. Kurihara Y, Kurihara H, Oda H, Maemura K, Nagai R, Ishikawa T, Yazaki Y. Aortic arch malformations and ventricular septal defect in mice deficient in endothelin-1. *J Clin Invest*. 1995;96:293-300.

Chapter 5

Ventricular filling after venous clipping or injection with endothelin-1 and endothelin receptor antagonists

Introductory remarks

Ventricular diastolic filling is an important feature of the ventricle as it determines preload and thus cardiac output. Diastolic filling can be partitioned into a passive filling component and an active filling component. During the passive phase blood flows from the atrium to the ventricle due to the pressure-gradient. Hereafter, active filling is established by atrial contraction. During development the ratio of passive to active filling volume decreases because the active filling increases geometrically. The atrioventricular flow pattern may be a mechanical-biologic link to ventricular chamber growth and a determination of ventricular chamber volume. The venous clip procedure temporarily reduces the mechanical load on the myocardium. Therefore, we investigated the influence of the venous clip intervention on ventricular diastolic filling characteristics at stage 24 using simultaneous Doppler measurements over the dorsal aorta and atrioventricular canal. Furthermore, the influence of endothelin-1 or endothelin receptor antagonist infusion on ventricular diastolic filling was established as well.

5.1 Ventricular diastolic filling characteristics in stage 24 chick embryos after extra-embryonic venous obstruction

Summary

Alteration of extra-embryonic venous blood flow in stage 17 chick embryos results in well-defined cardiovascular malformations. We hypothesise that the decreased dorsal aortic blood volume flow observed after venous obstruction results in altered ventricular diastolic function in stage 24 chick embryos. A microclip was placed at the right lateral vitelline vein in a stage 17 (52-64 h of incubation) chick embryo. At stage 24 (4.5 days of incubation), we measured simultaneously dorsal aortic and atrioventricular blood flow velocities with a 20-MHz pulsed-Doppler velocity meter. The fraction of passive and active filling was integrated and multiplied by dorsal aortic blood flow to obtain the relative passive and active ventricular filling volumes. Data were summarized as mean ± SEM and analyzed by t-test. At similar cycle lengths ranging from 557 to 635 ms ($p>0.60$), dorsal aortic blood flow and stroke volume measured in the dorsal aorta were similar in stage 24 clipped and normal embryos. Passive filling volume (0.07 ± 0.01 mm^3) was decreased and active filling volume (0.40 ± 0.02 mm^3) was increased in the clipped embryo when compared to the normal embryo (0.15 ± 0.01

mm^3, 0.30±0.01 mm^3, respectively) (p<0.003). In the clipped embryos, the passive/active ratio was decreased compared to normal embryos (p<0.001). Ventricular filling components changed after partially obstructing the extra-embryonic venous circulation. These results suggest that material properties of the embryonic ventricle are modified after temporarily reduced hemodynamic load.

Introduction

The formation of the four-chambered heart is a complex and dynamic interaction between the basic gene program that regulates growth and differentiation and the mechanical forces generated by the functioning heart. To study the influence of hemodynamics on heart morphogenesis, we used a chick embryo intervention model in which extra-embryonic blood flow can be manipulated. Intracardiac blood flow patterns were altered by a redirection of venous inflow through permanent obstruction of the right vitelline vein with a microclip. We previously showed that this intervention produced a specific set of cardiac malformations, namely ventricular septal defects, valve anomalies and pharyngeal arch artery malformations [1,2]. The similarity of these structural cardiac anomalies in the chick embryo to those observed in patients with congenital heart disease argues for the importance of intracardiac hemodynamics as a key epigenetic factor in embryonic cardiogenesis [3].

We recently demonstrated that venous clipping has major acute effects on hemodynamics in the stage 17 chick embryo [4]. For the total study period of five hours, dorsal aortic blood flow remains lower compared to baseline values, whereas heart rate shows a recovery to baseline within two hours after clipping [4]. This dramatic reduction in total circulating blood volume after clipping could influence the functional characteristics of the embryonic heart. Since the early developing cardiovascular system is not yet innervated [5], cardiovascular function is sensitive to mechanisms or interventions that alter hemodynamic load like in the venous clip model. In contrast to the mature cardiovascular system, the embryonic heart lacks the ability to acutely alter heart rate to compensate for reduced ventricular preload [6]. We therefore, hypothesize that the decreased blood volume flow observed in the venous clip embryo would affect ventricular diastolic function.

Embryonic diastolic function can be investigated using pulsed-Doppler measurements of blood velocity and flow. The combination of simultaneous atrioventricular and dorsal aortic blood flow profiles accurately defines passive and active ventricular filling volumes [7]. We studied embryonic cardiovascular performance in the stage 24-chick embryo during normal growth and development and after venous clip intervention.

Material and Methods

Fertilized White Leghorn chicken (*Gallus domesticus L.)* eggs (Charles River Laboratories, Extertal, Germany) were incubated blunt-end up at 37-38ºC and staged according to Hamburger and Hamilton [8]. Embryos that were dysmorphic, exhibited arrhythmias or overt bleeding were excluded. At stage HH 17 (52-64 h of incubation) the embryo was exposed by creating a window in the shell followed by removal of the overlying shell membranes. Adjacent to the right lateral vitelline vein, the vitelline membrane was removed and a small incision was made in the yolk sac membrane. An aluminum microclip was used to clip the right lateral vitelline vein [1,2]. After venous ligation, the window was sealed with tape and the eggs returned to the incubator until stage HH 24 (4.5 days of incubation).

Dorsal aortic blood flow velocity and atrioventricular (AV) blood flow velocity were recorded using a 20-MHz pulsed Doppler velocity meter (model 545C-4, Iowa Doppler Products, Iowa City, USA). Dorsal aortic blood velocity was measured with a 750-μm piezoelectric crystal positioned at a 45º angle towards the dorsal aorta at the level of the developing wing bud. Internal aortic diameter was calculated from a magnified video image displaying the dorsal aorta using a custom-built analysis program (IMAQ Vision, National Instruments, Austin, TX, USA) [9]. Atrioventricular blood flow velocity was measured with a second crystal positioned at the apex of the heart towards the AV orifice. The Doppler audio signals were digitized at 24 kHz and stored on hard disk. Using complex fast Fourier transform analysis, the maximum velocity waveform was reconstructed. A more detailed description of this method has been published previously [9]. Passive filling (P) was defined in the AV flow velocity waveform from end-systole to the onset of the A-wave, and active filling (A) from the onset of the A-wave to the onset of systole (Fig. 1). Portions of passive and active filling overlapped each other at faster heart rates. The demarcation between the passive and active velocities was dependent on heart rate, but was most conspicuous as heart rate slowed. Therefore, heart rate was decreased to 100 bpm by cooling of the embryo. Although environmental temperature directly influences hemodynamics [10] a slowed heart rate of approximately 100 bpm was necessary to discriminate between the passive and active filling phase and to study both groups under similar conditions. Cycle length was defined as the time between consecutive beats obtained from the dorsal aortic velocity waveform. Dorsal aortic and both passive and active AV velocity profiles were integrated over time. Dorsal aortic blood flow, an estimate of cardiac output, was calculated as the product of the integrated velocity curve and the cross-sectional area of the dorsal aorta. Passive ventricular filling volume equaled dorsal aortic stroke volume multiplied by the fraction of passive filling area

and active ventricular filling volume equaled dorsal aortic stroke volume multiplied by the fraction of the active filling area [7].

Fifteen clipped and fifteen normal embryos were measured at stage 24. For each embryo we analyzed five consecutive cycles. The data are presented as mean ± SEM and a statistical analysis was carried out using an unpaired t-test. When data was not normally distributed according to the Shapiro-Wilk test, a logarithmic transformation was performed prior to establishing difference between the two study groups. Statistical significance was reached at p < 0.05. Calculations were performed with SPSS 10.1 software (SPSS Inc, Chicago, IL).

Fifteen clipped and fifteen normal embryos were measured at stage 24. For each embryo we analyzed five consecutive cycles. The data are presented as mean ± SEM and a statistical analysis was carried out using a paired t-test. Statistical significance was reached at p < 0.05. Calculations were performed with SPSS 10.1 software (SPSS Inc, Chicago, IL).

Results

The cycle length and heart rate were similar between the two study groups (p>0.60). The mean cycle length was 593 ± 7 ms in the clipped embryo and 597 ± 5 ms in the normal embryo corresponding to a mean heart rate of 101 ± 1 bpm vs. 100 ± 1 bpm in the clipped and normal embryo, respectively. As a result of this slowed heart rate the passive and active filling phase of the AV velocity waveform during diastole were well defined (Fig. 1). The AV velocity waveform during ventricular systole coincided with the dorsal aortic flow velocity (Fig. 1).

Dorsal aortic blood flow and stroke volume were similar in the clipped and normal embryos at stage 24 (Fig. 2 and 3). In the clipped embryos, mean passive ventricular filling volume decreased by 53%, while mean active ventricular filling volume increased 33%, when compared with normal controls (Fig. 3). The passive filling volume accounted for 15% of the stroke volume in the clipped embryos and 33% in the normal embryos. The ratio of passive to active ventricular filling volume was significantly decreased in the clipped embryos compared to normal embryos (0.19 ± 0.02 $vs.$ 0.50 ± 0.04) (p<0.001).
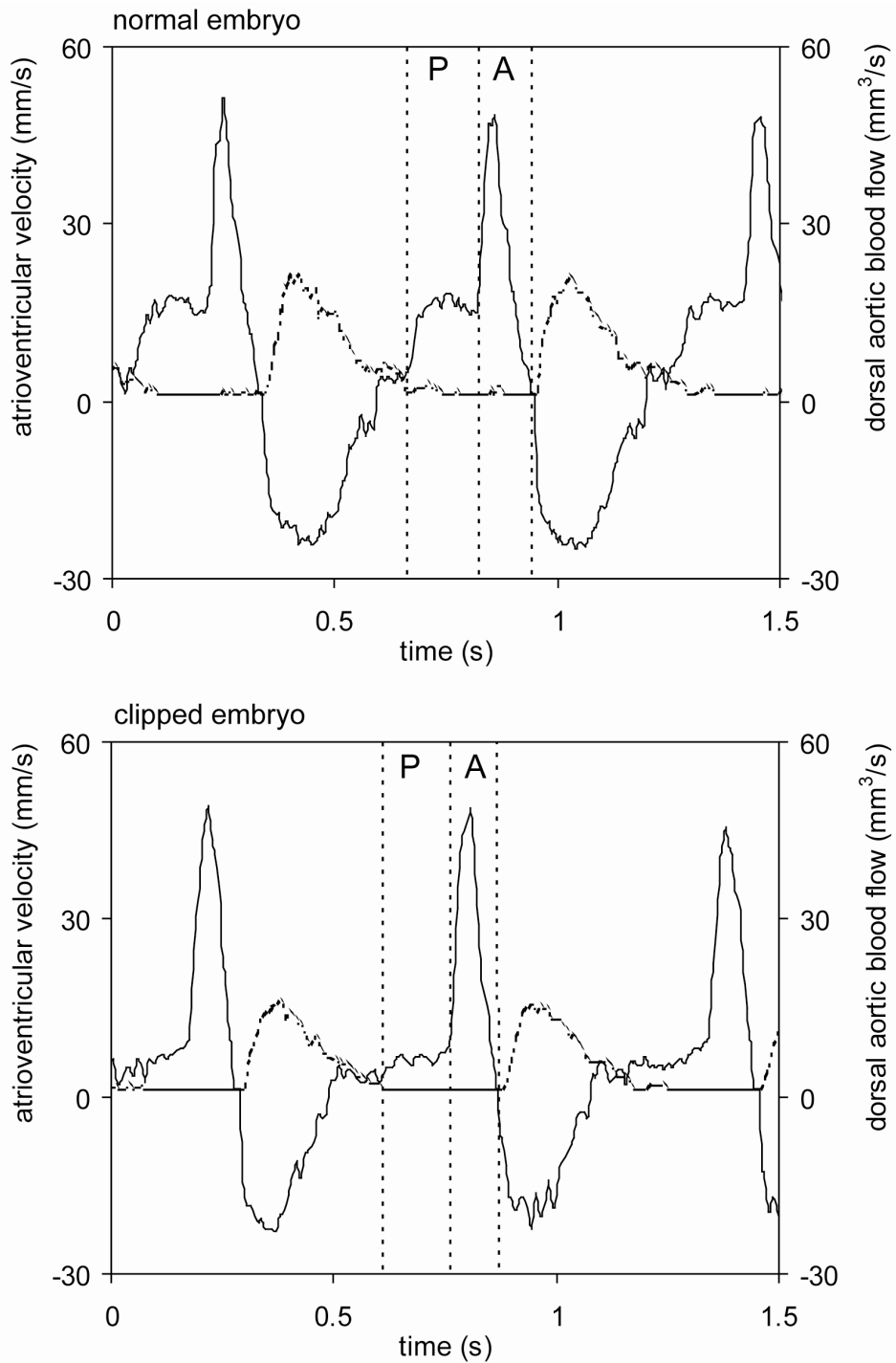
Figure 1.

An example of simultaneously recorded tracings of atrioventricular velocity (solid line) and dorsal aortic blood flow (dashed line) in a normal (upper panel) and clipped (lower panel) stage 24 chick embryo. Diastole is partitioned into two components: the passive phase indicated by P and the active phase indicated by A.
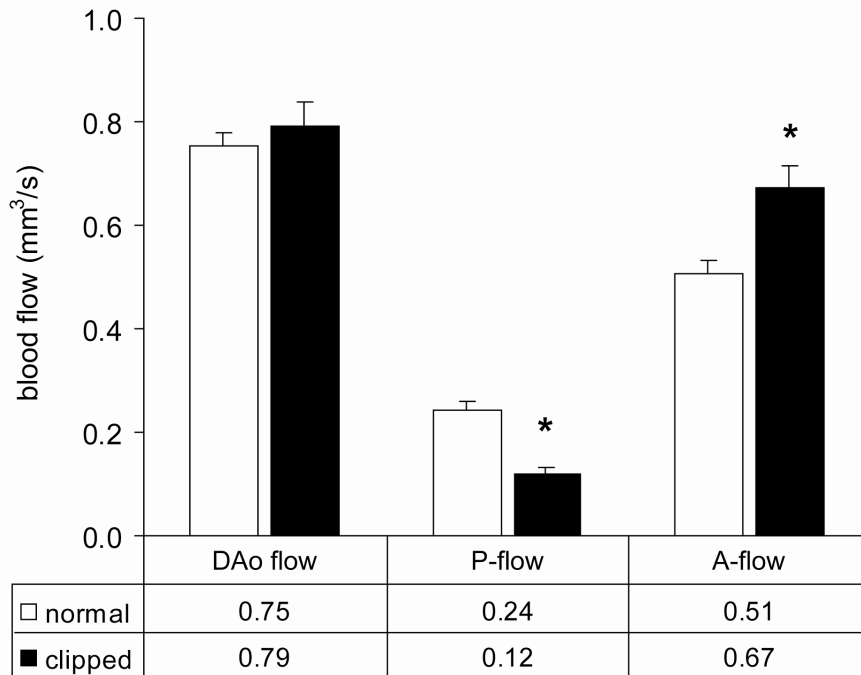
Figure 2.

Dorsal aortic (DAo) blood flow and passive (P) and active (A) components of atrioventricular blood flow measured in normal (open bars, n=15) and clipped (solid bars, n=15) chick embryos at stage 24. Data presented as mean ± SEM. *p<0.003 *vs*. control.

Figure 3.

Dorsal aortic (DAo) stroke volume and passive (P) and active (A) ventricular filling volumes measured in normal (open bars, n=15) and clipped (solid bars, n=15) chick embryos at stage 24. Data presented as mean ± SEM. *p<0.003 *vs*. control.

Discussion

The present study extends our ongoing investigation of embryonic cardiovascular function after venous clipping experiments at stage 17. We used simultaneous measurements of atriove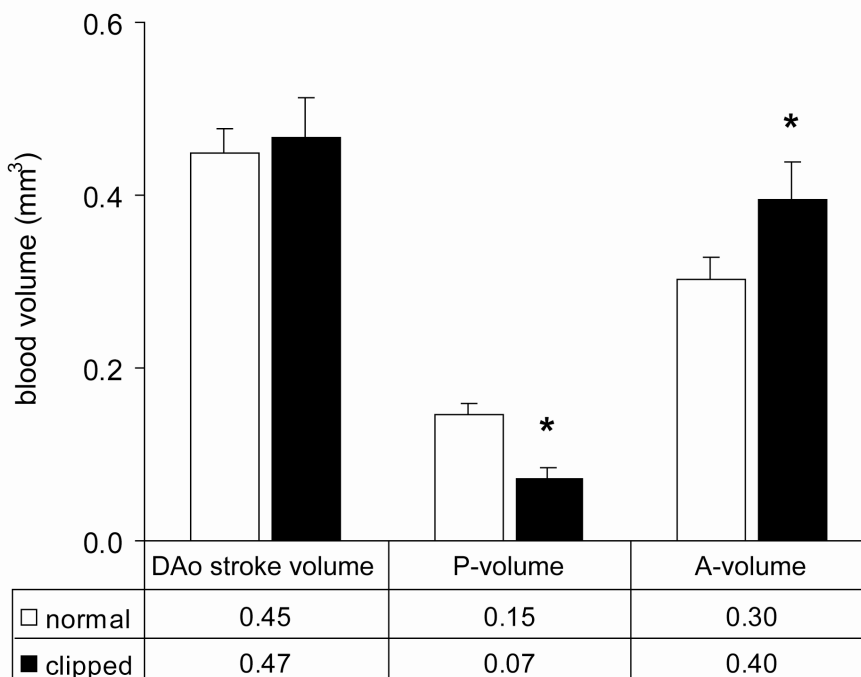ntricular blood flow velocity and dorsal aortic blood flow to study ventricular diastolic filling characteristics after vitelline vein ligation. Our data of atrioventricular inflow patterns after venous clipping showed a reduced contribution of passive filling in favor of atrial contraction to ventricular filling at stage 24, whereas stroke volume measured in the dorsal aorta was similar between clipped and control embryos at this stage.

Rerouting of venous inflow by permanent obstruction of the right vitelline vein in the early chick embryo results in cardiovascular malformations: ventricular septal defects, valve anomalies and pharyngeal arch artery malformations [2]. Results of our hemodynamic study revealed that during the first five hours after clipping dorsal aortic blood flow is markedly decreased and is unable to return to baseline values [4]. However, dorsal aortic blood flow measurements obtained 24 hours (stage 21) after clipping demonstrated similar results in clipped and control embryos (unpublished data). We suggest that the reduction in blood flow for at least five hours may begin a cascade of events that result in the cardiovascular malformations observed later during development.

Proper functional loading is essential for normal cardiac morphogenesis, as the structure and function of the developing heart are intimately linked. Subjecting the chick embryonic heart to mechanically altered loading conditions modifies the myocardial architecture [11]. Decreased mechanical loading of the left ventricle by left atrial ligation results in reduced levels of proliferation in the left ventricular compact layer and trabeculae [12]. During normal maturation of the heart, myofibrils increase in number and alignment and this will probably affect the myocardial properties of the ventricle [13]. In the same left atrial ligation model, Tobita *et al.* [14] demonstrated an increase in passive stiffness of embryonic myocardium in response to reduced mechanical load. Microtubules, important regulators of cellular organization and fibrillogenesis, seem to be associated with the response of the embryonic myocardium to altered load. An increase in microtubular density and an acceleration of myofiber maturation were observed in the embryonic heart after altered mechanical load and were related to the increased passive stiffness noted after left atrial ligation [15].

Venous clipping also reduces mechanical load and is likely to modify the myocardial architecture and this may subsequently result in increased passive stiffness of the embryonic myocardium. This is supported by morphologic examination of venous clipped embryos demonstrating, that in addition to delayed cardiac looping and impaired cushion formation,

the compact layer of ventricular myocardium was thinner and ventricular trabeculation was reduced [16]. These morphological changes in developing myocardium could also have impact on diastolic function and contribute to observed changes in ventricular filling patterns.

In contrast, data of atrioventricular inflow patterns after left atrial ligation showed reduced contribution of atrial contraction to ventricular filling and decreased peak velocity from stage 21 to stage 27 [17]. In the left atrial ligation model the decrease in volume load is chronic, whereas in the venous clip model the reduction in volume load is temporary. We, therefore, suggest that the embryonic ventricle responds to temporarily reduced loading conditions by a change in ventricular passive properties resulting in a reduction in passive filling that is compensated by an increase of atrial contraction to maintain constant cardiac output.

Experimental disruptions of the venous return by vitelline vein obstruction or left atrial ligation cause cardiovascular malformations [2,18]. These observations indicate that responses of cardiac tissue to altered biomechanical forces including blood flow and shear stress are critical determinants of cardiac development. Also a role for hemodynamics in modulation of shape and arrangements of endocardial cells in the embryonic chick has been reported [19]. In addition, cultured vascular endothelial cells rearrange their cytoskeletal architecture and change their gene expression profiles in response to flow-induced forces [20-23]. Thus, experimentally induced flow alterations that translate fluid shear stress to changes in gene expression are likely candidate regulating mechanisms for the response of the developing heart to reduced loading conditions. The hypothesis that fluid shear stress plays an important role in embryonic cardiogenesis was recently substantiated by a study performed in zebrafish embryos. This study describes the quantitative *in vivo* analysis of intracardiac blood flow and shear stress in zebrafish embryos. Their data strongly suggest that shear stress forces play some role in the regulation of embryonic cardiogenesis [3].

In conclusion, early venous obstruction results in altered diastolic ventricular filling of the stage 24-chick embryo. Our study supports the paradigm that alteration in mechanical loading is a mechanism that can produce changes in cardiac function and structure.

5.2 Altered ventricular diastolic filling characteristics in HH24 chicken embryos after venous infusion of endothelin-1 and endothelin receptor antagonists at HH18

In preparation

Summary

Cardiovascular malformations in the venous clip model for chicken embryos are similar to malformations observed in knockout mice studies of components of the endothelin-1/endothelin-converting-enzyme-1/endothelin receptor A (ET-1/ECE-1/ETA) cascade. *ET-1* expression is decreased in the heart 3 hrs after clipping. Also ventricular diastolic filling is disturbed 2 days after clipping. Therefore, we hypothesize that the endothelin cascade is involved in the development of functional cardiac impairment and cardiovascular malformations after venous clipping.

Endothelin-1 and endothelin receptor antagonists were infused into the blood stream of HH18 embryos and ventricular diastolic filling characteristics were studied at HH24, followed by cardiovascular morphologic investigation at HH35. The results were compared to sham-operated embryos. Furthermore, the effect of ET-1 and receptor antagonists on expression of *ET-1*, *ECE-1*, *ETA*, and Lung Krüppel-like factor (*KLF2*) was investigated, and the cardiovascular localisation of *ETA* and *ETB* receptor mRNA from HH18 to HH24 was determined using in situ hybridisation (ISH).

We found a reduced diastolic passive-filling component of ventricular filling in embryos infused with ET-1, ETA and the combined ETA-ETB antagonist, which was more than compensated by an increased active-filling component. The passive-filling component was not affected after infusion of the ETB antagonist. In 42% of the experimental embryos a thinner ventricular myocardium was found compared to 20% in sham embryos. No major cardiovascular malformations were observed. In vitro administration of ET-1 or endothelin receptor antagonists confirmed that ETA and ETB receptors act differently within cardiac function. ISH revealed that *ETA* mRNA is predominantly expressed in the myocardium, whereas *ETB* is mostly expressed in the endocardium.

The results found in the present study suggest that the endothelin pathway is involved in the development of functional cardiac impairment observed in the venous clip model and plays an important role in development of cardiac function in general. We conclude that cardiovascular malformations after venous clipping arise from a combination of hemodynamic changes and subsequent altered gene expression patterns, including those of the endothelin pathway.

Introduction

The formation of the four chambered heart results from the complex and dynamic interaction between the basic gene program that regulates growth and differentiation and the mechanical forces generated by the functioning heart. When mechanical forces such as shear stress are impaired, or when genes involved in growth and differentiation are not functioning correctly, malformations may arise.

In the venous clip model the right lateral vitelline vein of a chicken embryo is permanently ligated. Due to this ligation blood flow patterns through the heart are changed, resulting in functional cardiac impairment and cardiovascular malformations [2,24,25]. For up to 5 hours after venous clipping, dorsal aortic mean and peak blood flows are decreased, leading to a decrease in shear stress [4]. Previously, we have shown that the genes endothelin-1 (*ET-1*), Lung Krüppel-like factor (*KLF2/LKLF*), and endothelial nitric oxide synthase (*NOS-3/eNOS*) are shear related *in vivo* in the chicken embryo [26]. After a 3-hour ligation the dorsal aortic expression of these genes is altered: *ET-1* is increased, and *KLF2* and *NOS-3* are both down-regulated (Groenendijk, unpublished). This confirms that indeed decreased aortic blood flow is accompanied by diminished local shear stress after venous clip.

ET-1 is part of the endothelin-1/endothelin-converting-enzyme-1/endothelin receptor A (ET-1/ECE-1/ETA) signalling cascade, which is important in cardiac development [27]. The cardiovascular malformations in the venous clip model [28] are similar to the malformations observed in knockout mice studies of components of the ET-1/ECE-1/ETA cascade [27,29,30]. In addition, *ET-1* expression after a 3-hour venous clip is decreased in the heart (Groenendijk, unpublished). This suggests that the endothelin cascade might be involved in the development of malformations induced by venous clipping.

In a previous study we demonstrated that ventricular diastolic filling is disturbed two days after clipping (HH24) [24]. Using simultaneous Doppler measurements of the dorsal aorta and atrioventricular canal, we found a reduced diastolic passive-filling component of ventricular filling, which was compensated by an increased active-filling component in clipped embryos.

To unravel the cascade of events thought to occur after venous clipping, we infused ET-1 and endothelin receptor antagonists into a vitelline vein at HH18. We studied embryonic ventricular diastolic function, using pulsed-Doppler measurements of blood velocity and flow in HH24 chicken embryos, two days after the extra-embryonic venous infusion. Furthermore, we examined the cardiovascular morphology of the infused embryos at HH35. This was done in order to test the hypothesis that disturbed *ET-1* expression after venous clipping is responsible for the observed functional cardiac impairment and cardiovascular malformations

in this model. Both the ventricular diastolic filling and morphology were compared to the results of sham-operated embryos. To examine the possible influence on gene expression ET-1 or endothelin receptor antagonists were also administered to endocardial cell cultures, after which gene expression was determined. The localisation of the mRNA of ETA and ETB receptors was investigated as well as ET-1 exerts its function through these receptors.

Material and Methods

Animals and intravenous infusions

Fertilised White Leghorn chicken (*Gallus domesticus* L.) eggs (Charles River Laboratories, Extertal, Germany) were incubated blunt-end up at 37-38ºC and staged according to Hamburger and Hamilton [8]. Embryos that were dysmorphic, exhibited arrhythmias or overt bleeding were excluded. At HH18 the embryos were exposed by creating a window in the shell followed by removal of the overlying shell membranes. Adjacent to the right lateral vitelline vein, the vitelline membrane was removed and a glass micropipette was inserted into one of the third order branches of the right lateral vitelline vein. One µl of the following substances was slowly infused without any force, to keep changes in hemodynamics to a minimum: endothelin 1 (Bachem, Brunschwig Chemie, Germany) at a concentration of 10^{-7}mol/L in Phosphate Buffered Saline (PBS) (n=16), the ETA antagonist BQ-123 (Bachem) (n=17) and ETB antagonist BQ-788 (Sigma-Aldrich) (n=18), both at a concentration of 10^{-5} mol/L in PBS, and a combined ETA/ETB antagonist PD145065 (Sigma-Aldrich) at a concentration of 10^{-4} mol/L in PBS (n=17). Indigo carmine blue (0.25 g/mL) was added for visualization of the solution during *in vivo* infusion. The embryos were compared with sham-operated animals (n=13) in which only PBS with indigo carmine was infused.

After this extra-embryonic venous infusion, the window was sealed with tape and the eggs were reincubated for measurement of the blood flow velocity at HH24 (embryonic day 4.5). The embryos were sacrificed at HH35 (embryonic day 9) for histological examination. Prior to fixation the embryos and the hearts were macroscopically evaluated for overt malformations.

Measurements

Dorsal aortic blood flow velocity and atrioventricular (AV) blood flow velocity were recorded using a 20-MHz pulsed Doppler velocity meter (model 545C-4, Iowa Doppler Products, Iowa City, USA). Dorsal aortic blood velocity was measured with a 750-μm piezoelectric crystal positioned at a 45º angle towards the dorsal aorta at the level of the developing wing bud. Internal aortic diameter was calculated from a magnified video image displaying the dorsal aorta using a custom-built analysis program (IMAQ Vision, National Instruments, Austin, TX, USA) [9]. Atrioventricular blood flow velocity was measured with a second crystal positioned at the apex of the heart towards the AV orifice. The Doppler audio signals were digitised at 24 kHz and stored on hard disk. Using complex fast Fourier transform analysis, the maximum velocity waveform was reconstructed. A more detailed description of this method has been published previously [9]. Passive filling (P) was defined in the AV flow velocity waveform from the end of the isovolumic relaxation period to the onset of the A-wave, and active filling (A) from the onset of the A-wave to the onset the isovolumic contraction period (Fig. 1). Portions of passive and active filling overlapped each other at faster heart rates. The demarcation between the passive and active velocities was dependent on heart rate, but was most conspicuous as heart rate slowed. Therefore, heart rate was decreased to approximately 110 bpm by cooling of the embryo. Although environmental temperature directly influences hemodynamics [10] a slowed heart rate of approximately 110 bpm was necessary to discriminate between the passive and active filling phase and to study both groups under similar conditions. Cycle length was defined as the time between consecutive beats obtained from the dorsal aortic velocity waveform. Dorsal aortic and both passive and active AV velocity profiles were integrated over time. Dorsal aortic blood flow, an estimate of cardiac output, was calculated as the product of the integrated velocity curve and the cross-sectional area of the dorsal aorta. The passive component of ventricular blood flow was defined as mean aortic blood flow multiplied by the fraction of passive filling area, and the active component of ventricular blood flow was defined as mean aortic blood flow multiplied by the fraction of the active filling area. Passive ventricular filling volume equalled dorsal aortic stroke volume multiplied by the fraction of passive filling area. Active ventricular filling volume equalled dorsal aortic stroke volume multiplied by the fraction of the active filling area [7].

Statistical analysis

Eighty-one chicken embryos were measured at HH24. We compared embryos that received an infusion with ET-1, ETA antagonist, ETB antagonist, or ETA/ETB antagonists with sham embryos. For each embryo we analysed five consecutive cycles per measurement. The data are presented as mean ± SEM and a statistical analysis was carried out using an unpaired t-test. When data was not normally distributed according to the Shapiro-Wilk test, a logarithmic transformation was performed prior to establishing difference between the study groups and sham embryos. Statistical significance was reached at $p < 0.05$. Calculations were performed with SPSS 10.1 software (SPSS Inc, Chicago, IL).

Morphological and histological examination

After the Doppler measurements at HH24 the embryos were reincubated until HH35. From the embryos that survived until this stage, we randomly selected embryos (n=6 per substance) for morphological and histological examination.

Embryos were fixed in 4% paraformaldehyde in 0.1M phosphate buffer for 24 hrs, followed by dehydration in graded ethanol and were embedded in paraffin. After this the embryos were serially sectioned transversely to the arterial pole at 5μm and mounted on glass slides. Routine immunohistochemical staining was performed using an overnight incubation with the primary antibody HHF35 (DAKO, Denmark) against muscle actin [31] diluted 1:500 in PBS with 0.05% Tween-20 (PBST) and 1% Bovine Serum Albumin (BSA). After rinsing in PBS the sections were incubated with horseradish peroxidase-conjugated rabbit anti-mouse antibody (1:250, DAKO, Denmark) for 75 minutes. Following thorough rinsing with PBS, the sections were treated with 0.04% diaminobenzidine tetrahydrochloride (DAB)/$0.006^0/_{00}$ H_2O_2 in 0.05mol/L Tris-maleic acid (pH 7.6) for 10 minutes at room temperature. The sections were counter-stained with Mayer's Haematoxylin, dehydrated, and mounted in Entellan.

Radioactive In Situ Hybridisation

In a separate set of control embryos we determined the localisation of mRNA for the endothelin-1 receptors ETA and ETB in the chicken heart at HH18 (n=3, stage of infusion), HH20 (n=2), HH22 (n=2) and HH24 (n=2, stage of measurements), essentially as described before (Groenendijk *et al.*, 2004). ^{35}S-labelled chicken specific riboprobes were produced from a 845 bp (nucleotides 2256-3101) ETA fragment, and a 440 bp (nucleotides 339-778) ETB fragment, that were cloned in pBSK (ETA) or pCRII (Invitrogen, ETB). After

linearisation sense and antisense cRNA was transcribed in transcription buffer, 0.01mol/L dithiothreitol, 0.25mmol/L G/A/CTP mix, 1.4U/µL RNase-inhibitor, and 1.5U/µL of the appropriate RNA polymerase (ETB: SP6; ETA: T3) in the presence of 2.31MB ^{35}S-UTP. Concentration of the probes was normalised to 1×10^5 cpm/µL. All sense probes showed negative hybridisation results (not shown).

In vitro experiments

To quantify the effect of exogenous endothelin and the receptor antagonists on expression of *ET-1*, *ECE-1*, *ETA* and *KLF2* we added the substances to primary cultures of quail endocardial cells, and quantified expression levels by QRT-PCR. Fertilised quail (*Coturnix coturnix*) eggs were incubated to stage HH40 (14 days) at 37°C and 60-70% relative humidity, and were isolated. The ventricles of the embryos were used for isolation procedures. After opening along their longitudinal axes, the ventricles were incubated with the endocardial side down for 10 minutes at 37°C in 0.1% (w/v in PBS) Collagenase-A (Roche). The cells were flushed with medium, and by filtration on a 30µm filter (Miltenyi Biotec) sheets of cells were isolated. After this, the cells were seeded in fibronectin-coated (20µg/mL, Sigma) dishes in QEC medium consisting of M199/HEPES (Gibco) supplemented with 10% (v/v) Fetal Calf Serum (Gibco), 2% (v/v) Chicken Serum (Gibco), 2mmol/L L-Glutamine (Gibco), 250µg/ml Endothelial Cell Growth Supplement (Sigma), 1x antibiotic/antimyotic solution (Gibco), and 50µg/mL Gentamycin (Sigma). The cells were grown to confluency and passed once a week. They were used at p3, at which they were exposed for 5 hours to medium containing 10^{-7}mol/L ET-1, 10^{-5}mol/L BQ-123, or 10^{-5}mol/L BQ-788. Control cells were exposed to medium only. Quail cells were used in this in vitro study to be able to identify endothelial cells by immunostaining with the QH1 antibody [32]. Co-staining for actin with 1A4 showed a 70%/30% mixture of endothelial cells and myocardium (not shown).

RNA isolation and QRT-PCR

From each sample total RNA was isolated (RNeasy, Qiagen) and prepared for quantitative real time amplification (QRT-PCR). RNA was treated with DNAse-I, and 500ng was reverse transcribed into cDNA with M-MuLV Reverse Transcriptase (Amersham). Equal amounts of cDNA were subjected in duplicate to QRT-PCR, using SYBR green I Master Mix (Applied Biosystems) on an MX3000P PCR machine (Stratagene) [33]. The reactions contained 1xPCR

Master Mix, 2µl cDNA template, and 10pmol of each primer. As negative controls no-template samples were used. The PCR program consisted of a hot start activation step of 10 min 95°C, followed by 50 cycles of 15 sec 95°C, 30 sec 58°C, and 30 sec 72°C. Dissociation analysis confirmed the amplification of unique targets and excluded the presence of primer-dimers. Sequence information of quail mRNAs was largely unavailable, therefore most primers in this study were based on chicken primers. The following gene specific primers: quail β-actin (GenBank: AF199488), chicken *KLF2* (BM490221), chicken *ET-1* (XM418943), chicken *ECE-1* (AF230274), and chicken *ETA* (AF040634), were designed using the Primer3 engine at http://frodo.wi.mit.edu/cgi-bin/primer3/primer3_www.cgi [34]. Equal amounts of RNA from control and experimental samples were analysed for β-actin expression. Ct values did not vary among these groups (not shown); therefore, this gene was used as normaliser. Relative expression levels were calculated [35], including gene specific values for amplification efficiencies derived from serial dilutions of cDNA and standard curve analysis. An independent samples t-test was used to compare the means between control and experimental samples. P-values <0.05 were considered significant.

Results

Doppler Measurements

Heart rate and cycle length were similar between the study groups and the sham embryos (smallest p>0.12). The mean heart rate in the sham embryos was 109 ± 1 bpm corresponding to a cycle length of 548 ± 4 ms. Figure 1 demonstrates that at this heart rate the passive and active filling phase of the AV velocity waveform during diastole are well-defined. It is also clear that the AV velocity waveform during ventricular systole coincides with the dorsal aortic flow velocity. Figure 2 shows all parameters after infusion of the different substances compared to shams.

ET-1:

Embryos infused with ET-1 demonstrated an increased dorsal aortic blood flow (0.87 ± 0.01 vs. 0.83 ± 0.01 µl/s, p<0.02). Stroke volume was increased by 3.0%, which was not significantly different. The passive ventricular filling volume was decreased by 26.9% (p=0.006) and the active filling volume was increased by 16.3% (p<0.01). This resulted in a decreased ratio of passive to active ventricular filling (0.30 ± 0.04 vs. 0.45 ± 0.03, p<0.01) after ET-1 infusion.

ETA receptor antagonist:

Chicken embryos treated with ETA antagonist had a significantly higher dorsal aortic blood flow than sham embryos (0.88±0.02 vs. 0.83±0.01 μl/s, p<0.05). Also dorsal aortic stroke volume was elevated by 4.4%. However, this was not a significant difference. The passive component of AV blood flow was lower (0.19±0.02 vs. 0.25±0.01 μl/s, p<0.01) in treated embryos and the active component higher (0.69±0.03 vs. 0.57±0.01 μl/s, p<0.01). The ratio of passive to active ventricular filling was therefore decreased by 36% (p<0.01) after ETA antagonist infusion.

ETB receptor antagonist:

Chicken embryos treated with ETB antagonist displayed a significantly higher dorsal aortic blood flow and stroke volume, i.e. 10.3% and 12.1% higher than sham embryos (p<0.001). The passive ventricular filling volume was not different from sham embryos (0.14±0.01 vs. 0.14±0.01 μl, p=0.5). The active ventricular filling volume was increased by 18.6% (p<0.001). This increase however, did not change the ratio of passive to active ventricular filling (0.39±0.05 vs. 0.45±0.03, p=0.1).

Combined ETA/ETB receptor antagonist:

The combined ETA/ETB antagonist caused an increase in dorsal aortic blood flow of 6.3% (p=0.001) and in stroke volume of 5.2% (p<0.01). The passive ventricular filling flow component was decreased (0.19±0.01 vs. 0.25±0.01 μl/s, p<0.01) and the active flow component was increased (0.69±0.01 vs. 0.57±0.01 μl/s, p<0.001) after infusion with ETA/ETB antagonist, resulting in a decreased ratio of passive to active ventricular filling by 36% (p<0.001).
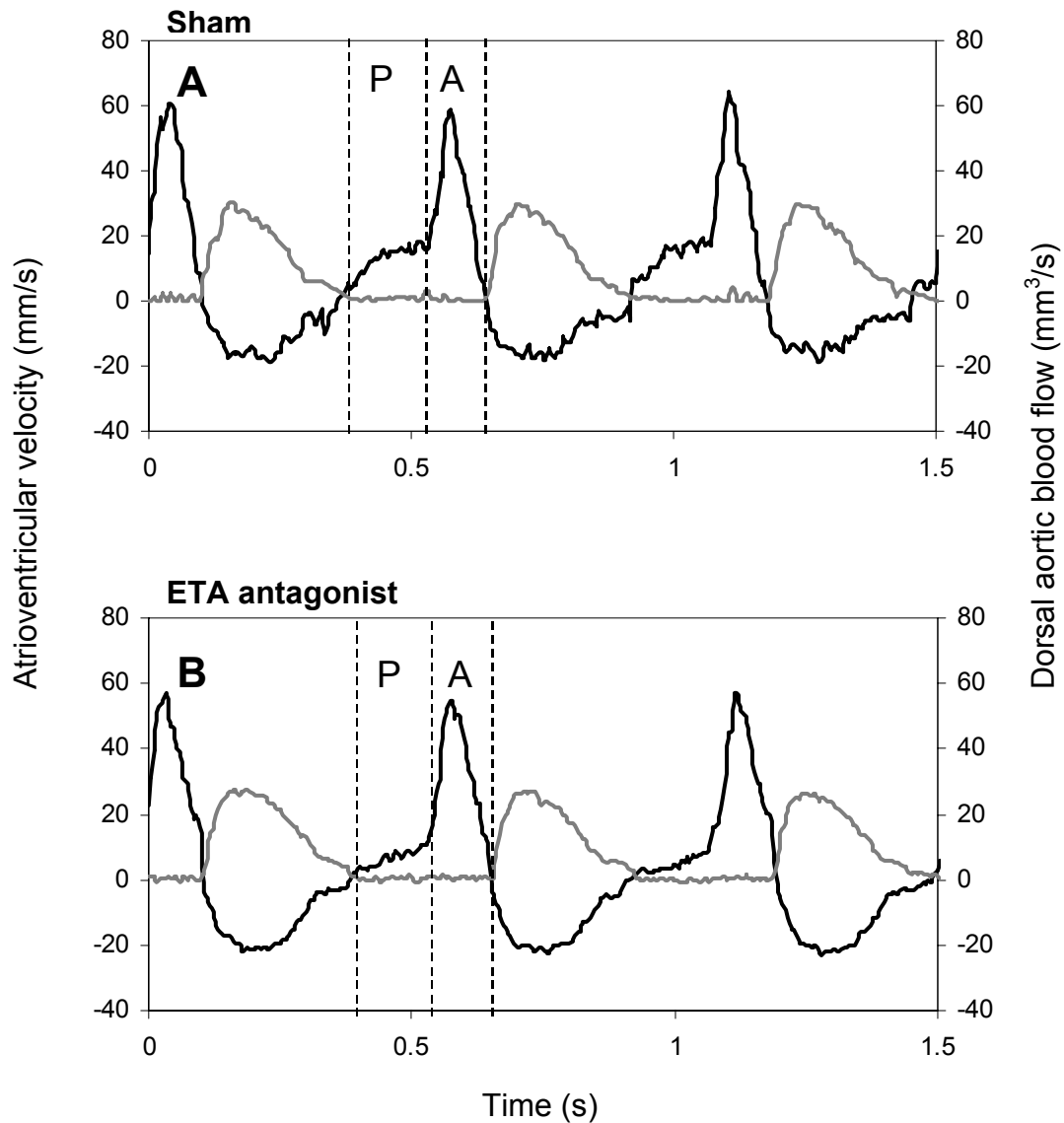
Figure 1.

An example of simultaneously recorded tracings of atrioventricular flow velocity (black line) and dorsal aortic blood flow (grey line) in a sham-operated embryo (A) and ETA antagonist treated embryo (B) at HH24. Diastole is portioned into the passive phase (P) and the active phase (A). From the figure it is clear that after ETA antagonist infusion the passive component is decreased, whereas the active component is increased.

Figure 2.

Effects of ET-1, ETA-, ETB-, and combined ETA/ETB antagonist infusion as compared to sham embryos (black line) on dorsal aortic blood flow (panel A), stroke volume (panel B), the passive component of atrioventricular blood flow (panel C), the active component of atrioventricular blood flow (panel D), and the ratio of passive to active ventricular filling (panel E). * P < 0.05 *vs*. shams.

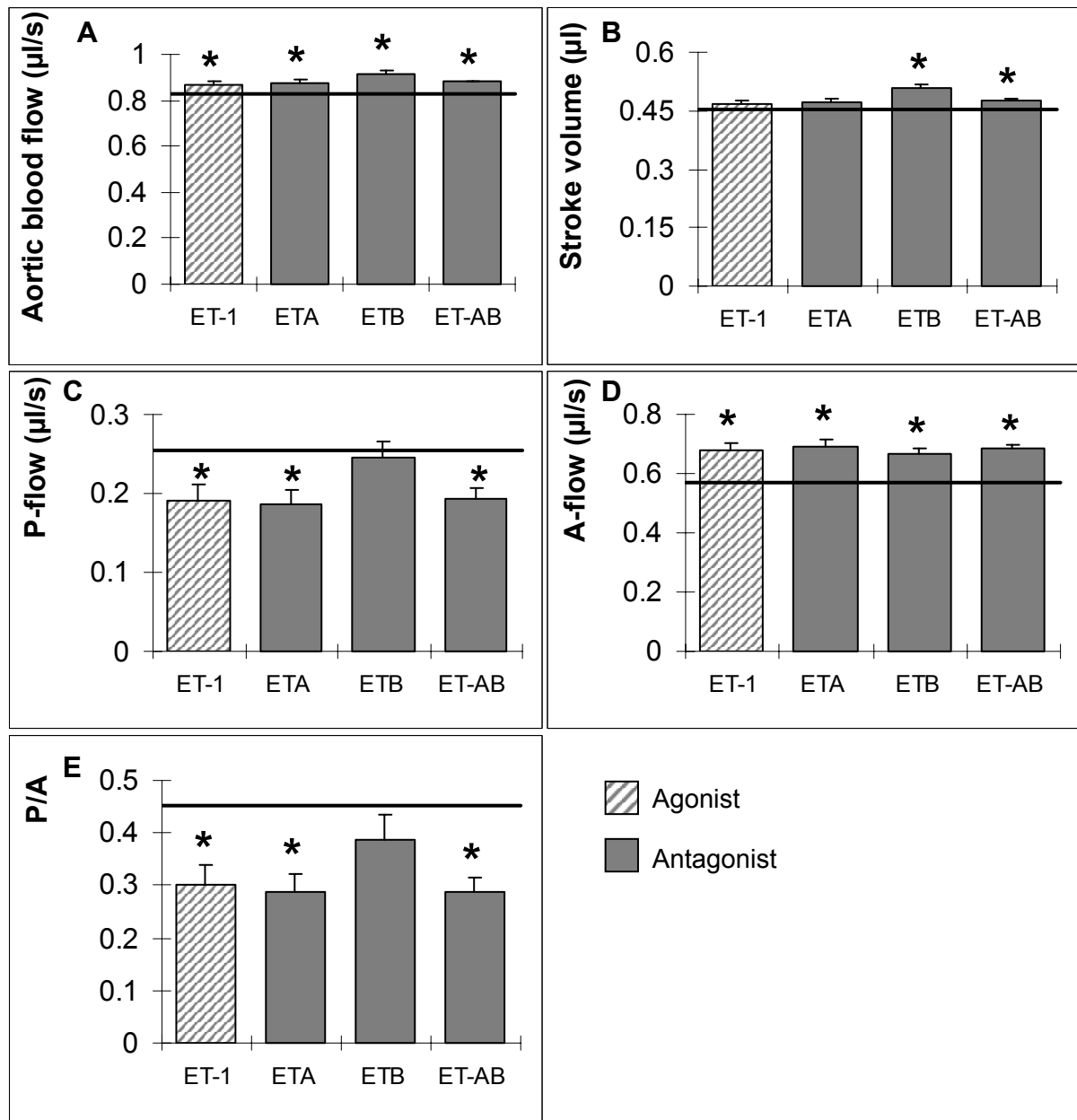Morphology of malformations

Macroscopically, no major malformations of the heart and pharyngeal arch arteries could be observed after infusion of either substance. Microscopically, minor malformations such as (pinpoint) ventricular septum defects, hypoplastic pharyngeal arch arteries, and thinner ventricular myocardium were encountered (Fig. 3). The total number of minor malformations was higher in the experimental embryos than in the shams. In the sham embryos 20% showed abnormalities, in the experimental embryos this was 68%, with the highest prevalence in the embryos treated with the ETA antagonist (100%), and the lowest prevalence in the ETB antagonist treated embryos (40%). Decreased size of the compact layer of the ventricular myocardium was the most common malformation occurring in 42% of the experimental embryos (50% in ET-1; 75% ETA antagonist; 40% ETB antagonist; 33% ETA/ETB antagonist) compared to 20% in sham embryos.

As VSDs are accompanied by impaired myocardialisation of the outflow tract septum[16], this was investigated using the anti-muscle actin antibody HHF35. All embryos infused with either ET-1, ETA antagonist, ETB antagonist or the combined receptor blocker showed normal myocardialisation of the outflow tract (OFT) septum (not shown).

Gene expression

Normal expression of *ETA* at stage HH18 was present in all the myocardium of the common atrium, the atrioventricular canal (AVC), the ventricle and the outflow tract. During development up to HH24 this was the same, all myocardium showed *ETA* expression (Fig. 4).

At stage HH18 *ETB* expression (Fig. 5) was present in the endocardium of the atrium, but predominantly on the lateral sides, and on the basal side of the myocardium. In the narrow part of the AVC mRNA was also only present in the endocardium at the lateral sides, and in the myocardium on the basal side. Going downstream in the AVC the endocardium was negative for *ETB*. The myocardium on the (left) lateral side was positive. The endocardium lining the ventricular trabeculations showed strong expression. The myocardium of the ventricle was also positive, like the OFT endocardium. During development to HH24 (Fig. 5), the endocardial lining of the atria becomes positive. The myocardium of the atria is positive predominantly in the ventral/lateral walls. The endocardium of the AVC was negative, like the myocardium. The endocardium along the ventricular trabeculations showed strong expression, the myocardium surrounding it was also positive. The OFT-myocardium was negative, whereas the endocardium showed a patchy expression.
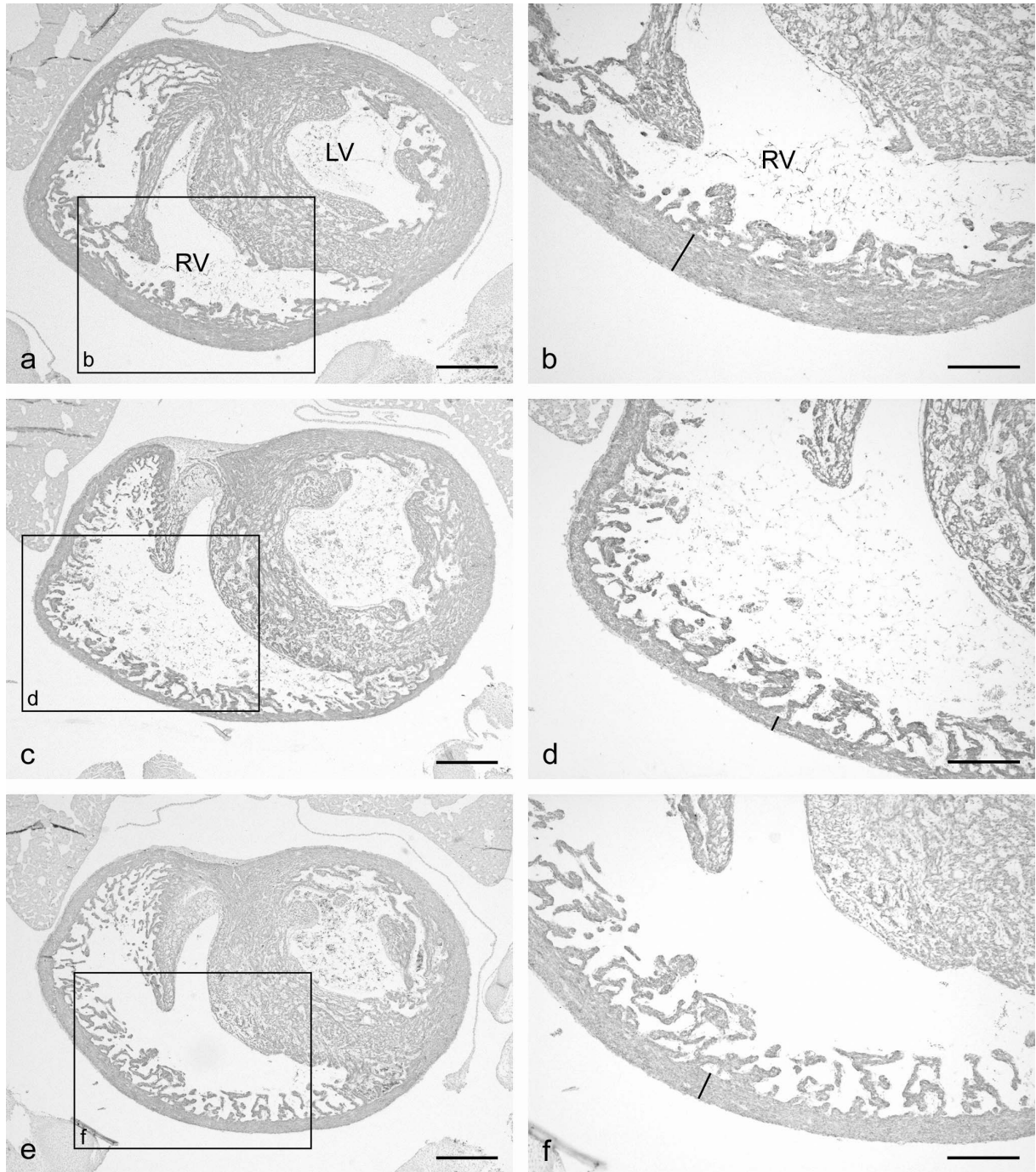
Figure 3.

Sections of HHF35-stained chicken embryonic ventricles at stage HH35. a, b: sham embryo. c, d: embryo infused with ET-1. e, f: embryo infused with the ETA/ETB receptor antagonist, and is also representative for embryos treated with ETA or ETB blockers. The thickness of the compact myocardium is indicated with a line in b, d, and f. Note that the ventricular myocardium is thinner in embryos treated with either ET-1 or ET receptor antagonists compared to shams. Bars in a, c and e: 300μm. Bars in b, d and f: 200 μm.
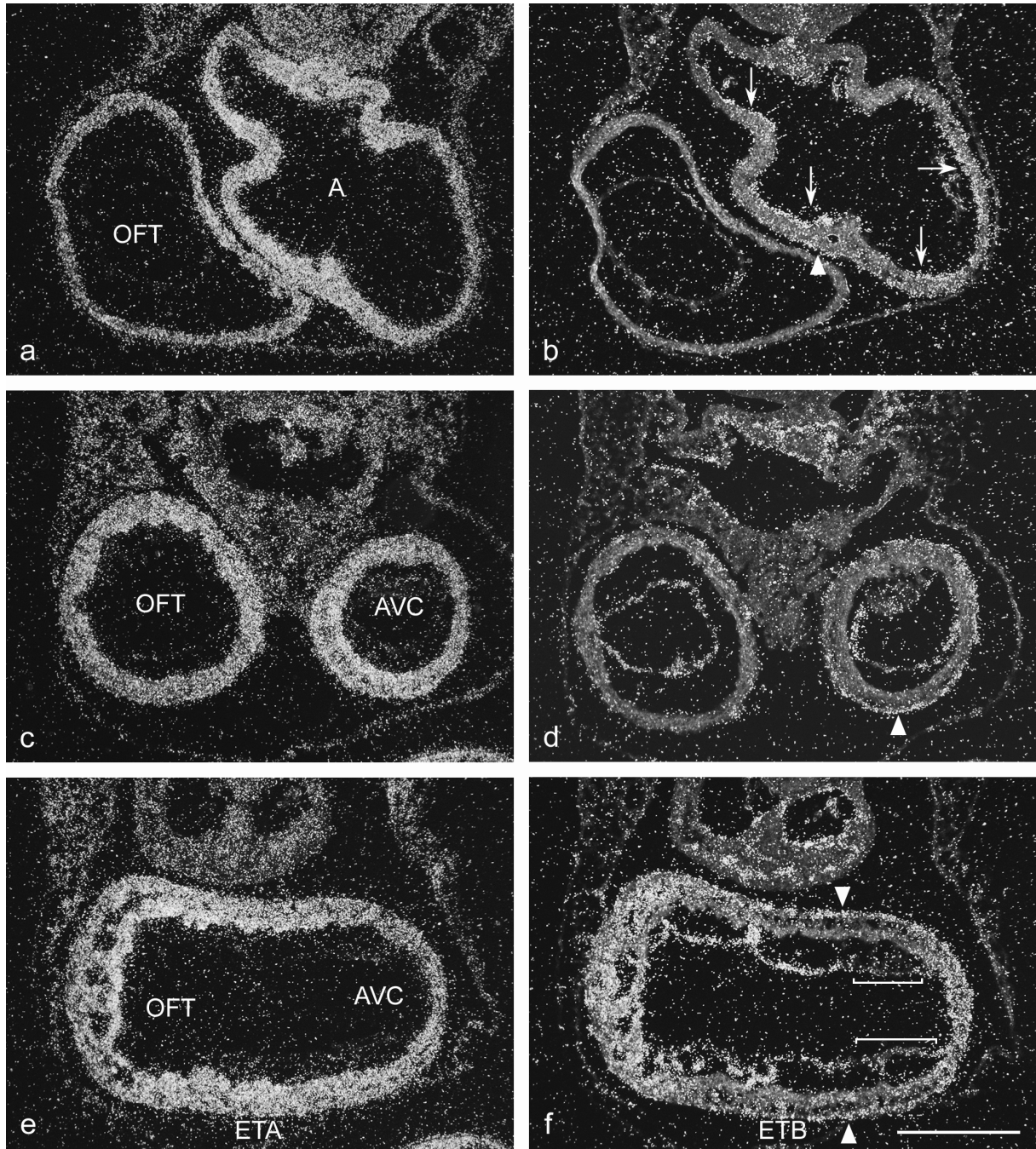
Figure 4.

ISH sections of a HH18 chicken embryo heart showing ETA (a, c, e) and ETB (b, d, f) mRNA expression in adjacent sections. Note that ETA is expressed in the myocardium, and not in the endocardium. ETB is predominantly expressed in the endocardium of the common atrium (A; arrows in b), narrow part of the atrioventricular canal at the lateral sides (AVC; d), the ventricle (trabecular part in f), and outflow tract (OFT; d, f). The distal part of the OFT shows less mRNA (b). The downstream part of the AVC also shows little expression (brackets in f). In the myocardium ETB is also locally present. The myocardium of the atrium is slightly positive (b), the ventricular yocardium, however, shows stronger expression (trabecular part in f). Note the border of positive myocardium in the atrium and AVC (arrowheads in b, d, f). Bar is 200μm.
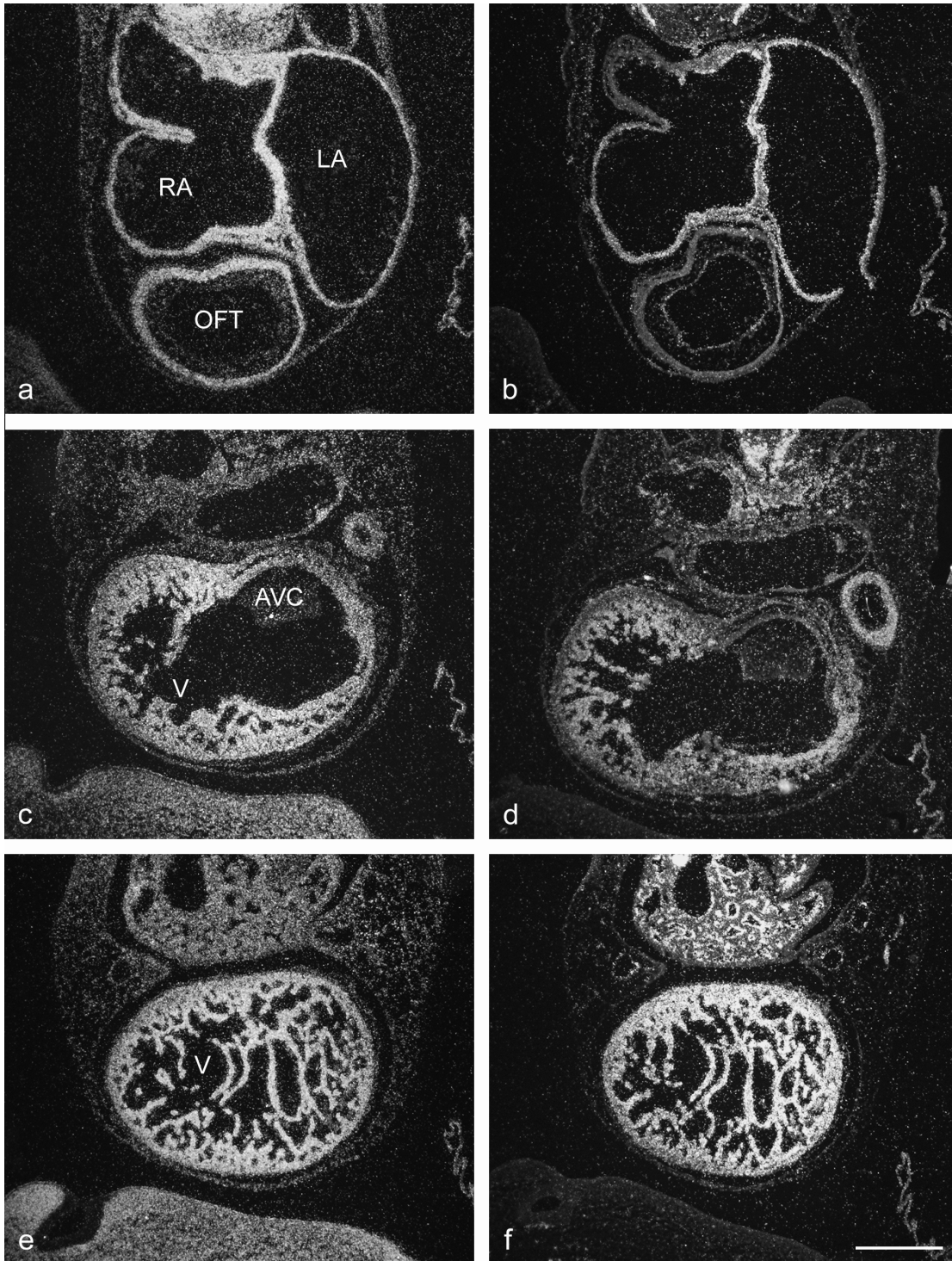
Figure 5.

ISH sections of a stage HH24 chicken heart showing ETA (a, c, e) and ETB (b ,d, f) mRNA expression. ETA is expressed in myocardium, and not in endocardium. ETB mRNA is predominantly present in the endocardium. However, endocardium of the complete atrioventricular canal (AVC) is negative (d). The ventricular (V) endocardium is strongly positive (d, f), whereas the endocardium of the outflow tract (OFT) shows less expression (b). The myocardium of the left and right atria (LA, RA; b) shows slight ETB expression. The myocardium of the AVC is negative (d), whereas the ventricular myocardium is positive (f). The compact myocardium shows less mRNA than the trabeculations (d). The OFT myocardium is negative (b). Bar is 300µm.

In vitro experiments

The results on gene expression of the addition of ET-1, ETA- or ETB antagonist to cultured quail heart endothelial cells (QHEC) for 5 hours is summarized in Figure 6. Application of the substances did not result in changes in the expression of *KLF2* compared to control cells. Exposure to the ETA antagonist, however, showed a significant decrease in *ET-1* expression, whereas the ETB antagonist resulted in enhancement of *ET-1* mRNA. *ETA* expression appears elevated with both ETA and ETB receptor antagonists, although significance was not reached. The same accounts for *ECE-1* mRNA, where exposure to the ETA receptor antagonist shows a significant increase. Addition of ET-1 had no effects on expression of the investigated genes.

Relative quantification endocardial expression
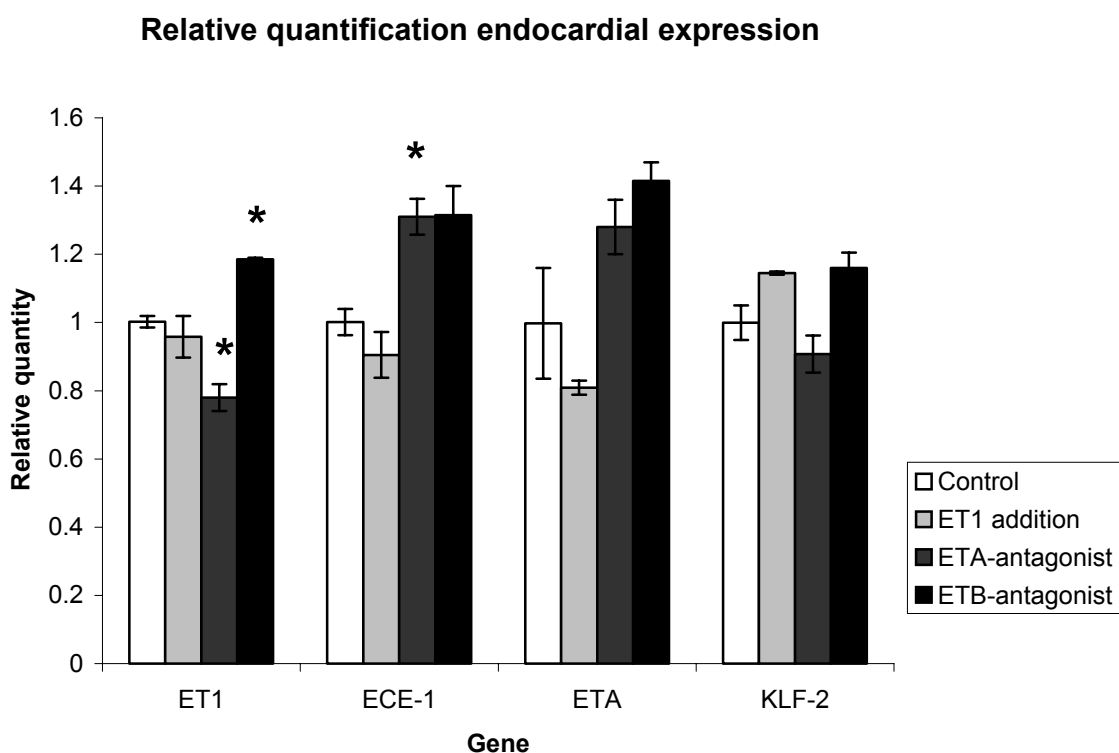
Figure 6.

Relative quantity of *ET-1*, *ECE-1*, *ETA* and *KLF2* mRNA from primary quail endocardial cell cultures after a 5-hour administration of ET-1, Endothelin receptor A or B antagonists, or PBS (control). Note that ET-1 addition does not lead to changes in mRNA levels. ETA antagonists, however, cause a decrease in *ET-1* mRNA and an increase of *ECE-1* levels; *ETA* mRNA appears to be increased. ETB antagonists show, in contrast to ETA blockers, an increase in *ET-1* mRNA. *ECE-1* and *ETA* levels appear to be up-regulated as well. *KLF2* mRNA is not affected by any of the administered substances.

Discussion

The venous clip model was developed to examine the relation between disturbed blood flow and cardiac development. Because the ET-1/ECE-1/ETA pathway has been shown to be responsive to changes in blood flow, we investigated whether disturbances in this cascade are responsible for both functional cardiac impairment and cardiovascular malformations as seen after venous clipping. For this purpose endothelin-1 and endothelin receptor antagonists were infused into the blood stream of HH18 embryos and ventricular diastolic filling characteristics were studied at HH24, followed by cardiovascular morphologic investigation at HH35. Furthermore, the effect of ET-1 and receptor antagonists on expression of *ET-1*, *ECE-1*, *ETA*, and *KLF2* was investigated.

In vitro experiments

The *in vitro* part of this study demonstrates that the different ET-receptor antagonists have the same, stimulating effect on *ECE-1* and *ETA* expressions, but a differential effect on *ET-1* mRNA in endocardial and heart muscle cells. While the ETA receptor antagonist causes down-regulation of *ET-1*, the ETB antagonist causes up-regulation. This confirms that ETA and ETB receptors act differently within cardiac function [36,37]. This was also demonstrated by the different reactions to ETA or ETB blockade on the passive filling component.

Doppler measurements

ET-1 has a negative inotropic and vasodilative effect through the ETB receptor and a positive inotropic and vasoconstrictive effect through the ETA receptor [36-39]. These effects, however, are direct and last for a couple of hours at the most [40,41]. Therefore, two days after treatment with ET-1 we encounter long-term consequences of this intervention.

Exogenous ET-1 causes an increase in blood flow probably due to the positive inotropic effect of the ETA receptor, which is expressed in the myocardium at both HH18 and 24. The ETB receptor is also expressed in the ventricular myocardium at HH18. However, ET-1 has a stronger affinity for the ETA receptor. This could explain the dominance of a positive inotropic effect through the ETA receptor. Stroke volume is elevated, however not significantly. This may be caused by a 2% higher heart rate compared to the shams. The passive component of diastolic filling was significantly reduced after ET-1 infusion. This might be due to increased collagen synthesis in the heart through both the ETA and ETB receptor, leading to a stiffer and less compliant ventricle [42]. In response to decreased passive

filling cardiac output is maintained by an increased active filling component, which assures growth of the embryo.

Unexpectedly ETA antagonist infusion increases blood flow. As the ETA receptor exerts a positive inotropic effect, we expected a diminished blood flow after blocking the receptor. Our *in vitro* data, however, show that when the ETA receptor is blocked, ETA mRNA is up-regulated, which indicates a compensatory mechanism. Possibly this effect lasts until HH24, resulting in a higher blood flow, via the positive inotropic effect of the ETA receptors. Stroke volume was elevated as well, however, this was not significant, due to a slightly higher heart rate of 1.3% as compared to sham embryos. The following explanation could be found for the decreased passive filling component. At HH35 about 50% of the embryos displayed thinner ventricles. This suggests that ventricular development is hampered, which could affect passive filling. Decreased size of the compact layer of the myocardium has been described in several other models, including the antisense *Ets* and the venous clip model [16,43]. The increased active component would assure maintenance of cardiac output at an adequate level. Furthermore, an increased inotropic state of the atrium due to up-regulation of the ETA receptors could be responsible for the latter observation.

By blocking the ETB receptor and thus the negative inotropic effects, the positive inotropic influence of the ETA receptor will prevail, resulting in the demonstrated increased blood flow and stroke volume. Growth of the ventricle and its compliance are probably not altered, which might explain the unchanged passive filling component. However, the active filling component was increased. Normally, the ETB receptors that are present in the atrial myocardium and endocardium counteract the positive inotropic effect of the ETA receptors. Blocking the ETB receptors could enhance atrial contraction, resulting in increased active ventricular filling.

The combined ETA-ETB antagonist demonstrated increased blood flow and stroke volume. Since ETA mRNA is up-regulated after single ETA and single ETB blockade, it is very likely that ETA mRNA is also increased after inhibition of both receptors. This will result in a more positive inotropic state through the ETA receptor and increased contractility two days after infusion of the combined antagonist. ET-1 normally stimulates proliferation of cardiac fibroblasts via the ETA receptor [32,44]. Therefore, blockade of the ETA receptor may also inhibit proliferation in the heart, resulting in decreased ventricular wall thickness. This explains the decreased passive filling component as described above. Compensation by the increased active component ensures cardiac output.

In the venous clip model similar changes in ventricular diastolic filling were demonstrated: the passive filling component was reduced by 53 % and the active component was increased by 33% after clipping [24]. In the present study however, the passive filling component was decreased by approximately 25% after infusion with ET-1, ETA- or combined ETA/ETB antagonist and the active filling was increased by ± 20%. These results suggest that perturbations in the endothelin pathway are responsible for disturbed diastolic filling in the venous clip model. However, a single infusion of these substances results in less severe diastolic functional impairment compared to the venous clip model, in which the intervention is permanent.

Morphology of malformations

Microscopically minor cardiovascular malformations were encountered after infusion of the different substances compared to sham infused embryos. In the venous clip model *ET-1* expression is decreased in the heart after 3 hours (Groenendijk, unpublished), and cardiovascular malformations develop [28]. These malformations are similar to the ones in knockout mice of *ET-1*, *ECE-1* and *ETA* [27,29,30]. Taken together, it would be conceivable that infusions of endothelin-1 or endothelin receptor antagonists in particular can lead to major malformations. Kempf *et al.* (1998)[45] performed experiments in chicken embryos comparable to the present study, and showed malformations of the heart and branchial arch derivatives. The anomalies of the branchial arch derivatives were supposed to be neural crest cell (NCC) related. In that study an ETA or ETA/ETB antagonist was administered onto the shell membrane between HH11 and HH24. In this way the neural crest cells were reached, and malformations of the outflow tract and branchial arches, to which NCC migrate, were evoked. In our study NCC may not be involved, as endothelin and the antagonists are infused into the blood stream, acting from the endothelial side of the vascular system, where they have to pass the endothelial barrier. This may explain the absence of these malformations in the present study. Another explanation is found in the timing of infusion. Antagonists administered at HH11-HH14 displayed the largest number of and the most severe malformations [45]. When administered during other developmental stages the embryos were much less affected, which led to the conclusion that there is a narrow time-window in the development of NCC-derived structures in the branchial arches that is ET-1/ECE-1/ETA dependent. Presumably, our infusions of antagonists at HH18 were too late to induce major NCC-related malformations.

In the venous clip model large VSDs are formed in the majority of embryos. A single infusion of ET-1, ETA-, ETB-, or a combined receptor antagonist at HH18 does not result in major

morphological malformations at HH35. Myocardialisation of the OFT is not impaired. If this was the case this would result in a VSD, or at least a delay in closure of the ventricular septum, as VSDs and impaired myocardialisation share a common origin [16]. Only isolated minor malformations are encountered. We assume that multiple infusions may lead to more severe cardiac malformations, such as found in the venous clip model, which involves a permanent venous ligation and where gene expression can be assumed to be altered for a longer period of time. Additionally, endogenous ET-1 is secreted at the abluminal side of the endocardial cells [46,47]. Therefore, a change in gene expression will have more impact on the myocardium than a single administration of ET-1 that is present at the luminal side as a consequence of infusion.

In the venous clip model the permanent ligation of the right lateral vitelline vein alters shear stress for at least 5 hrs [4] and subsequently the expression of shear stress responsive genes like *ET-1*, *KLF*2 and *NOS-3* (Groenendijk *et al*., 2005, unpublished). Thus, after clipping more genes will be disturbed than only those involved in the endothelin pathway, and diastolic functional changes are stronger. This suggests that the combination of altered hemodynamics and gene expression, including those of the endothelin pathway, causes the observed cardiovascular malformations after clipping.

In summary

The results found in the present study suggest that the endothelin pathway is involved in the development of functional cardiac impairment present in the venous clip model and plays an important role in development of cardiac function in general. We did not observe major cardiovascular malformations after infusions of the different substances. Presumably a single infusion causes fewer disruptions in cardiac developmental processes than evoked by the venous clip intervention. We conclude that cardiovascular malformations after venous clipping arise from a combination of hemodynamic changes and subsequent altered gene expression patterns, including those of the endothelin pathway.

5.3   References

1.   Hogers B, DeRuiter MC, Baasten AM, Gittenberger-de Groot AC, Poelmann RE. Intracardiac blood flow patterns related to the yolk sac circulation of the chick embryo. *Circ Res*. 1995;76:871-7.

2.   Hogers B, DeRuiter MC, Gittenberger-de Groot AC, Poelmann RE. Unilateral vitelline vein ligation alters intracardiac blood flow patterns and morphogenesis in the chick embryo. *Circ Res*. 1997;80:473-481.

3.   Hove JR, Koster RW, Forouhar AS, Acevedo-Bolton G, Fraser SE, Gharib M. Intracardiac fluid forces are an essential epigenetic factor for embryonic cardiogenesis. *Nature*. 2003;421:172-177.

4.   Stekelenburg-de Vos S, Ursem NT, Hop WC, Wladimiroff JW, Gittenberger-De Groot AC, Poelmann RE. Acutely altered hemodynamics following venous obstruction in the early chick embryo. *J Exp Biol*. 2003;206:1051-1057.

5.   Pappano AJ. Ontogenetic development of autonomic neuroeffector transmission and transmitter reactivity in embryonic and fetal hearts. *Pharmacological Reviews*. 1977;29:3-33.

6.   Casillas CB, Tinney JP, Keller BB. Influence of acute alterations in cycle length on ventricular function in chick embryos. *Am J Physiol*. 1994;267:H905-11.

7.   Hu N, Connuck DM, Keller BB, Clark EB. Diastolic filling characteristics in the stage 12 to 27 chick embryo ventricle. *Pediatr Res*. 1991;29:334-337.

8.   Hamburger V, Hamilton HL. A series of normal stages in the development of the chick embryo. *J Morphol*. 1951;88:49-92.

9.   Ursem NTC, Struijk PC, Poelmann RE, Gittenberger-de Groot AC, Wladimiroff JW. Dorsal aortic flow velocity in chick embryos of stage 16 to 28. *Ultrasound Med Biol*. 2001;27:919-24.

10.   Wispé J, Hu N, Clark EB. Effect of environmental hypothermia on dorsal aortic blood flow in the chick embryo, stages 18 to 24. *Pediatr Res*. 1983;17:945-8.

11.   Sedmera D, Pexieder T, Rychterova V, Hu N, Clark EB. Remodeling of chick embryonic ventricular myoarchitecture under experimentally changed loading conditions. *Anat Rec*. 1999;254:238-52.

12.   Sedmera D, Hu N, Weiss KM, Keller BB, Denslow S, Thompson RP. Cellular changes in experimental left heart hypoplasia. *Anat Rec*. 2002;267:137-45.

13.   Clark EB, Hu N, Dummett JL, Vandekieft GK, Olson C, Tomanek R. Ventricular function and morphology in chick embryo from stages 18 to 29. *Am J Physiol*. 1986;250:H407-H413.

14.   Tobita K, Schroder EA, Tinney JP, Garrison JB, Keller BB. Regional passive ventricular stress-strain relations during development of altered loads in chick embryo. *Am J Physiol Heart Circ Physiol*. 2002;282:H2386-96.

15.   Schroder EA, Tobita K, Tinney JP, Foldes JK, Keller BB. Microtubule involvement in the adaptation to altered mechanical load in developing chick myocardium. *Circ Res*. 2002;91:353-359.

16.   Hogers B, Gittenberger-de Groot AC, DeRuiter MC, Mentink MMT, Poelmann RE. Cardiac inflow malformations are more lethal and precede cardiac outflow malformations. Chick embryonic venous clip model. In: Hogers B, ed. *The role of blood flow in normal and abnormal heart development*. Wageningen: Ponsen & Looijen BV; 1998:79-100.

17.   Tobita K, Keller BB. Right and left ventricular wall deformation patterns in normal and left heart hypoplasia chick embryos. *Am J Physiol Heart Circ Physiol*. 2000;279:H959-69.

18.   Harh JY, Paul MH, Gallen WJ, Friedberg DZ, Kaplan S. Experimental production of hypoplastic left heart syndrome in the chick embryo. *Am J Cardiol*. 1973;31:51-6.

19.   Icardo JM. Endocardial cell arrangement: role of hemodynamics. *Anat Rec*. 1989;225:150-5.

20.   Davies PF, Tripathi SC. Mechanical stress mechanisms and the cell. An endothelial paradigm. *Circ Res*. 1993;72:239-45.

21.   Topper JN, Gimbrone MA. Blood flow and vascular gene expression: fluid shear stress as a modulator of endothelial phenotype. *Mol Med Today*. 1999;5:40-46.

22.   Galbraith CG, Skalak R, Chien S. Shear stress induces spatial reorganization of the endothelial cell cytoskeleton. *Cell Motil Cytoskeleton*. 1998;40:317-30.

23.   Yoshigi M, Clark EB, Yost HJ. Quantification of stretch-induced cytoskeletal remodeling in vascular endothelial cells by image processing. *Cytometry*. 2003;55A:109-18.

24.   Ursem NTC, Stekelenburg-de Vos S, Wladimiroff JW, Poelmann RE, Gittenberger-de Groot AC, Hu N, Clark EB. Ventricular diastolic characteristics in stage-24 chick embryos after extra-embryonic venous obstruction. *J Exp Biol*. 2004;207:1487-1490.

25.   Stekelenburg-de Vos S, Steendijk P, Ursem NT, Wladimiroff JW, Delfos R, Poelmann RE. Systolic and Diastolic Ventricular Function Assessed by Pressure-Volume Loops in the Stage 21 Venous Clipped Chick Embryo. *Pediatr Res*. 2005;57:16-21.

26.   Groenendijk BCW, Hierck BP, Gittenberger-De Groot AC, Poelmann RE. Development-related changes in the expression of shear stress responsive genes KLF-2, ET-1, and NOS-3 in the developing cardiovascular system of chicken embryos. *Dev Dyn*. 2004;230:57-68.

27.   Kurihara Y, Kurihara H, Oda H, Maemura K, Nagai R, Ishikawa T, Yazaki Y. Aortic arch malformations and ventricular septal defect in mice deficient in endothelin-1. *J Clin Invest*. 1995;96:293-300.

28.   Hogers B, DeRuiter MC, Gittenberger-de Groot AC, Poelmann RE. Extraembryonic venous obstructions lead to cardiovascular malformations and can be embryolethal. *Cardiovasc Res*. 1999;41:87-99.

29.   Yanagisawa H, Yanagisawa M, Kapur RP, Richardson JA, Williams SC, Clouthier DE, de Wit D, Emoto N, Hammer RE. Dual genetic pathways of endothelin-mediated intercellular

signaling revealed by targeted disruption of endothelin converting enzyme-1 gene. *Development*. 1998;125:825-36.

30. Clouthier DE, Hosoda K, Richardson JA, Williams SC, Yanagisawa H, Kuwaki T, Kumada M, Hammer RE, Yanagisawa M. Cranial and cardiac neural crest defects in endothelin-A receptor-deficient mice. *Development*. 1998;125:813-24.

31. Tsukada T, Tippens D, Gordon D, Ross R, Gown AM. HHF35, a muscle-actin-specific monoclonal antibody. I. Immunocytochemical and biochemical characterization. *Am J Pathol*. 1987;126:51-60.

32. Pardanaud L, Altmann C, Kitos P, Dieterlen-Lievre F, Buck CA. Vasculogenesis in the early quail blastodisc as studied with a monoclonal antibody recognizing endothelial cells. *Development*. 1987;100:339-349.

33. Hierck BP, Molin DG, Boot MJ, Poelmann RE, Gittenberger-de Groot AC. A chicken model for DGCR6 as a modifier gene in the DiGeorge critical region. *Pediatr Res*. 2004;56:440-8.

34. Rozen S, Skaletsky H. Primer3 on the WWW for general users and for biologist programmers. *Methods Mol Biol*. 2000;132:365-86.

35. Pfaffl MW. A new mathematical model for relative quantification in real-time RT-PCR. *Nucleic Acids Res*. 2001;29:2002-2007.

36. Kelso EJ, McDermott BJ, Silke B, Spiers JP. Endothelin(A) receptor subtype mediates endothelin-induced contractility in left ventricular cardiomyocytes isolated from rabbit myocardium. *J Pharmacol Exp Ther*. 2000;294:1047-52.

37. Leite-Moreira AF, Bras-Silva C, Pedrosa CA, Rocha-Sousa AA. ET-1 increases distensibility of acutely loaded myocardium: a novel ETA and Na+/H+ exchanger-mediated effect. *Am J Physiol Heart Circ Physiol*. 2003;284:H1332-9.

38. Marsault R, Feolde E, Frelin C. Receptor externalization determines sustained contractile responses to endothelin-1 in the rat aorta. *Am J Physiol*. 1993;264:C687-93.

39. Hirata Y, Emori T, Eguchi S, Kanno K, Imai T, Ohta K, Marumo F. Endothelin receptor subtype B mediates synthesis of nitric oxide by cultured bovine endothelial cells. *J Clin Invest*. 1993;91:1367-73.

40. Vierhapper H, Wagner O, Nowotny P, Waldhausl W. Effect of endothelin-1 in man. *Circulation*. 1990;81:1415-8.

41. Sirvio ML, Metsarinne K, Saijonmaa O, Fyhrquist F. Tissue distribution and half-life of 125I-endothelin in the rat: importance of pulmonary clearance. *Biochem Biophys Res Commun*. 1990;167:1191-5.

42. Guarda E, Katwa LC, Myers PR, Tyagi SC, Weber KT. Effects of endothelins on collagen turnover in cardiac fibroblasts. *Cardiovasc Res*. 1993;27:2130-4.

43. Lie-Venema H, Gittenberger-de Groot AC, van Empel LJ, Boot MJ, Kerkdijk H, de Kant E, DeRuiter MC. Ets-1 and Ets-2 transcription factors are essential for normal coronary and myocardial development in chicken embryos. *Circ Res*. 2003;92:749-56.

44. Fujisaki H, Ito H, Hirata Y, Tanaka M, Hata M, Lin M, Adachi S, Akimoto H, Marumo F, Hiroe M. Natriuretic peptides inhibit angiotensin II-induced proliferation of rat cardiac fibroblasts by blocking endothelin-1 gene expression. *J Clin Invest*. 1995;96:1059-65.

45. Kempf H, Linares C, Corvol P, Gasc JM. Pharmacological inactivation of the endothelin type A receptor in the early chick embryo: a model of mispatterning of the branchial arch derivatives. *Development*. 1998;125:4931-41.

46. Yoshimoto S, Ishizaki Y, Mori A, Sasaki T, Takakura K, Murota S. The role of cerebral microvessel endothelium in regulation of cerebral blood flow through production of endothelin-1. *J Cardiovasc Pharmacol*. 1991;17 Suppl 7:S260-3.

47. Wagner OF, Christ G, Wojta J, Vierhapper H, Parzer S, Nowotny PJ, Schneider B, Waldhausl W, Binder BR. Polar secretion of endothelin-1 by cultured endothelial cells. *J Biol Chem*. 1992;267:16066-8.

Chapter 6

General discussion

The purpose of the present thesis was to investigate our hypotheses regarding the development of cardiovascular malformations in the venous clip model. Firstly, we hypothesized that the venous clip intervention leads to instantaneous changes in hemodynamic parameters. Secondly, we hypothesized that venous clipping could lead to long-term changes in ventricular function. Thirdly, we hypothesized that the endothelin cascade is involved in the development of functional cardiac impairment and cardiovascular malformations after venous clipping. We used two approaches to obtain different parameters of cardiac function at several stages of development. Doppler measurements were made using a 20-MHz pulsed Doppler meter. This technique allowed determination of dorsal aortic blood flow velocities and ventricular diastolic filling characteristics. Furthermore, intraventricular blood pressure and ventricular blood volume were obtained using the servo-null pressure system and video imaging with a stereo microscope. This method enabled pressure-volume loop reconstruction and analysis, from which intrinsic ventricular systolic and diastolic properties were assessed. We used the venous clip chick embryo model, as this intervention leads to specific cardiovascular malformations. We suspected that hemodynamics could be affected as well, because of the intricate relationship between cardiac morphogenesis and cardiac function.

In figure 1 the findings of the studies presented in this thesis are combined. Starting at the top: the venous clip intervention at HH17. This causes an acute decrease in dorsal aortic blood volume flow as described in chapter 3. Blood volume flow remains below baseline level for at least 5 hrs [1]. This leads to a diminished mechanical load on the myocardium of the ventricle. Mechanical load regulates ventricular growth [2,3]. During normal development the ventricular wall volume will increase in size. Hogers *et al.* observed a delay in ventricular development after clipping [4]. The venous clip thus probably slows down the ventricular growth and differentiation process. This is presumably caused by altered gene expression. Eventually cardiovascular malformations are developed [5,6].

The marked decrease in mean blood flow after clipping also affects shear stress, as shear stress depends directly on volume flow [7]. Endothelial cells sense these changes in shear stress, which lead to alterations in gene expression by activation of a shear stress responsive element in the promotor region of the gene [8,9]. Groenendijk *et al.* demonstrated developmental stage-
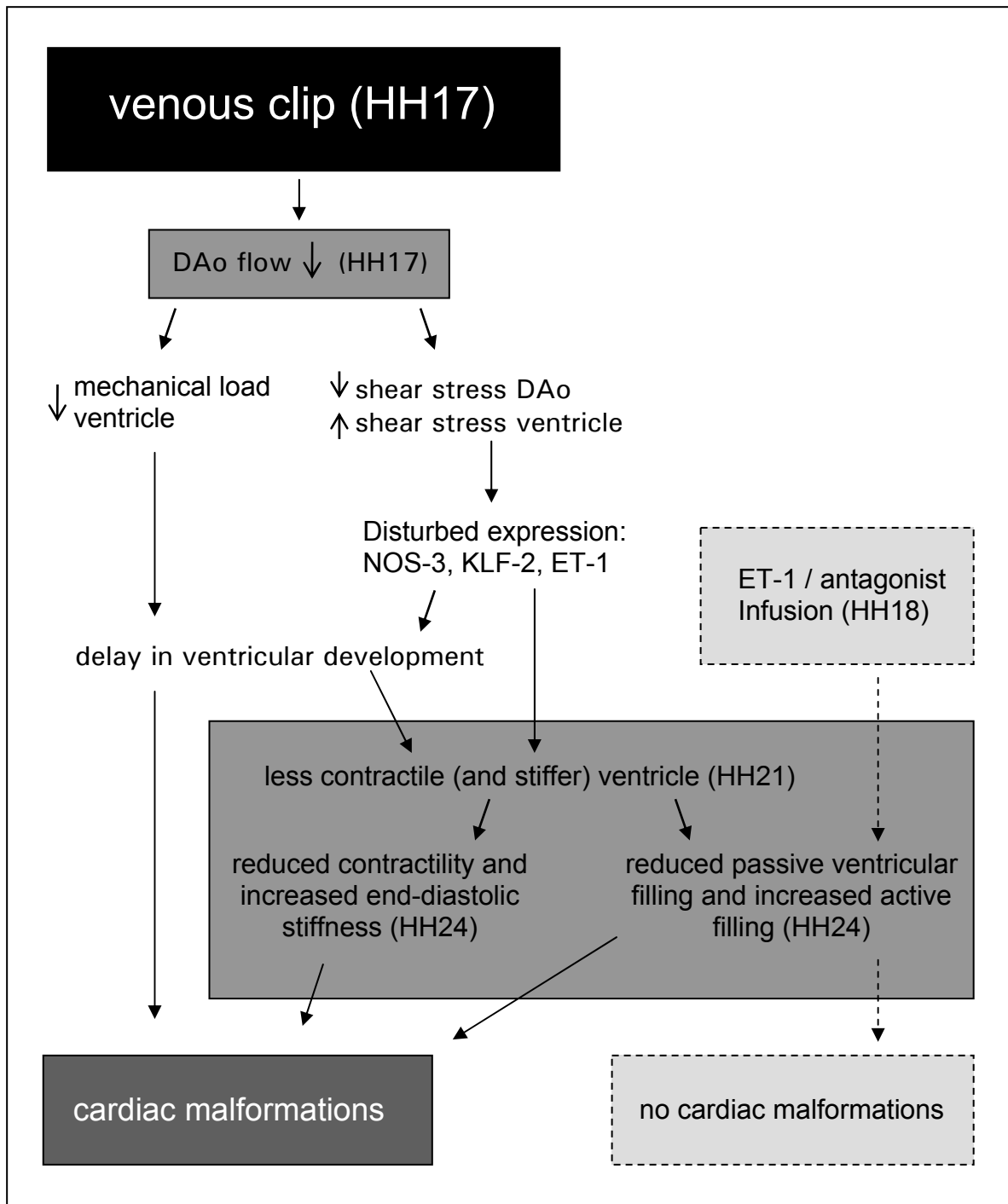
Figure 1.

Schematic overview of the results presented in this thesis.

▪ Represents the venous clip intervention.

▪ Represents functional findings after the venous clip intervention (chapter 3, 4 and 5.1).

▫ Represents the endothelin-1/antagonist infusion study (chapter 5.2)

▪ Represents cardiac malformations caused by venous clipping.

related cardiovascular expression of the transcription factor KLF-2 (Krüppel-like factor-2), ET-1 (endothelin-1) and NOS-3 (endothelial nitric oxide synthase), which are shear stress responsive genes [10]. Gene expression levels 3hrs after clipping confirmed that shear stress is diminished in the dorsal aorta. ET-1 expression is increased and KLF-2 and NOS-3 expression is down- regulated (Groenendijk *et al.*, 2004, unpublished data). The expression of ET-1 inside the ventricle is decreased 3hrs after clipping (Groenendijk *et al.*, 2004, unpublished data). This is probably caused by a change in intracardiac blood flow patterns, which were observed by Hogers *et al.* leading to local changes in shear stress [5]. Especially the endothelin-1/ETA signalling cascade appears to be important in cardiovascular development. ET-1 has a positive inotropic and vasoconstrictive effect through the ETA receptor [11]. Knockout mice studies of this cascade demonstrate a spectrum of cardiovascular malformations, which strongly resemble those seen in our venous clip model [12-14]. As ET-1 expression is diminished in the heart after clipping, this suggests that the endothelin cascade might be involved in the development of the malformations in our model. Ventricular development might be impaired due to disturbed expression of these genes. Through the ETA receptor, ET-1 mediates proliferation of cardiac fibroblasts of neonatal rats and canines [15,16]. This contrasts with Hafizi *et al.* who demonstrated that ET-1 inhibits cell growth in human cardiac fibroblasts over a period of 48 hrs while concomitantly being able to stimulate collagen synthesis [17]. The exact influence of disturbances in ET-1/ETA signalling cascade on ventricular development in the chick embryo is not clear yet. This cascade is important in other models. Therefore, we assume that in the chick embryo it may also influence ventricular development. Reduced mechanical load and/or altered gene expression probably lead to delayed or impaired ventricular development.

Not only ventricular morphology is abnormal. Ventricular function is affected as well. At HH21 we demonstrated reduced contractility of the ventricle and the ventricular wall tended to be stiffer using pressure-volume loop analysis as described in chapter 4. At HH24 contractility was even more reduced. This indicates that the mechanism causing a disturbed ventricular function is an ongoing process that results in a less contractile ventricle. At HH24 diastolic stiffness was significantly increased indicating a less compliant ventricle. As the embryonic ventricle is relatively non-compliant and compliance increases during development [18-20], our data suggest that this process lags behind after venous clipping.

In stage 24 we also observed changes in ventricular diastolic filling using simultaneous Doppler measurements of the dorsal aorta and atrioventricular canal, described in chapter 5. A reduced diastolic passive-filling component of ventricular filling was compensated by an

increased active-filling component in clipped embryos [21]. Probably the stiffer ventricular wall causes this decrease in passive filling, which is compensated by increased atrial contraction, thereby maintaining cardiac output at a sufficient level. Changes in diastolic function may be a critical regulatory pathway during cardiac morphogenesis [22]. After left atrial ligation Schroder *et al.* demonstrated an increase in microtubule density and β-tubulin protein [3]. They observed increased myocardial stiffness in response to reduced mechanical load. They argued that microtubules mediate the transport of materials necessary for the production of new cellular structures. As a consequence they may also play a role in mediating the adaptive response of the developing myocardium to altered mechanical load. This also holds for the venous clip model since in our model mechanical load is reduced. We assume that changes in microtubule density and organisation leads to increased diastolic stiffness in the clipped embryos thereby causing reduced diastolic passive ventricular filling.

In chapter 5 we described the influence of ET-1 and endothelin antagonist infusions on diastolic ventricular filling. Changes in ventricular diastolic filling after these infusions are similar to the observations made in the venous clip model. This suggests that disturbances in the endothelin pathway are responsible for the disturbed diastolic function in the venous clip model. However, compared to the venous clip model, diastolic functional impairment is less severe, probably due to the short intervention by single infusion of these substances. This also explains why we did not observe major cardiovascular malformations after the infusions. Presumably a single infusion causes fewer disruptions in cardiac developmental processes than the venous clip intervention does. In the venous clip model the permanent ligation of the right lateral vitelline vein alters shear stress for at least 5 hrs and subsequently the expression of shear stress responsive genes like ET-1, KLF-2 and NOS-3 [1](Groenendijk *et al.* unpublished data). Thus, it is conceivable that after clipping more genes are disturbed than those involved in the endothelin pathway. This suggests that a combination of altered gene expression patterns and hemodynamic changes causes the observed cardiovascular malformations after clipping.

The question arises as to how the results described in this thesis can be linked to the human embryo. The most severe human congenital cardiac malformations are already developed before we are able to visualise the human embryonic heart in detail using ultrasonography. In the majority of cases complex multifactorial genetic factors in combination with environmental influences are thought to be responsible [23]. We hypothesise that these combinations lead to altered gene and protein expression, which in turn result in hampered blood flow patterns inside the embryonic heart. Both altered gene expression and hampered

blood flow will result in cardiovascular malformations as described in the venous clip model. Also disturbed placental development may affect blood flow. Completion of the anatomical structure of the embryonic heart coincides with trophoblast invasion and early development of the placenta. When the process of trophoblast invasion is disturbed, extra-embryonic blood flow may be affected leading to altered flow and shear stress in the embryo, causing cardiovascular malformations.

Very recently, the chick genome has been sequenced [24]. It contains approximately one billion base pairs of sequence and an estimated 20,000-23,000 genes. In future research a prominent role for genomics and especially proteomics has to be reserved next to physiological studies [25,26]. These relative new fields of research enable determination of gene expression patterns and identification of proteins in the organism. Protein function is determined by the amount and structure of the protein. Structural changes in proteins caused by mutations can impair their function leading to diseases. It would be interesting to know whether the venous clip intervention causes alterations in protein production, and if so what kind of proteins are affected. Knowledge of these issues can give more insight into normal and abnormal cardiovascular developmental processes in chicks and humans.

References

1.   Stekelenburg-de Vos S, Ursem NT, Hop WC, Wladimiroff JW, Gittenberger-De Groot AC, Poelmann RE. Acutely altered hemodynamics following venous obstruction in the early chick embryo. *J Exp Biol*. 2003;206:1051-1057.

2.   Clark EB, Hu N, Frommelt P, Vandekieft GK, Dummett JL, Tomanek RJ. Effect of increased pressure on ventricular growth in stage 21 chick embryos. *Am J Physiol*. 1989;257:H55-H61.

3.   Schroder EA, Tobita K, Tinney JP, Foldes JK, Keller BB. Microtubule involvement in the adaptation to altered mechanical load in developing chick myocardium. *Circ Res*. 2002;91:353-359.

4.   Hogers B, Gittenberger-de Groot AC, DeRuiter MC, Mentink MMT, Poelmann RE. Cardiac inflow malformations are more lethal and precede cardiac outflow malformations. Chick embryonic venous clip model. In: Hogers B, ed. *The role of blood flow in normal and abnormal heart development*. Wageningen: Ponsen & Looijen BV; 1998:79-100.

5.   Hogers B, DeRuiter MC, Gittenberger-de Groot AC, Poelmann RE. Unilateral vitelline vein ligation alters intracardiac blood flow patterns and morphogenesis in the chick embryo. *Circ Res*. 1997;80:473-481.

6.   Hogers B, DeRuiter MC, Gittenberger-de Groot AC, Poelmann RE. Extraembryonic venous obstructions lead to cardiovascular malformations and can be embryolethal. *Cardiovasc Res*. 1999;41:87-99.

7.   Goldsmith HL, Turitto VT. Rheological aspects of thrombosis and haemostasis: basic principles and applications. ICTH-Report--Subcommittee on Rheology of the International Committee on Thrombosis and Haemostasis. *Thromb Haemost*. 1986;55:415-435.

8.   Malek AM, Izumo S. Control of endothelial cell gene expression by flow. *J Biomech*. 1995;28:1515-28.

9.   Fisher AB, Chien S, Barakat AI, Nerem RM. Endothelial cellular response to altered shear stress. *Am J Physiol Lung Cell Mol Physiol*. 2001;281:L529-533.

10.   Groenendijk BC, Hierck BP, Gittenberger-De Groot AC, Poelmann RE. Development-related changes in the expression of shear stress responsive genes KLF-2, ET-1, and NOS-3 in the developing cardiovascular system of chicken embryos. *Dev Dyn*. 2004;230:57-68.

11.   Leite-Moreira AF, Bras-Silva C. Inotropic effects of ETB receptor stimulation and their modulation by endocardial endothelium, NO, and prostaglandins. *Am J Physiol Heart Circ Physiol*. 2004;287:H1194-9.

12.   Kurihara Y, Kurihara H, Oda H, Maemura K, Nagai R, Ishikawa T, Yazaki Y. Aortic arch malformations and ventricular septal defect in mice deficient in endothelin-1. *J Clin Invest*. 1995;96:293-300.

13.   Yanagisawa H, Yanagisawa M, Kapur RP, Richardson JA, Williams SC, Clouthier DE, de Wit D, Emoto N, Hammer RE. Dual genetic pathways of endothelin-mediated intercellular

signaling revealed by targeted disruption of endothelin converting enzyme-1 gene. *Development*. 1998;125:825-36.

14.   Clouthier DE, Hosoda K, Richardson JA, Williams SC, Yanagisawa H, Kuwaki T, Kumada M, Hammer RE, Yanagisawa M. Cranial and cardiac neural crest defects in endothelin-A receptor-deficient mice. *Development*. 1998;125:813-24.

15.   Piacentini L, Gray M, Honbo NY, Chentoufi J, Bergman M, Karliner JS. Endothelin-1 stimulates cardiac fibroblast proliferation through activation of protein kinase C. *J Mol Cell Cardiol*. 2000;32:565-76.

16.   Tsuruda T, Jougasaki M, Boerrigter G, Huntley BK, Chen HH, D'Assoro AB, Lee SC, Larsen AM, Cataliotti A, Burnett JC, Jr. Cardiotrophin-1 stimulation of cardiac fibroblast growth: roles for glycoprotein 130/leukemia inhibitory factor receptor and the endothelin type A receptor. *Circ Res*. 2002;90:128-34.

17.   Hafizi S, Wharton J, Chester AH, Yacoub MH. Profibrotic effects of endothelin-1 via the ETA receptor in cultured human cardiac fibroblasts. *Cell Physiol Biochem*. 2004;14:285-92.

18.   Friedman WF. The intrinsic physiologic properties of the developing heart. *Prog Cardiovasc Dis*. 1972;15:87-111.

19.   Keller BB, Tinney JP, Hu N. Embryonic ventricular diastolic and systolic pressure-volume relations. *Cardiol Young*. 1994;4:19-27.

20.   Anderson PA. The heart and development. *Semin Perinatol*. 1996;20:482-509.

21.   Ursem NTC, Stekelenburg-de Vos S, Wladimiroff JW, Poelmann RE, Gittenberger-de Groot AC, Hu N, Clark EB. Ventricular diastolic characteristics in stage-24 chick embryos after extra-embryonic venous obstruction. *J Exp Biol*. 2004;207:1487-1490.

22.   Hu N, Connuck DM, Keller BB, Clark EB. Diastolic filling characteristics in the stage 12 to 27 chick embryo ventricle. *Pediatr Res*. 1991;29:334-337.

23.   Nora JJ. Causes of congenital heart diseases: old and new modes, mechanisms, and models. *Am Heart J*. 1993;125:1409-19.

24.   International Chicken Genome Sequencing Consortium. Sequence and comparative analysis of the chicken genome provide unique perspectives on vertebrate evolution. *Nature*. 2004;432:695-716.

25.   McGregor E, Dunn MJ. Proteomics of heart disease. *Hum Mol Genet*. 2003;12 Spec No 2:R135-44.

26.   Prentice H, Webster KA. Genomic and proteomic profiles of heart disease. *Trends Cardiovasc Med*. 2004;14:282-8.

Summary

Chapter 1

Congenital heart disease affects approximately 2-3% of children born each year. The aetiology of these cardiovascular malformations is still largely unclarified. Knowledge of normal and abnormal cardiac development is necessary in order to improve medical and surgical outcome. As the present techniques do not allow real-time investigation of early cardiac development in human pregnancies, we used the chick embryo as a model. This model shares morphological characteristics of the human embryo during early cardiac development. Furthermore, an intervention model was available in which specific cardiovascular malformations can be induced. By obstructing the right lateral vitelline vein (venous clipping) alterations in intracardiac blood flow patterns are caused eventually leading to outflow tract anomalies. This model enables investigation of the relationship between cardiac morphogenesis and cardiac function as described in this thesis.

Chapter 2

This chapter deals with the techniques and methods that were used to obtain different parameters of cardiac function in the normal and venous clipped chick embryo. The venous clip procedure is described. The theory behind Doppler ultrasound and its use in this thesis is outlined, as well as the reproducibility of the blood flow velocity waveform recordings. Detailed information on the servo-null pressure system and intraventricular blood volume measurements is presented. Assessment of ventricular function is obtained by analysis of pressure-volume loops.

Chapter 3

The instantaneous effects of clipping the right lateral vitelline vein on blood volume flow in the stage 17-chick embryo was studied using dorsal aortic Doppler measurements. Heart rate, peak systolic velocity, time-averaged velocity, peak blood flow, mean blood flow, peak acceleration and stroke volume decreased acutely after venous clipping and only three out of seven parameters (heart rate, time-averaged velocity and mean blood flow) showed a recovery to baseline values during the 5 h study period. The venous clip intervention has major acute effects on hemodynamics in the chick embryo. These effects may be responsible for the observed cardiac malformations after clipping.

Chapter 4

Long-term consequences of the venous clip intervention for ventricular function were determined one day (HH21) and two days (HH24) after clipping using pressure-volume loop analysis. At HH21 steady state hemodynamic parameters demonstrated no significant differences between the venous clipped and control embryos. However analysis of pressure-volume relations showed a significantly lower end-systolic elastance in the clipped embryos indicating reduced contractility. Diastolic stiffness tended to be increased after clipping but the difference did not reach statistical significance. At HH24 end-systolic volume was significantly higher in clipped embryos. End-systolic pressure and end-diastolic pressure were also increased. No significant differences were demonstrated for other baseline hemodynamic parameters. Analysis of pressure-volume relations showed a significantly lower end-systolic elastance in the clipped embryos indicating reduced contractility. Diastolic stiffness was significantly increased indicating reduced compliance.

These findings support the hypothesis that development of ventricular function in the embryonic heart is affected by mechanical load. Venous obstruction interferes with normal myocardial development resulting in impaired intrinsic systolic and diastolic ventricular function. Changes in ventricular function may precede morphological derangements in later developmental stages.

Chapter 5

The first part of this chapter describes the study on the influence of the venous clip intervention on ventricular diastolic filling using simultaneous Doppler measurements over the dorsal aorta and atrioventricular canal. At similar cycle lengths dorsal aortic blood flow and stroke volume measured in the dorsal aorta were comparable in HH24 clipped and normal embryos. Passive filling volume was decreased with 53% and active filling volume was increased with 33% in the clipped embryos, leading to a decreased passive/active ratio. These results suggest that material properties of the embryonic ventricle are modified after temporarily reduced hemodynamic load. In conclusion, early venous obstruction results in altered diastolic ventricular filling in the stage 24-chick embryo. Changes in cardiac function and structure can be produced by alterations in mechanical loading.

In the second part of the chapter the same simultaneous Doppler measurements were performed after infusion of endothelin-1 or endothelin receptor antagonist. The passive filling component was decreased with approximately 25% after infusion with ET-1, ETA- or combined ETA/ETB receptor antagonist. The active filling was increased with ± 20%. These

changes in ventricular diastolic filling are similar to the observations made in the venous clip model. This suggests that disturbances in the endothelin pathway are responsible for the impaired diastolic function in the venous clip model. We did not observe major cardiovascular malformations after the infusions. Presumably a single infusion causes fewer disruptions in cardiac developmental processes than the venous clip intervention does. The combination of altered gene expression patterns and hemodynamic changes probably causes the observed cardiovascular malformations after clipping.

Samenvatting

Hoofdstuk 1

Ieder jaar wordt bij 2-3% van de pasgeborenen een congenitale hartafwijking geconstateerd. De oorzaak van deze cardiovasculaire afwijkingen is grotendeels onbekend. Kennis van normale en abnormale hartontwikkeling is nodig om de uitkomst van medische en chirurgische behandeling te verbeteren. Omdat de huidige beeldvormende technieken ontoereikend zijn om vroege hartontwikkeling te bestuderen in de mens hebben we gebruikgemaakt van het kippenembryo model. De morphologische eigenschappen van dit model komen overeen met die van de mens tijdens vroege hartontwikkeling. We beschikken daarnaast over een interventie model waarin specifieke cardiovasculaire afwijkingen kunnen worden geïnduceerd. Door de rechter laterale vitelline vene af te klemmen (veneus clippen) worden veranderingen in intracardiale bloedstroomprofielen veroorzaakt, wat uiteindelijk leidt tot afwijkingen in het uitstroomgebied. Dit model maakt het mogelijk om de relatie tussen morphologie van het hart en hartfunctie te onderzoeken zoals beschreven in dit proefschrift.

Hoofdstuk 2

Dit hoofdstuk behandelt de technieken en methodes welke gebruikt zijn om de verschillende hartfunctie parameters te verkrijgen in normale en veneus geclipte kippenembryo's. De veneuze clip procedure wordt beschreven. Zowel de theorie achter Doppler echografie en het gebruik hiervan in dit proefschrift wordt uiteengezet, als ook de reproduceerbaarheid van bloeddoorstroming snelheidsmetingen. Gedetailleerd worden het servo-null druksysteem en de intraventriculaire bloedvolume metingen beschreven. Ventrikelfunctie wordt vastgesteld met behulp van druk-volume relaties.

Hoofdstuk 3

De directe effecten van het clippen van de rechter laterale vitelline vene in het stadium 17 kippenembryo op bloedvolume doorstroming werden bestudeerd met behulp van dorsale aorta Doppler metingen. Hartslag, maximale systolische doorstromingssnelheid, gemiddelde systolische doorstromingssnelheid, maximaal doorstromingsvolume, gemiddeld doorstromingsvolume, maximale acceleratie en slagvolume zijn acuut verlaagd na veneus clippen en slechts drie van de zeven parameters (hartslag, gemiddelde systolische doorstromingssnelheid en gemiddeld doorstromingsvolume) herstelden zich tot baseline

waarden tijdens de 5 uur durende studieperiode. De veneuze clip interventie heeft grote gevolgen voor de hemodynamiek in het kippenembryo. Dit zou de oorzaak kunen zijn voor de waargenomen hartafwijkingen na clippen.

Hoofdstuk 4

Lange termijn gevolgen van de veneuze clip interventie voor ventrikelfunctie werden vastgesteld één dag (HH21) en twee dagen (HH24) na clippen door middel van druk-volume relatie analyse. In HH21 toonden de basis hemodynamische parameters geen significante verschillen tussen de veneus geclipte en controle embryo's. Maar analyse van druk-volume relaties liet een significant lagere eind-systolische elasticiteit in de geclipte embryo's zien, wat wijst op een verlaagde contractiliteit. Diastolische stijfheid was verhoogd na clippen, maar niet significant. In HH24 was het eind-systolische volume significant hoger in geclipte embryo's. Eind-systolische druk en eind-diastolische druk waren ook verhoogd. Voor overige basis hemodynamische parameters werden geen significante verschillen gevonden. Analyse van de druk-volume relaties toonde een significant lagere eind-systolische elasticiteit en dus contractiliteit. Diastolische stijfheid was significant verhoogd, dit duidt op een verminderde compliantie.

Deze bevindingen ondersteunen de hypothese dat ontwikkeling van ventrikelfunctie in het embryonale hart wordt beïnvloed door mechanische lading. Veneuze obstructie interfereert met normale myocardiale ontwikkeling resulterend in gestoorde intrinsieke systolische en diastolische ventrikelfunctie. Veranderingen in ventrikelfunctie kunnen voorafgaan aan morphologische afwijkingen in latere ontwikkelingsstadia.

Hoofdstuk 5

Het eerste deel van dit hoofdstuk beschrijft de studie naar de invloed van de veneuze clip interventie op ventriculaire diastolische vulling door middel van simultane Doppler metingen over de dorsale aorta en het atrioventriculaire kanaal. Bij een gelijke hartcycluslengte waren bloeddoorstromingsvolume en slagvolume, gemeten in de dorsale aorta, vergelijkbaar in geclipte en normale embryo's van HH24. Het passieve vullingsvolume was afgenomen met 53% en het actieve vullingsvolume was toegenomen met 33% in geclipte embryo's, wat resulteerde in een verlaagde passieve/actieve ratio. Deze resultaten suggereren dat materiaal eigenschappen van het embryonale ventrikel zijn veranderd na tijdelijk verlaagde mechanische lading.

In het tweede deel van dit hoofdstuk werden dezelfde simultane Doppler metingen verricht na infusie van endotheline-1 of endotheline receptor antagonisten. De passieve vullingscomponent was verlaagd met ongeveer 25% na infusie met ET-1, ETA- of gecombineerde ETA/ETB receptor antagonist. De actieve vulling was verhoogd met ± 20%. Deze veranderingen in ventriculaire diastolische vulling zijn vergelijkbaar met bevindingen in het veneuze clip model. Dit suggereert dat verstoringen in de endotheline cascade verantwoordelijk zijn voor de afwijkende diastolische functie in het veneuze clip model. We vonden geen grote cardiovasculaire afwijkingen na de infusies. Het is aannemelijk dat een enkele infusie minder verstoringen in het hartontwikkelingsproces veroorzaakt dan de veneuze clip interventie. De combinatie van veranderde genexpressiepatronen en hemodynamische veranderingen leidt waarschijnlijk tot de gevonden cardiovasculaire afwijkingen na clippen.

List of publications

Joosten AMS, de Vos S, van Opstal D, Brandenburg H, Gaillard JLJ, Vermeij-Keers C. Full monosomy 21, prenatally diagnosed by in situ hybridisation. Prenatal Diagnosis. 1996;17:3:271-275.

van Stuijvenberg M, Suur MH, de Vos S, Tjiang GCH, Steyerberg EW, Derksen-Lubsen G, Moll HA. Informed consent, parental awareness, and reasons for participating in a randomised controlled study. Arch Dis Child. 1998;179:120-125.

van Stuijvenberg M, de Vos S, Tjiang GC, Steyerberg EW, Derksen-Lubsen G, Moll HA. Parents' fear regarding fever and febrile seizures. Acta paediatr. 1999;88(6):618-622.

Stekelenburg-de Vos S, Ursem NTC, Hop WC, Wladimiroff JW, Gittenberger-de Groot AC, Poelmann RE. Acutely altered hemodynamics following venous obstruction in the early chick embryo. J Exp Biol. 2003 Mar;206(Pt 6):1051-7.

Ursem NTC, Stekelenburg-de Vos S, Wladimiroff JW, Poelmann RE, Gittenberger-de Groot AC, Hu N, Clark EB. Ventricular diastolic filling characteristics in stage-24 chick embryos after extra-embryonic venous obstruction. J Exp Biol. 2004 Apr;207(Pt 9):1487-90.

Stekelenburg-de Vos S, Steendijk P, Ursem NTC, Wladimiroff JW, Delfos R, Poelmann RE. Systolic and diastolic ventricular function assessed by pressure-volume loops in the stage 21 venous clipped chick embryo. Pediatr Res 2005;57:16-21.

Vennemann P, Lindken R, Groenendijk BCW, Stekelenburg-de Vos S, Ten Hagen TL, Ursem NTC, Poelmann RE, Westerweel J, Hierck BP. In vivo micro particle image velocimetry measurements of blood-plasma in the embryonic avian heart. J Biomech. 2005. In press.

Stekelenburg-de Vos S, Steendijk P, Ursem NTC, Wladimiroff JW, Poelmann RE. Impaired ventricular function after extra-embryonic venous obstruction, a pressure-volume loop assessment in the stage 24-chick embryo. In preparation.

Poelmann RE, Gittenberger-de Groot AC, Groenendijk BCW, Hierck BP, Hogers B, Nieuwstadt FTM, Pourquie MJBM, Steendijk P, Stekelenburg-de Vos S, Ursem NTC, Wladimiroff JW. Shear stress in the developing cardiovascular system. In: Artman M, Woodrow BD, Strivastava D, Nakazawa M. eds *Cardiovascular Development and Congenital Malformations, Molecular and Genetic Mechanisms*. New York: Blackwell Futura Co; 2005.

Stekelenburg-de Vos S, Groenendijk BCW, Weijden AT, Ursem NTC, Hierck BP, Wladimiroff JW, Poelmann RE. Altered ventricular diastolic filling characteristics in HH24 chicken embryos after venous infusion of endothelin-1 and endothelin receptor antagonists at HH18. In preparation.

Curriculum vitae

Sandra Stekelenburg-de Vos was born on the 31st of December 1973 in Rotterdam, The Netherlands. She passed secondary school at the J.C. De Glopper scholengemeenschap in Capelle aan den IJssel. She attended Medical School at the Erasmus University in Rotterdam from 1992 – 1998. From December 1998 – July 1999 she worked as a resident at the department of Obstetrics and Gynaecology of the Diaconessen Hospital in Leiden. From August 1999 – January 2001 she worked as a resident at the department of Obstetrics and Gynaecology of Hospital Leyenburg in The Hague. From February 2001 – January 2005 she worked as a PhD student at the division of Prenatal Diagnosis of the department of Obstetrics and Gynaecology of the Erasmus MC in Rotterdam performing the studies described in this thesis. From February 2005 – May 2005 she worked as a resident at the department of Obstetrics and Gynaecology of the Amphia Hospital in Breda. In July 2005 she started her training in Obstetrics and Gynaecology at the Albert Schweitzer Hospital in Dordrecht.

Dankwoord

Uiteraard wil ik alle mensen die geholpen hebben bij de totstandkoming van dit proefschrift bedanken. Allereerst gaat mijn dank uit naar mijn twee promotores Prof.dr. J.W. Wladimiroff en Prof.dr. R.E. Poelmann (Rob) voor de enthousiaste begeleiding en heldere visie op de soms lastige wetenschappelijke vraagstukken waar ik tegenaan liep. Altijd wisten jullie mijn kijk op de resultaten weer te veranderen en te verbeteren.

Ik bedank ook alle leden van de kleine en grote promotiecommissie voor hun bereidwilligheid om hierin zitting te nemen.

Lieve Nicolette (Ursem), jou ben ik de meeste dank verschuldigd. Jij was niet alleen mijn dagelijkse begeleidster, maar ook mijn kamergenoot, inspirator en co-promotor. Ik heb veel van je geleerd. We denken over vele dingen op dezelfde manier en hebben daardoor veel lol gehad samen. Het was altijd gezellig en ik kon overal en altijd bij je terecht met zowel werkgerelateerde maar zeker ook persoonlijke zaken. Het was welgemeend een voorrecht om met jou te werken.

Beste Piet (Struijk), jij en de 22^e verdieping, dat zijn twee onlosmakelijk met elkaar verbonden eenheden. Bedankt voor je bijles over statistische aangelegenheden, maar vooral bedankt voor het opluisteren van de koffiepauzes met alles waar alleen jij je druk over kan maken! Ik vind het bewonderenswaardig hoe hard je werkt aan je eigen boekje en toch altijd nog tijd vindt om anderen te adviseren.

Dear Simona (Boito), I always enjoyed your typical Italian way of doing things. You always made me smile with your stories about Mrs. Bomans and the dog. I still miss you.

Lieve Anneke (Verkleij), Marianne (Coolman) en Annelous (Berends), ook jullie kwamen naar de 22e en het werd steeds gezelliger. Bedankt voor jullie vriendschap en jullie luisterend oor bij voor- en tegenspoed. Ik kijk uit naar jullie boekjes!

De overige onderzoekers in het bijzonder Nanette (Roelofsma), Hilmar (Bijma), Aagje (Bais), Manon (van Seters) en Annemarie (Mulders) wil ik bedanken voor de gezelligheid op de kopkamer.

De mensen uit Leiden, hartelijk bedankt voor jullie interesse voor de fysiologische kant van het kippenembryo. Bianca (Groenendijk), je was een fijne mede-AIO op dit project. Voor jou is het einde nu ook in zicht. We vormden een goed team tijdens de lange uren die we samen hebben vertoefd achter de microscoop en ik bedank je nogmaals voor je inzet voor ons project. Ik bewonder je doorzettingsvermogen.

Beerend (Hierck) bedankt voor je bijdrage aan de discussies over interpretatie van resultaten.

Paul (Steendijk), ik wil je hartelijk bedanken voor mijn inwijding in de wereld van de pressure-volume loops. Je hebt veel werk gehad aan alle analyses, en ook toen je laptop gestolen was en je alles opnieuw kon uitvoeren was dit supersnel weer gebeurd. Ook je bijdrage aan de artikelen is van onschatbare waarde. Bedankt!

De mensen uit Delft, bedankt voor de gezellige shear stress vergaderingen. René (Delfos) met name bedank ik voor zijn werk aan het servo-null pressure systeem. Het blijft toch een zeer ingewikkeld technisch apparaat voor een simpele dokter zoals ik. Mathieu (Pourquie), Ralph (Lindken), Peter (Vennemann) en Prof.dr.ir. Jerry Westerweel, bedankt voor jullie input en meedenken. Jullie hebben bewezen dat Delftse techneuten toch ook normale mensen zijn.

Prof.dr.ir. F.T.M. Nieuwstadt (Frans), bedankt voor uw interesse in de biologische aspecten van het project. Ik vond het een eer u gekend te hebben. Uw rustige en vaderlijke uitstraling zal ik nooit vergeten.

Lieve Gerda (Verduijn) en Annemarie (Swaak-Kragten) en uiteraard ook jullie mannen Jeroen en Pieter, bedankt voor jullie vriendschap. Jullie waren zowel mijn getuigen bij mijn huwelijk als nu ook mijn paranimfen. We delen lief en leed met z'n zessen en ik hoop dat we nog lang van elkaar mogen blijven genieten. Jullie zijn ontzettend belangrijk voor mij.

Schoonouders, familieleden, vrienden en vriendinnen, bedankt voor jullie interesse in mijn onderzoek.

Lieve ouders, van jongs af aan hebben jullie mij steeds gestimuleerd om het beste uit mezelf te halen. Jullie stonden altijd achter me en dankzij jullie ben ik geworden tot wie ik ben. Bedankt voor jullie liefde en nimmer aflatende steun.

Als allerlaatste wil de belangrijkste persoon in mijn leven bedanken. Allerliefste Erik, jij betekent alles voor mij. Jij hebt steeds achter al mijn beslissingen gestaan en mij gesteund door dik en dun! De klus is geklaard, op naar de volgende uitdaging. Ik blijf geloven in ons motto 'de aanhouder wint'.

Sandra